

A SEMI-EMPIRICAL SELF-CONSISTENT FIELD MOLECULAR
ORBITAL (SCF-MO) STUDY OF THE GROUND STATE
PROPERTIES OF SUBSTITUTED NAPHTHALENE
COMPOUNDS

BY

ADENIYI OLADEPO ADEKUNLE
B.Sc. (Hons.) Chemistry, M.Sc.
Physical Chemistry (Ibadan)

A THESIS IN THE DEPARTMENT OF CHEMISTRY
SUBMITTED TO THE FACULTY OF SCIENCE IN PARTIAL
FULFILMENT OF THE REQUIREMENTS FOR THE AWARD
OF THE DEGREE OF
MASTER OF PHILOSOPHY
OF THE
UNIVERSITY OF IBADAN

MARCH 1990

DEDICATION

I dedicate this piece of work to the memory of my great father, Chief M.P. Adekunle, who, in his lifetime, insisted that I must know GOD and taught me the best of values of life, and who also, at the time my etchy capacity for patience was beginning to wear distinctly thin, implored me to at least finish this task, if only as indicator of my vast potentials for genuine greatness.

UNIVERSITY OF IBADAN LIBRARY

ABSTRACT

The ground and excited state properties of naphthalene and some of its derivatives have been studied.

The molecular orbitals were evaluated using the modified Huckel Molecular Orbital (HMO) theory and the calculated molecular properties such as dipole moments, electronic transition frequencies, have been compared with experimental values.

The electronic absorption spectra of some of the compounds were further studied in detail as to their band systems and characteristics, solvent polarity effects and hydrogen bonding effects. The dipole moment changes from ground to excited states were generally determined to be high. A linear regression analysis obtained for plots of the ' L_b ' band maxima (ν_{obs}) versus solvent physical properties and solvent empirical parameters has shown that there is no meaningful correlation between solvent dielectric constant (ϵ) and solvent induced shifts.

The oscillator strengths have been found to be

generally low for the examined compounds in all the solvents. However, the electronic relaxation times calculated for each of the compounds give strong indication as to the likelihood of the band systems arising from mixed states. The relationship between relaxation times, τ , and solvent viscosities, η , allows the prediction of large changes in spherical symmetries of the two band systems (1L_a and 1L_b) in both 1-naphthylamine and 4-nitro-1-naphthylamine. A possible existence of free internal rotation in the excited states of these molecules, has thus been suggested.

The infrared spectra have been studied in the solid state and in solution and the vibrational frequencies assigned by making correlations with spectra of substituted benzene compounds and other related compounds. The substituent modes for each of the compounds have been discussed in detail.

ACKNOWLEDGEMENTS

To Professor J.A. Faniran and Dr. B.B. Adeleke, for providing enviable academic leadership;

To Head(s) of Department of Chemistry, for allowing me the use of research facilities at Ibadan;

To my brothers and sisters, for their genuine love, understanding, patience and financial support;

To Jummy;

To Government College, Ibadan Old Boys Association (1972-76 Class Set) for aiding me financially in a superb display of our high-quality human minds and a most beautiful demonstration of our spirit of magnanimity;


To all my numerous friends and admirers all over the world, for their confidence in my capabilities, for their fellowship and moral support;

To Mrs. A.M. Pettèrs, for typing the thesis wonderfully, and Mr. Olaoye for preparing the illustrations; and finally

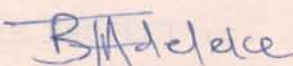
To God, for granting me life, boosted with enough courage to withstand most trying times and complete an almost impossible task.

CERTIFICATION

We certify that this work was carried out under our supervision by Mr. A.O. Adekunle in the Department of Chemistry, University of Ibadan, Nigeria.



J.A. Faniran
B.Sc.(Ibadan), Ph.D.
(Queens)
Professor of Chemistry
University of Ibadan



B.B. Adeleke
B.Sc.(Ibadan), Ph.D.
(Queens)
Reader in Chemistry
University of Ibadan

TABLE OF CONTENTS

	<u>Page</u>
TITLE	i
DEDICATION	ii
ABSTRACT	iii
ACKNOWLEDGEMENT	v
CERTIFICATION	vi
TABLE OF CONTENTS	vii
LIST OF FIGURES	x
LIST OF TABLES	xix
ABBREVIATIONS	xxix
CHAPTER 1: INTRODUCTION	1
1.1 GENERAL	1
1.2 MOLECULAR ORBITAL CALCULATIONS	17
1.3 SPECTRAL AND MOLECULAR PROPERTIES	23
1.4 AIMS AND OBJECTIVES OF PROJECT	38
CHAPTER 2: THEORETICAL BACKGROUNDS	40
2.1 MOLECULAR ORBITAL CALCULATIONS	40
2.1.1 Huckel Molecular Orbital Theory	40
2.1.2 The Omega (ω) Technique	49

	<u>Page</u>
2.1.3 Calculations Involving Heteroatoms ...	50
2.1.4 Bond Orders, Charge Distributions and Free Valence Index ...	51
2.1.5 Ionization Potentials ...	53
2.1.6 Dipole Moments ...	54
2.2 TRANSITION DIPOLE MOMENT ...	59
2.3 OSCILLATOR STRENGTH ...	62
2.4 RADIATIVE LIFE-TIME, τ , OF EXCITED STATE ...	63
2.5 SOLVENT EFFECTS ON ELECTRONIC SPECTRA ...	64
2.6 GROUP THEORETICAL ANALYSIS OF NAPHTHALENE AND ITS DERIVATIVES	66
CHAPTER 3: EXPERIMENTAL SECTION ...	72
3.1 REAGENTS AND SOLVENTS ...	72
3.1.1 Preparation and Purification of Reagents ...	72
3.1.2 Purification of Solvents	74
3.2 SPECTRAL MEASUREMENTS ...	78
3.2.1 Ultraviolet Spectra ...	78
3.2.2 Infrared Spectra ...	79
3.2.3 Physical Data on Reagents and Solvents ...	80

	<u>Page</u>
CHAPTER 4: RESULTS AND DISCUSSIONS ...	83
4.1 HUCKEL MOLECULAR ORBITAL CALCULATIONS ...	83
4.1.1 Molecular Orbital Energies	87
4.1.2 Charge Distributions and Bond Orders ...	101
4.2 THE ELECTRONIC SPECTRA ...	116
4.3 SOLVENT EFFECT ON ELECTRONIC SPECTRA ...	127
4.4 GROUND AND EXCITED STATE DIPOLE MOMENTS ...	151
4.5 OSCILLATOR STRENGTHS AND RADIATIVE LIFETIMES OF EXCITED STATES ...	170
4.6 INFRARED SPECTRA ...	180
CHAPTER 5: CONCLUSION ...	213
5.1 RECOMMENDATION FOR FURTHER WORK	
LIST OF REFERENCES ...	215

LIST OF FIGURES

Figure		Page
1	Positions in naphthalene ...	1
2	naphthalene molecule showing π - clouds above and below plane of rings ...	2
3	Resonance structures of naphthalene ...	3
4	Haworth synthetic pathways for naphthalene and derivatives ...	5
5	Synthesis of β -substituted naphthalenes from substituted benzenes ...	6
6	Introduction of alkyl (or aryl) substituents into α -position of naphthalene ...	6
7	1-nitronaphthalene ...	7
8	Halogéno-naphthalenes ...	7

Figure		Page
9	Preparation of α -substituted naphthalenes via 1-nitronaphthalene and 1-bromonaphthalene ...	7
10	Preparation of naphthalene sulfonic acids ...	8
11	The naphthols ...	8
12	The naphthylamines ...	9
13	Preparation of naphthols from naphthalene sulfonic acids ...	9
14	Preparation of naphthols from naphthylamines ...	9
15	Synthesis of β -substituted naphthalenes via diazonium salts	10
16	Products of further substitution in a mono substituted naphthalene	11
17	4-bromo-1-naphthylamine, 4-nitro-1-naphthylamine and 2-nitro-1-naphthol ...	69

Figure		Page
18	Atomic indices for substituted naphthalenes, substituted naphthols and substituted nitronaphthalenes	... 85
19	Molecular diagrams showing charge densities in brackets and π -bond orders along bonds for 1-mono substituted naphthalenes	... 102
20	Molecular diagrams showing charge densities in brackets and π -bond orders along bonds for 2-mono substituted naphthalenes	... 103
21	Molecular diagrams showing charge densities in brackets and π -bond orders along bonds for 2-substituted naphthols	... 104
22	Molecular diagrams showing charge densities in brackets and π -bond orders along bonds for 4-substituted naphthols	... 105

Figure		Page
23	Molecular diagrams showing charge densities in brackets and π -bond orders along bonds for 2-substituted nitronaphthalenes	106
24	Molecular diagrams showing charge densities in brackets and π -bond orders along bonds for 4-substituted nitronaphthalenes	107
25	The electronic absorption spectra of naphthalene in various solvents	128
26	The electronic absorption spectra of 1-naphthol in various solvents	129
27	The electronic absorptive spectra of 1-naphthylamine in various solvents	130
28	The electronic absorption spectra of 1-nitronaphthalene in various solvents	131
29	The electronic absorption spectra of 4-nitro-1-naphthylamine in various solvents ...	132

Figure		Page
30	The electronic absorption spectra of 4-bromo-1-naphthylamine in various solvents ...	133
31	Plots of ν_{\max} vs $\epsilon - 1/2 \epsilon + 1$ for a: 1-naphthol b: 4-nitro-1-naphthylamine c: naphthalene d: 1-naphthylamine e: 1-nitronaphthalene from different solvents.	146
32	Plots of ν_{\max} vs $n^2 - 1/n^2 + 2$ for a: 1-naphthol b: 4-nitro-1-naphthylamine c: naphthalene d: 1-naphthylamine e: 1-nitronaphthalene from different solvents.	147
33	Plots of ν_{\max} vs π^* for a: 1-naphthol b: 4-nitro-1-naphthylamine c: naphthalene d: 1-naphthylamine e: 1-nitronaphthalene from different solvents.	148

Figure		Page
34	Alternative π -charges in the ring of 1-methyl naphthalene ...	152
35	Valence structures of charge distribution in 1-naphthylamine and 1-naphthol ...	153
36	Plots of $\nu_{\max} ('L_b)$ vs $2(D-1)/(2D+1)$ for a: 1-naphthol b: 4-nitro-1-naphthylamine c: naphthalene d: 1-naphthylamine e: 1-nitronaphthalene f: 4-bromo-1-naphthylamine from different solvents.	158
37	Plots of $\nu_{\max} ('L_a)$ vs $2(D-1)/(2D+1)$ for a: 1-naphthol b: 4-nitro-1-naphthylamine c: naphthalene d: 1-naphthylamine e: 1-nitronaphthalene f: 4-bromo-1-naphthylamine from different solvents.	159

Figure		Page
38	A plot of X vs Y in Rao's method of estimating excited state dipole moment of the $'L_b$ band in naphthalene ...	163
39	A plot of X vs Y in Rao's method of estimating excited state dipole moment of the $'L_b$ band in 1-naphthylamine ...	164
40	A plot of X vs Y in Rao's method of estimating excited state dipole moment of the $'L_b$ band in 1-naphthol	165
41	A plot of X vs Y in Rao's method of estimating excited state dipole moment of the $'L_b$ band in 1-nitronaphthalene ...	166
42	A plot of X vs Y in Rao's method of estimating excited state dipole moment of the $'L_b$ band in 4-nitro-1-naphthylamine ...	167
43	A plot of X vs Y in Rao's method of estimating excited state dipole	

Figure		Page
	moment of the $'L_b$ band in 4-bromo-1-naphthylamine ...	168
44	A plot of log of relaxation times, τ , vs log of solvent viscosities η , for the absorption band systems of naphthalene ...	175
45	A plot of log of relaxation times, τ , vs log of solvent viscosities η , for the absorption band systems of 1-naphthol ...	176
46	A plot of log of relaxation times, τ , vs log of solvent viscosities η , for the absorption band systems of 1-naphthylamine ...	177
47	A plot of log of relaxation times, τ , vs log of solvent viscosities η , for the absorption band system of 1-nitronaphthalene ...	178
48	A plot of log of relaxation times, τ , vs log of solvent viscosities η , for the absorption band systems of 4-nitro-1-naphthylamine ...	179

Figure		Page
49	Infrared spectra of naphthalene (a) as solid in KBr; (b) as solution in CCl_4 ...	182
50	Infrared spectra of 1-naphthol (a) as solid in KBr; (b) as solution in CCl_4 ...	184
51	Infrared spectra of 1-naphthylamine (a) as solid in KBr; (b) as solution in CCl_4 ...	186
52	Infrared spectra of 1-nitro naphthalene (a) as solid in KBr; (b) as solution in CCl_4 ...	188
53	Infrared spectra of 4-nitro-1- naphthylamine (a) as solid in KBr; (b) as solution in CCl_4	190
54	Infrared spectra of 2-nitro-1- naphthol (a) as solid in KBr; ...	192
55	Infrared spectra of 4-bromo-1- naphthylamine as solid in KBr ...	193

LIST OF TABLES

<u>Table</u>		<u>Page</u>
1	Symmetry types and characters of naphthalene of D_{2h} point group ...	67
2	Selection rules for D_{2h} structure of naphthalene ...	68
3	Symmetry types and characters of C_s point group ...	70
4(a)	Physical data on reagents. ...	81
(b)	Physical data on solvents ...	82
5	Bond lengths and bond moments used in HMO calculations ...	84
6	Number of electrons contributed per substituent group ...	86
7	Energies of the occupied and lowest unoccupied molecular orbitals (E_1 , E_2 , ...) in β units for 1-monosubstituted naphthalenes ...	88
8	Energies of the occupied and lowest unoccupied molecular orbitals (E_1 , E_2 , ...) in β units for 2-monosubstituted naphthalenes ...	89

<u>Table</u>	<u>Page</u>
9	Energies of the occupied and lowest unoccupied molecular orbitals (E_1 , E_2, \dots) in β units for 2-substituted naphthols ... 90
10	Energies of the occupied and lowest unoccupied molecular orbitals (E_1 , E_2, \dots) in β units for 4-substituted naphthols ... 91
11	Energies of the occupied and lowest unoccupied molecular orbitals (E_1 , E_2, \dots) in β units for 2-substituted nitronaphthalene ... 92
12	Energies of the occupied and lowest unoccupied molecular orbitals (E_1 , E_2, \dots) in β units for 4-substituted nitronaphthalenes ... 93
13	Total energies (E_π), delocalization energies (DE_π), bonding energies per electron (BEPE) and delocalization energies per electron (DEPE) in β units for 1-monosubstituted naphthalenes ... 94

<u>Table</u>		<u>Page</u>
14	Total energies (E_{λ}), delocalization energies (DE_{λ}), bonding energies per electron (BEPE) and delocalization energies per electron DEPE in β units for 2-monosubstituted naphthalenes	95.
15	Total energies (E_{λ}), delocalization energy (DE_{λ}), bonding energies per electron (BEPE) and delocalization energies per electron (DEPE) in β units for 2-substituted naphthols	96
16	Total energies (E_{λ}), delocalization energies (DE_{λ}), bonding energies per electron (BEPE) and delocalization energies per electron (DEPE) in β units for 4-substituted naphthols	97
17	Total energies (E_{λ}), delocalization energies (DE_{λ}), bonding energies per electron (BEPE) and delocalization energies per electron (DEPE) in β units for 2-substituted nitro-naphthalenes ...	98

<u>Table</u>	<u>Page</u>
18	Total energies (E_{λ}), delocalization energies (DE_{λ}), bonding energies per electron (BEPE) and delocalization energies per electron (DEPE) in β units for 4-substituted nitro-naphthalene.. 99
19	Correlation of substituents with Hammetts constant ... 108
20	Charge distributions for some 1- and 2-monosubstituted naphthalenes 109
21	$\bar{\lambda}$ -Bond orders for some 1- and 2-monosubstituted naphthalenes ... 110a
22	$\bar{\lambda}$ -Bond orders for some 2- and 4-substituted nitronaphthalenes ... 112
23	$\bar{\lambda}$ -Bond orders for some 2- and 4-substituted naphthols ... 114
24	HMO calculated transition frequencies in nm, ν and oscillator strengths for 1-mono substituted naphthalenes 118

<u>Table</u>	<u>Page</u>
25 HMO calculated transition frequencies in nm, and oscillator strengths for 2-monosubstituted naphthalenes	119
26 HMO calculated transition frequencies in nm, and oscillator strengths for 2-substituted naphthols ...	120
27 HMO calculated transitions frequencies in nm, and oscillator strengths for 4-substituted naphthols ...	121
28 HMO calculated transition frequencies in nm, and oscillator strengths for 2-substituted nitronaphthalenes	122
29 HMO calculated transition frequencies in nm, and oscillator strengths for 4-substituted nitronaphthalenes	123
30 Electronic absorption spectra of substituted naphthalenes in various solvents ...	134
31 Calculated oscillator strengths (f), half-bandwidths ($\nu_{1/2}$), dipole moments (D) in various solvents for naphthalene ...	137

<u>Table</u>	<u>Page</u>
32	Calculated oscillator strengths (f), half-bandwidths ($\nu_{1/2}$), dipole moments (D) in various solvents for 1- naphthol 138
33	Calculated oscillator strengths (f), half-band widths ($\nu_{1/2}$), dipole moments (D) in various solvents for 1-naphthylamine 139
34	Calculated oscillator strengths (f), half-bandwidths ($\nu_{1/2}$), dipole moments (D) in various solvents for 1- nitronaphthalene 140
35	Calculated oscillator strengths (f), half-bandwidths ($\nu_{1/2}$), dipole moments (D) in various solvents for 4-bromo- 1-naphthylamine 141
36	Calculated oscillator strengths (f), half-bandwidths ($\nu_{1/2}$), dipole moments (D) in various solvents for 4-nitro- 1-naphthylamine 142

TablePage

37	Linear regression parameters obtained from plots of the 1L_b band maxima (ν_{obs}) vs solvent physical properties and solvent empirical parameters for: (a) Naphthalene (b) 1-naphthol (c) 1-naphthylamine (d) 1-nitronaphthalene (e) 4-nitro-1-naphthylamine (f) 4-bromo-1-naphthylamine	144
38	Calculated ground state dipole moments compared with experimental values for 1- and 2-monosubstituted naphthalenes in Debyes.	155
39	Calculated ground state dipole moments compared with experimental values for 2- and 4-substituted nitronaphthalenes in Debyes.	156
40	Calculated ground state dipole moments compared with experimental values for 2- and 4-substituted naphthols in Debyes.	157

<u>Table</u>	<u>Page</u>	
41	Molecular volumes, dipole moments in the ground and excited states estimated by McRae's method for ' L_a ' and ' L_b ' bands	161
42	Molecular volumes, dipole moments in the ground and excited states estimated by Rao's method for ' L_b ' band	162
43	Relaxation times, $\tau(\nu)$, of naphthalene in various solvents	172
44	Relaxation times, $\tau(\nu)$, of 1-naphthol in various solvents	172
45	Relaxation times, $\tau(\nu)$, of 1-naphthylamine in various solvents	173
46	Relaxation times, $\tau(\nu)$, of 1-nitronaphthalene in various solvents	173
47	Relaxation times, $\tau(\nu)$, of 4-bromo-1-naphthylamine in various solvents	174
48	Relaxation times, $\tau(\nu)$, of 4-nitro-1-naphthylamine in various solvents	174

<u>Table</u>		<u>Page</u>
49	Assignment of observed infra-red frequencies (cm^{-1}) of naphthalene for (a) solid spectra (b) solution spectra.	194
50	Assignment of observed infra-red frequencies (cm^{-1}) of 1-naphthol for (a) solid spectra (b) solution spectra.	196
51	Assignment of observed infra-red frequencies (cm^{-1}) of 1-naphthylamine for (a) solid spectra (b) solution spectra.	198
52	Assignment of observed infra-red frequencies (cm^{-1}) of 1-nitronaphthalene for (a) solid spectra (b) solution spectra.	200
53	Assignment of observed infra-red frequencies (cm^{-1}) of 4-nitro-1-naphthylamine for (a) solid spectra (b) solution spectra.	202

<u>Table</u>		<u>Page</u>
54	Assignment of observed infra-red frequencies (cm^{-1}) of 2-nitro-1-naphthol (solid spectra).	204
55	Assignment of observed infra-red frequencies (cm^{-1}) of 4-bromo-1-naphthalene (solid spectra).	206

UNIVERSITY OF IBADAN LIBRARY

ABBREVIATIONS

i.r	-	infra-red
kBr	-	potassium bromide
e.s.r	-	electron spin resonance
K	-	Kelvin
n.m.r	-	nuclear magnetic resonance
MINDO	-	Modified-Intermediate-Neglect-of-Differential-Overlap
MO	-	molecular orbital
PRDDO	-	partial retention of diatomic differential overlap
LCAO	-	linear combination of atomic orbitals
C.I	-	Configuration Interaction
ρ	-	Hammett substituent constant
π	-	pi
n	-	refractive index
HMO	-	Huckel Molecular Orbital
ω	-	Omega
ρ	-	charge density
μ	-	dipole moment
M	-	transition dipole moment
f	-	oscillator strength
τ	-	radiative lifetime of excited state.

CHAPTER 1

INTRODUCTION

1.1 GENERAL

Naphthalene belongs to a class of organic compounds called aromatics [1]. This class is characterized by having carbon atoms in six-membered rings, each atom of the ring being bonded to only one atom outside the ring. Naphthalene is the simplest and most important of fused-ring aromatic hydrocarbons.

Naphthalene, $C_{10}H_8$ is a colourless solid with melting point $80.3^{\circ}C$. It is insoluble in water but soluble in alcohol and has a characteristic odour. It can be obtained from coal-tar.

The positions in the naphthalene ring system are designated as in Figure 1. Any two isomeric monosubstituted naphthalenes are differentiated by the prefixes 1- and 2- or α - and β -.

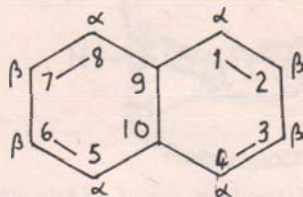


Figure 1; Positions in naphthalene.

The simplest electronic structure which can be drawn for $C_{10}H_8$ is that in which each carbon atom shares four electron pairs with other atoms, having alternating single and double bonds. A high degree of unsaturation is expected for this structure, but naphthalene is known to be resistant to the addition reactions characteristic of unsaturated compounds. The typical reactions are electrophilic substitution reactions in which hydrogen is displaced as hydrogen ion and the naphthalene ring system preserved. From the experimental standpoint, naphthalene is classified as aromatic on the basis of its properties. Also, from a theoretical standpoint, naphthalene has the structure required of an aromatic compound, containing flat six-membered rings. A consideration of the atomic orbitals shows that the structure can provide π -clouds containing six electrons per ring (Figure 2).

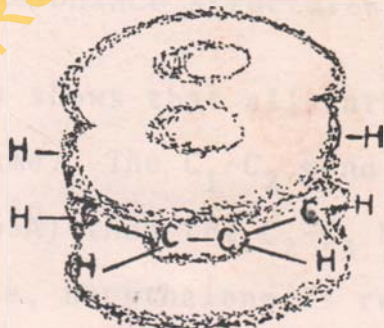


Fig. 2: Naphthalene molecule showing π -clouds above and below plane of rings

The ten carbon atoms lie at the corners of two fused hexagons. Each carbon is attached to three other atoms by σ -bonds. Since these σ -bonds result from the overlap of trigonal sp^2 orbitals all carbon and hydrogen atoms lie in a single plane. Above and below this plane, there is a cloud of π -electrons formed by the overlap of p-orbitals.

In terms of valence bond, naphthalene is considered to be a resonance hybrid of structures I, II and III (Figure 3), its resonance energy, shown by heat of combustion to be

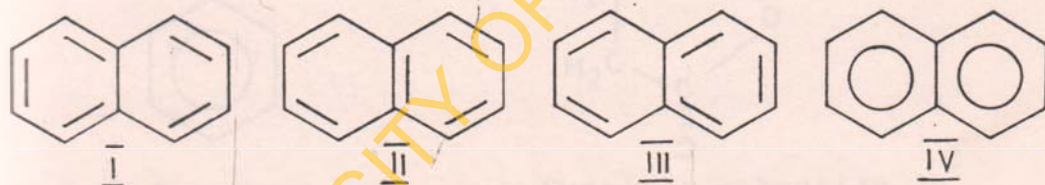


Figure 3: Resonance structures of naphthalene

X-ray analysis shows that all carbon-carbon bonds are not the same. The C_1-C_2 bond is considerably shorter (1.365\AA) than the C_2-C_3 bond (1.404\AA), but for convenience, naphthalene is represented as the single structure IV (Figure 3).

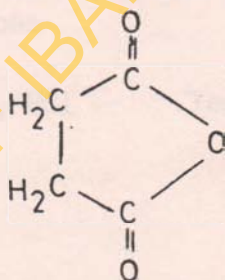
Naphthalene typically undergoes electrophilic

substitution, an electrophilic reagent finding the π -cloud as a source of available electrons, attaching itself to the ring to form an intermediate carbonium ion. The carbonium ion then gives up a proton to restore the stable aromatic system. Therefore, naphthalene is capable of undergoing oxidation or reduction, nitration, halogenation, sulfonation and Friedel-Crafts acylation reactions.

The Haworth synthesis, Figure 4 is one of the methods that can be used to make certain other naphthalene derivatives.



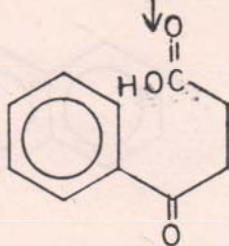
Benzene



Succinic anhydride

 AlCl_3

Friedel-Crafts acylation

 β -Benzoylpropionic acid

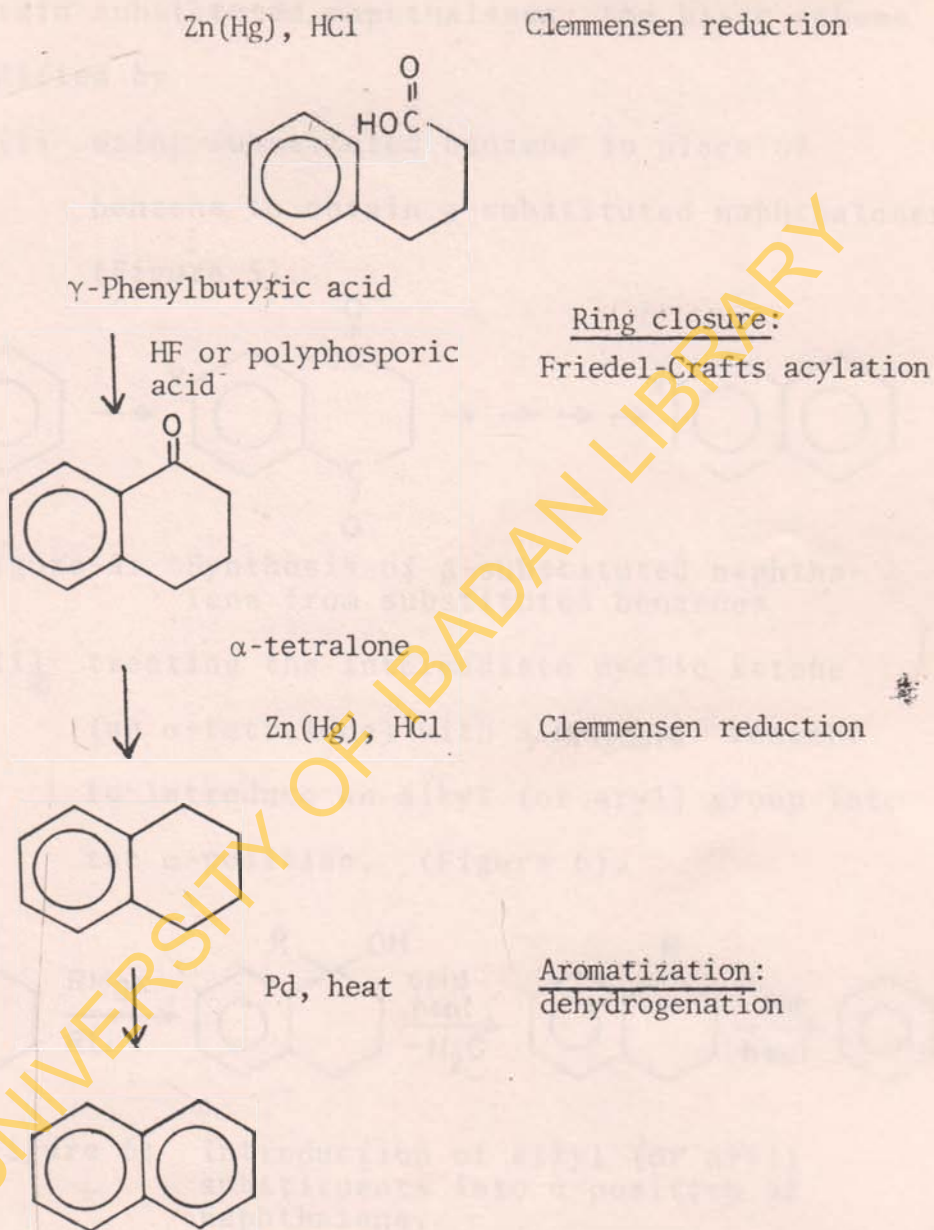


Figure 4: Haworth synthetic pathways for naphthalene and derivatives.

To obtain substituted naphthalenes, the basic scheme is modified by

- (i) using substituted benzene in place of benzene to obtain β -substituted naphthalenes (Figure 5).

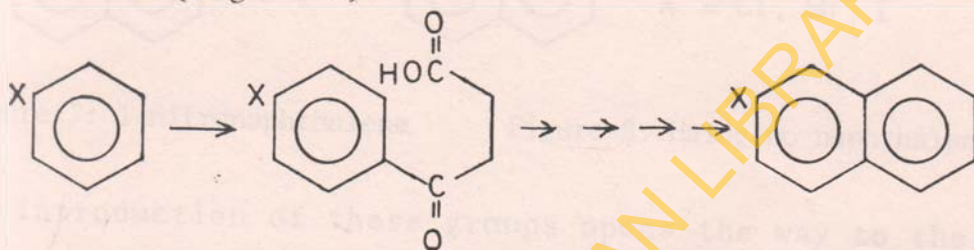


Figure 5: Synthesis of β -substituted naphthalene from substituted benzenes

- (ii) treating the intermediate cyclic ketone (an α -tetralone) with a Grignard reagent to introduce an alkyl (or aryl) group into the α -position. (Figure 6).

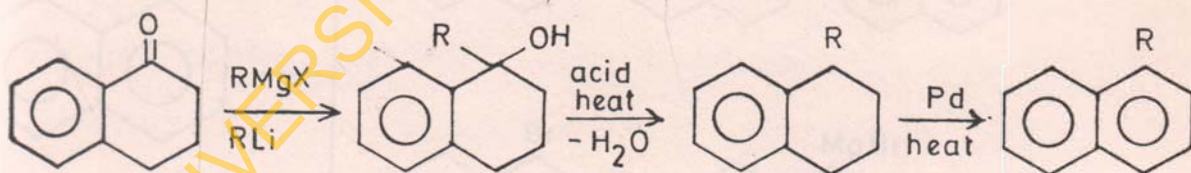
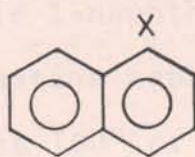
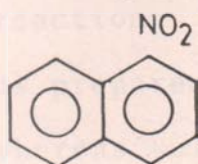


Figure 6: Introduction of alkyl (or aryl) substituents into α -position of naphthalene.

Nitration and halogenation of naphthalene take place almost exclusively in the 1-position, thus

1-Nitronaphthalene (Figure 7) and 1-halogeno naphthalene (Figure 8) are prepared by nitration and halogenation of naphthalene.



X = Cl, Br, I

Figure 7: 1-nitronaphthalene

Figure 8: Halogeno-naphthalene

The introduction of these groups opens the way to the preparation of a series of α -substituted naphthalenes, from 1-Nitronaphthalene via the amine and diazonium salts and from 1-bromonaphthalene via the Grignard reagent.

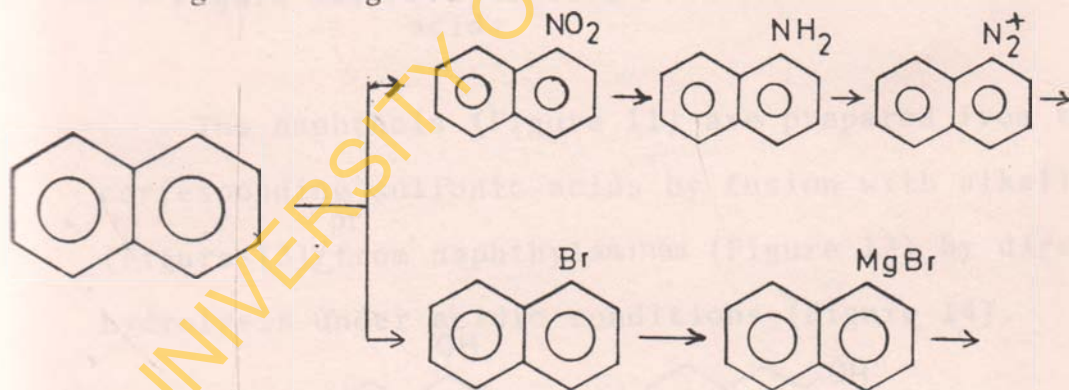


Figure 9: Preparation of α -substituted naphthalenes via 1-nitronaphthalene and 1-bromonaphthalene.

The orientation of substitution in sulfonation and Friedel-Crafts acylation is determined by the particular solvent used and the temperature of reaction. For example 1-naphthalene sulfonic acid is prepared by sulfonating naphthalene at 80°C whereas sulfonation at 160° or higher yields directly 2-naphthalene sulfonic acid (Figure 10).

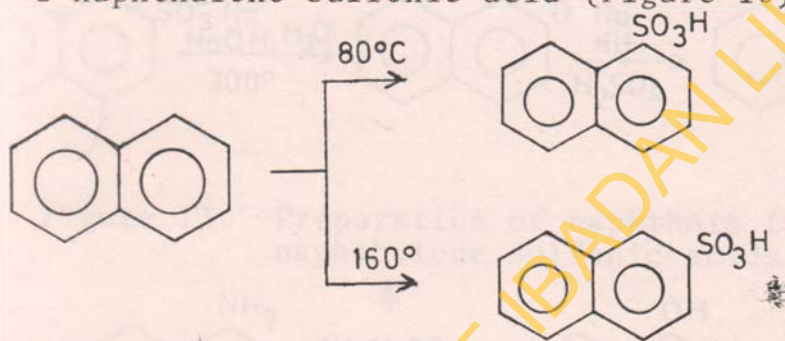


Figure 10: Preparation of naphthalene sulfonic acid.

The naphthols (Figure 11) are prepared from the corresponding sulfonic acids by fusion with alkali (Figure 13) or from naphthylamines (Figure 12) by direct hydrolysis under acidic conditions (Figure 14).

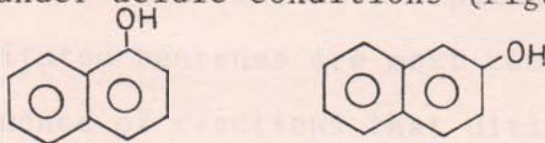


Figure 11: The naphthols.

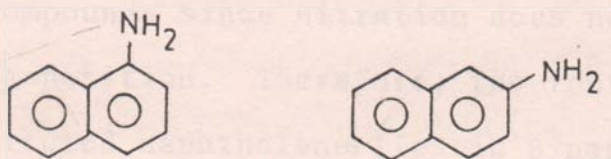


Figure 12: The naphthylamines.

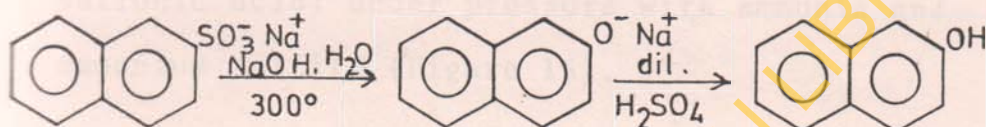


Figure 13: Preparation of naphthols from naphthalene sulfonic acids.

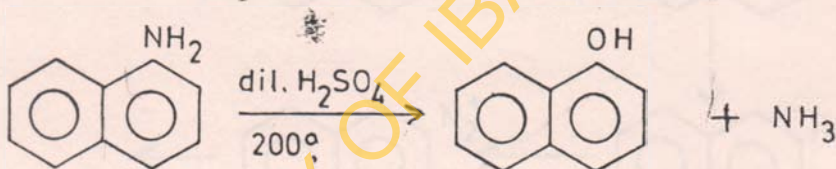


Figure 14: Preparation of naphthols from naphthylamines.

In general, the α -substituted naphthalenes, like the substituted benzenes are most commonly prepared by a sequence of reactions that ultimately goes back to a 1-nitro compound. The preparation of β -substituted naphthalenes cannot start with the

nitro compounds since nitration does not take place in the β -position. Therefore, the route to several β -substituted naphthalenes lies in β -naphthylamine and the versatile diazonium salts. β -naphthylamine is made by heating β -naphthol (obtained from the β -sulfonic acid) under pressure with ammonia and ammonium sulfite (Figure 15).

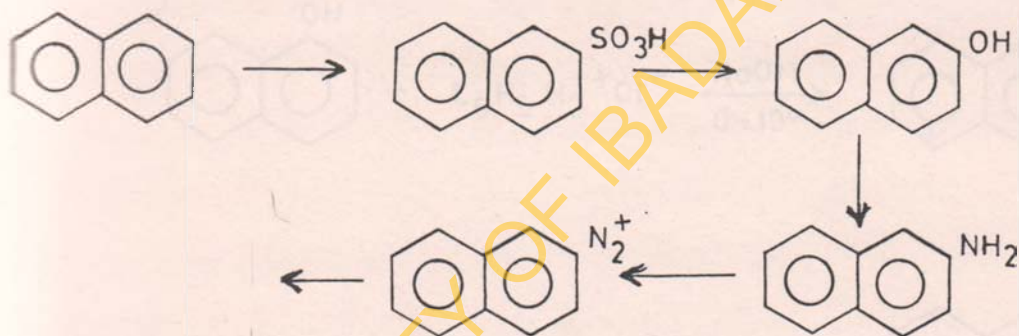


Figure 15: Synthesis of β -substituted naphthalenes via diazonium salts.

The major products of further substitution in a monosubstituted naphthalene are predicted by the following rules:

- (1) An activating group (electron-releasing) tends to direct further substitution into the same

ring. Thus, an activating group in position 1 directs further substitution to position 4 and to a lesser extent, to position 2, while an activating group in position 2 directs further substitution to position 1. (Figure 16).

- (2) A deactivating group (electron-withdrawing) tends to direct further substitution into the other ring (Figure 16).

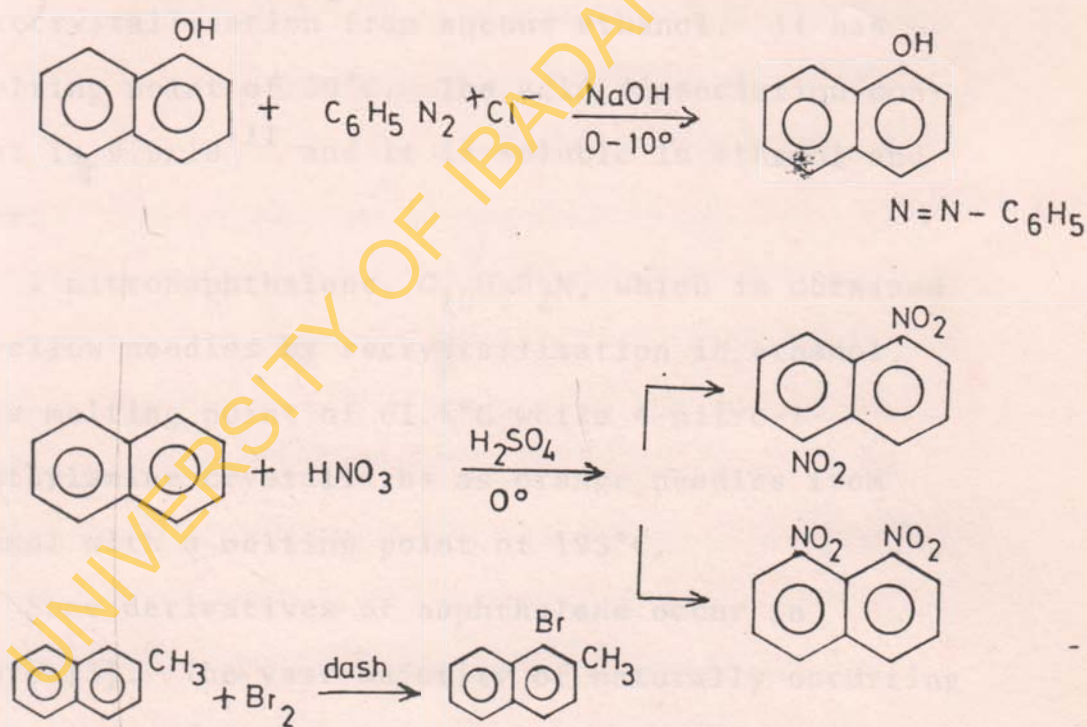


Figure 16: Products of further substitution in a monosubstituted naphthalene.

The rules do not always hold in sulfonation, because the reaction is reversible and at high temperature tends to take place at β -position.

1-naphthol, $C_{10}H_8O$ has a melting point of $94^\circ C$ and acid dissociation constant of 2.5×10^{-10} at $25^\circ C$ [2]. It is soluble in ethanol, ether, chloroform, benzene and water.

1-naphthylamine, $C_{10}H_9N$ is obtained as needles on recrystallization from aqueous ethanol. It has a melting point of $50^\circ C$. The acid dissociation constant is 9.9×10^{-11} and it is soluble in ethanol and ether.

1-nitronaphthalene, $C_{10}H_7O_2N$, which is obtained as yellow needles by recrystallization in ethanol, has a melting point of $61.5^\circ C$ while 4-nitro-1-naphthylamine crystallizes as orange needles from ethanol with a melting point of $195^\circ C$.

Some derivatives of naphthalene occur in nature [3]. The vast majority of naturally occurring derivatives of naphthalene are the quinones. The others are mainly related naphthols or naphthyl ethers. An increasing number of O-naphthoquinone, (mainly of

terpenoid origin), and binaphthaquinones have been found in recent years. For example, during a search for new antibiotics, several Marasmius spp were found to produce antibacterial substances [4]. One of the metabolites 6-methyl-1, 4 naphthoquinone was confirmed by direct comparison with a synthetic specimen prepared by Diels-Alder addition of isoprene to benzoquinone.

Other examples of naturally occurring quinones are Lawsone [5] and Juglone [6]. Lawsone is the dyeing principle of the ancient colouring matter, "henna", prepared from the leaves of Lawsonia alba which is cultivated in Africa and India for medicinal and dyeing purposes. Juglone is isolated from green walnut shells of Juglan regia. It is an effective sternutator like many other quinones and has weak fungicidal and bactericidal properties. As a toxic principle, it is used in activities ranging from catching of fish to the treatment of ringworm.

Microorganisms are known for their ability to break down to utilize aromatic compounds as a source of energy and of carbon. Many common soil bacteria

and fungi possess this ability to degrade aromatic compounds as an aspect of metabolism which is of considerable significance in the carbon cycle [7]. Thus, the biodegradation of naphthalene and its derivatives has been a subject of great interest. It is now known that the bacteria which are capable of degrading naphthalene and some of its derivatives do so by a stepwise process in which ring-fusion of one of the rings is followed by conversion to a phenol such as catechol or salicylic acid.

Dihydroarenediols, such as *trans*-1,2 dihydro-1, 2-dihydronaphthalene isolated from cultures of *Pseudomas nocardia* and other species grown on naphthalene have also been considered to be the compounds initially formed in this process [8,9]. Sequential induction experiments have also indicated that the oxidation product of the dihydroarenediol obtained from naphthalene is 1,2-dihydroxynaphthalene [10].

The degradation of the methylnaphthalene and 1-chloro- and 1-bromo naphthalene have been investigated [11,12]. Their oxidation appears to be similar to that of naphthalene; dihydroarenediol and substituted

salicyclic acids having been identified as intermediates.

It is not known yet, to what extent fungi can utilize naphthalene and its derivatives. Byrde et al [13], in a study of the metabolism of ω -(2-naphthyloxy)-n-alkyl carboxylic acids have found that Aspergillus niger is capable of hydroxylating these compounds in the 6-position and also of reducing the length of the alkyl side-chain by β -oxidation. In a subsequent investigation by Byrde et al [14] of Aspergillus niger, it has been shown that the substituted ring of 2-methoxynaphthalene is cleaved open and 4-methoxysalicyclic acid was identified as the only metabolic product.

The bioactivity and toxicology of naphthalene and its derivatives, as a subject, is of some interest. The ingestion of a toxic dose of naphthalene is known to cause gastro-enteric distress, tremors, convulsions, fever, changes in the formed elements of the blood and death from respiratory failures [15]. Naphthalene is also metabolized to α - and β -naphthols which, as hemolytic agents, are capable of producing

severe systemic intoxications such as kidney injury, jaundice, haemoglobinuria anemia, convulsions and coma. This type of haemolysis, because of a specific metabolic deficiency in glucose-6-phosphate dehydrogenase (G-6-PD) activity of the red blood cells is more frequent in black peoples than whites.

Although no human toxicity data are available, an oral administration of β -nitronaphthalene in rabbits induces degenerative and neurotic lesions in the brain, liver and kidneys [15]. Also, chronic intoxication of dinitronaphthalene is known to cause severe alterations of the liver, kidney, myocardium and brain tissues [16].

1-naphthalene sulfonic acid has been examined for potency and considered active as in-vitro inhibitors of the deamination of biogenic amine substrates by rat brain monoamine oxidase (MAO) [17]. Also, several commercial polychlorinated naphthalenes, including halowaxes have been found useful as hepatic microsomal enzyme inducers in the immature male rat [15]. An environmental pollution with a number of these polychlorinated naphthalenes are known to affect the sperm

density distributions of human males and make the distribution similar to those of prevasectomy patients [18].

A few of these derivatives of naphthalene also have serious applications in chemistry. The naphthalene anion is the first radical for which proton hyperfine splitting was observed in solution. This anion, in dimethylethoxide (DME) is used as a secondary standard in absolute determination of g-factors of other paramagnetic species [19]. Also, one important analytical usefulness of 2-nitroso-1-naphthol is as reagent for the determination of trace amounts of cobalt by the graphite furnace atomic absorption spectrometry [20].

Malignancies in man have been reported in several places, after only a few weeks of exposure to 2-naphthylamine [15].

1.2 MOLECULAR ORBITAL CALCULATIONS

The interaction of a substituent with an aromatic ring has been of great importance in determining the structures, stabilities and other properties of

many organic molecules. The earliest theoretical workers [21] on the subject were mainly concerned with π -interaction between the substituent and the aromatic system. Thus, one of the theoretical backgrounds recognized as providing very useful theoretical information in the prediction of various ground state properties of conjugated molecules and their derivatives is known as the Huckel Molecular Orbital (HMO) Theory [22].

Several workers have done molecular calculations of the naphthalene ring based on other theoretical backgrounds aside from the HMO. For examples, Dewar et al [23], using the SIMPLEX minimization algorithm have carried out detailed Modified-Intermediate-Neglect-of-Differential-Overlap (MINDO/2) calculations of naphthalene and found results to agree well with various π -approximations. There was the Self-Consistent-Field-Molecular-Orbital-Configuration Interaction (SCF-CI) calculations based on the Pariser-Parr-Pople method of the triplet-triplet transitions of benzene and naphthalene [24]. Geometries of conjugated hydrocarbons have been

calculated on a model based on the one-dimensional gas theory which seeks to improve the π -electron wavefunctions of conjugated molecules by taking changes of bondlength differences into account [25]. Also, the electron repulsion integrals and σ - π separation factor proposed by Tinland and Jaffe has been used in a Complete-Neglect-of-Differential-Overlap (CNDO/2) calculations of orbital energies of naphthalene [26,27]. The ionization potentials, electron affinities and equilibrium bondlengths calculated for naphthalene by Caldwell's systematic approximation to the Pople method [28] have led the Pople method to a form of Huckel theory which is self-consistent with respect to charges and bond orders.

However, fewer attempts [29-37] have been made to treat the electronic spectra and other properties of substituted aromatic compounds by molecular orbital theories. Kichisuke Nishimoto et al [30], applying an HMO treatment have been able to differentiate between the spectra of α - and β -naphthol. They have pointed out that in an aromatic derivative, the

peculiar degeneracy of the two excited configurations χ'_{1-2} and χ'_{2-1} of the parent hydrocarbon is removed by the perturbation of the substituent, and furthermore, that this perturbation leads to an interaction between all configurations. However, in α -substituted hydrocarbons with an auxochromic substituent in the α -position such as α -naphthol, χ'_{1-2} strongly interacts with χ'_{2-1} , but only slightly with χ'_{1-1} , so that the nature of the π - π^* absorption is practically the same as that of the parent hydrocarbon. In attempts to explain the electronic spectra of the β -derivatives, it was found that the common characteristics of the parent hydrocarbon were completely lost because all of the lower excited configurations interact strongly with each other and therefore it was necessary to consider the interaction among all configurations.

Leslie Forster and Kichisuke Nishimoto [31] using the Self-Consistent-Field (SCF) variant of the P.P.P. method have computed transition energies, intensities and charge distributions in the ground and excited states of α - and β -naphthol. The results

obtained have compared well with results from similar calculations by ASMO-CI method [32], the other commonly employed procedure which has been used for naphthalene and naphthols.

In trying to see whether it would be possible to interpret the electronic spectra of aromatic molecules containing polar substituents without configuration interaction, Bloor [33] has extended a model (previously used for substituted benzenes) to the interpretation of the K-band spectra of naphthalene substituted in the 4-position by the nitro, the cyano, the acetyl, the formyl groups and also by the electron-donating amino, methoxyl, bromo, chloro and iodo groups. Such interpretation of the K-band spectra has been found to be similar to the qualitative theory of Burawoy [34], which assumes that electron transfer in the ground state occurs by an inductive mechanism. However, the agreement between experiment and theory was found to be poor, since the theory predicted for substitution in 2-position, a bigger bathochromic shift of the K-band than substitution in the 1-position of naphthalene, whereas

the opposite should be true for both electron-attracting and electron-donating substituents. However, it is known that some other sophisticated calculations also overestimate the effect of substituents in the 2-position of naphthalene [35].

Ridley and Zeiner [36] have made observations of many interesting ambiguities and uncertainties in the experimental spectra of the azanaphthalenes. These observations have led them to employ a MINDO technique to calculate the electronic spectra of naphthalene and some mono-, di- and tetra-azanaphthalenes. The computer programme performed the LCAO-MO-SCF calculations from an input molecular geometry and atomic numbers in which a ground state calculation followed by configuration interaction calculation resulted in the desired spectroscopic transition energies and oscillator strengths.

To elucidate the molecular properties of naphthalene derivatives with auxochromic substituents such as methoxy, amino, halogen, etc. Kichisuke Noshimoto and Ryoichi Fujishiro [37] have studied the electronic structures of naphthalenediols, pointing

out that molecular properties such as charge distribution and electronic spectra, depend remarkably upon the type of substitution. It was also suggested that the 9-10 bond in naphthalene could play an important role in the conjugation interaction between the ring and the substituent.

1.3 SPECTRAL AND MOLECULAR PROPERTIES

Naphthalene is one of the few molecules for which near ultra-violet (uv) spectrum is fairly understood. The spectrum shows two band systems, a very weak one (system A) and the second one (B) which is much stronger. A careful vibrational analysis and polarization results on naphthalene in durene crystal have shown [38,39] that the small fraction of the absorption of system A, which is due to the pure electronic transition, is polarized along the long axis of the molecule (x-axis) ${}^1B_{3u} \leftarrow {}^1A_g^-$ while system B was found to be polarized along the short molecular axis (y-axis) ${}^1B_{2u}^+ \leftarrow {}^1A_g^-$ [40]. To examine the extent of coupling between these two transitions El Sayed [41] had used the

molecule isoquinoline (a β -azanaphthalene) to study the substitutional and solvent perturbation of the coupling between these two lowest electronic transition states in naphthalene. The experimental results obtained indicated that the originally very weak system A must be stealing its intensity under perturbation mainly from the originally perpendicular polarized B system and not from the similarly polarized higher energy system ${}^1B_{3u} + {}^1A_g^-$.

The effect of hydrogen bonding on near uv absorption spectra of α - and β -naphthol, which were used as the proton donors, had been studied by Nagakura and Gouterman [42]. The L_a and L_b bands were found to decrease gradually with the increasing concentration of the proton acceptor while new bands appeared on the longer wavelength sides of original bands.

Noboru Mataga [43], while studying solvent effects on the absorption and fluorescence spectra of naphthylamines had been able to demonstrate remarkable difference between the conjugation power of the hydroxy- and amino-groups on naphthalene. In

further consideration of the importance of these hydroxy- and amino-derivatives of benzenoid hydrocarbons, Tichy et al [44] have measured the electronic spectra of monoamino- and monohydroxy-derivatives of naphthalene in 50% aqueous methanol and also in alkaline 50% aqueous methanol. Several first bands of the absorption curves ($S_0 \rightarrow S_x$ transitions) were interpreted by means of the unmodified method of Pariser-Parr and Pople using the Mataga-Nishimoto approximation for the electron repulsion integrals.

The electronic-vibrational spectra of 1- and 2-monosubstituted naphthalene derivatives have been examined and the absorption curves for the most varied [45] $C_{10}H_7X$ ($X =$ substituent) derivatives found to be completely similar to that of naphthalene with respect to the number and characteristics of the bands and other responses to various perturbations of the molecules. The differences in the effect of X in positions 1 and 2 have also been explained by the fact that electrons could be displaced in two principal directions, transverse and longitudinal on excitation in the naphthalene molecule. Again, the

specific effects of introducing a conjugatable substituent at position 1 and position 2 on the ultraviolet absorption spectrum of naphthalene have been shown in the spectra of naphthylamines and naphthoic acids [46], and the localized region of the absorption spectrum related to the direction of polarization of the associated processes of electronic excitation.

The uv spectra of naphthalene, mono-, di- and tri-hydroxy naphthalenes have been recorded in ethanol and acid ethanol [47]. For the monohydroxy-naphthalenes, the distinctions between the 1- and 2-derivatives in neutral and acid solutions were again observed in alkaline solution, and although there was a bathochromic shift and a general smoothing of the curve, the characteristic three peaks of naphthalene were retained in 2-naphthol, whereas only two peaks were present in the 1-derivative. The introduction of the second hydroxyl group into the corresponding position in the unattached ring as the first, as in 1,5 naphthalenediol was found to have little effect upon the wavelength of absorption,

whereas in 1,4 naphthalenediol an entirely different absorption curve was obtained. The apparent difference in the polarizations of the molecule responsible for the curves in 1,4 and 1,5 diols was therefore believed to depend largely upon the suppression of the ionization of the two opposed hydroxyls in the same ring of the 1,4 diol.

The excited electronic states and polarization of electron transitions in molecules of 1,2 disubstituted naphthalenes containing donor and acceptor groups had been studied and their similarity to spectra of 1- and 2-monosubstituted naphthalenes established [48]. A connection between certain electronic transitions in molecules of 1,2 disubstituted naphthalenes with the corresponding transitions in molecules of monosubstituted ones and through them with transitions into $'L_a$, $'L_b$ or $'B_b$ excited states of a non-substituted molecule has been traced.

Milea [49], in studies of the uv spectra of monosubstituted naphthalenes in various solvents has found a linear relationship between the characteristic

band at $31,000 \text{ cm}^{-1}$ and the function $[f(n^2-1)/2n^2+1]$ where n = refractive index of solvent. The f/ν^3 ratio, where f = oscillator strength in the absorption band, ν = wavenumber and a = the radius of the supposed spherical cavity in which the solvated molecule is located, was approximately constant while the interaction of all the mono-substituted naphthalenes with the given solvent was nearly the same.

In a study of heavy-atom effects on the triplet lifetimes of naphthalene, the decrease in the lifetime with substitution for some mono- and polyhalo naphthalenes, have been found to vary with the square of the atomic spin-orbit coupling factor for the attached halogen and the position dependence qualitatively related to the unpaired spin-density distribution in the molecule [50]. Also, to understand the forbidden character in allowed electronic transitions of mono halo naphthalenes, Singh et al [51] have analyzed the singlet-singlet absorption and emission spectra of α -fluoro- and the absorption spectra of α -chloro-, α -iodo- and α -bromonaphthalenes.

They have also interpreted the appearance of strong vibronic and weak electronic bands in the longer wavelength system of α -chloro- and α -iodo-naphthalenes as the interaction of totally symmetrical vibrations, which interpretation is very rare for the molecules.

Several authors [52,53] have reported the infrared (ir) vibrations of naphthalene. For example, Daryl et al [52] in calculating the 33 planar vibration frequencies of the molecule and the deuterated molecules α -d₄, β -d₄, β -d₈ have used a valence force field containing 24 improved constants which were transferred from benzene constants using an iterative method of steepest descent. Also, the vibrational analysis of naphthalene has been presented using the D_{2h} symmetry group, with 40 of the 48 fundamental frequencies described [53].

To add substantial information to a complete rationalization of the vibrational behaviour of some naphthalene derivatives, their infrared absorption spectra of solution and powder samples have been measured and successfully assigned [54]. In the case of α -naphthol, some of the bands observed have

been interpreted by considering that the compound associated by hydrogen bonding in solid and maintain equilibrium between monomer and associated molecule in solution. More studies have been reported on the infrared spectroscopic investigations of hydrogen bonds in naphthols [55], both in solid and solution, and of amino (NH_2 -) band stretching frequencies in 1- and 2-naphthylamines [56]. The symmetrical vibration of the NH_2 group have been found to have the higher intensities and thus explained in terms of changes in hybridization of bond orbitals during stretching.

The infrared absorption spectra of some other monosubstituted naphthalenes have been obtained in solution and in pure states by several workers [57-60]. In some of these studies [58,60], a correlation chart has been given for the dependence of the characteristic C-H deformation frequencies on the position of substituents in the nucleus. Also, the near ir absorption spectra of 1-nitro-2 methoxy naphthalene, 2-nitro-1-methoxy naphthalene, 4 nitro-1-methoxy naphthalene, 1-nitro-2-naphthol, 8 nitro-

1-naphthol and 4-nitro-1-naphthol have been measured in the form of KBr pellets [58,61-65]. The resonance stabilization of the chelate ring between the $-NO_2$ and $-OH$ groups was found to be strongest in 1-nitro-2-naphthol and weakest in 8-nitro-1-naphthol.

The ir and Raman spectra measured for a series of mono- and di-halonaphthalenes in which the very low energy in-plane and out-of-plane halogen bending modes for the molecules were identified and assigned have aided their complete vibrational assignment [64]. The halogen stretching modes were found to be strongly coupled with the naphthalene skeletal modes. The Raman spectra of 1-, and 2-, methyl naphthalene, 1- and 2-naphthol, 1- and 2-bromo naphthalene and 1-naphthonitrile have, again, been, determined as solids in the melt at 200° , using Hg 4358 or 5461A for excitation [65].

Many reviews [66-69] have summarized the extensive electron spin resonance (e.s.r.) studies of naphthalene and its derivatives. For examples, the line widths of the e.s.r. spectra of naphthalene in dilute solutions at low temperatures have been carefully

investigated [66] while a computer simulation of its e.s.r. spectra in polycrystalline environments has been applied to the extraction of values of the Fermi contact hyperfine splittings [67]. The calculated exactly zero external field magnetic resonance spectrum of photoexcited naphthalene has given results which are comparable with available experimental information [68]. The broad e.s.r. spectrum observed on irradiation of naphthalene with X-rays or electron at liquid nitrogen temperature, has been ascribed to the naphthyl radical and found to decay according to the 1st order reaction kinetics [69].

The dependence of zero-field-splitting shift and spin-densities at substitutional carbon sites on the triplet lifetimes of naphthalene derivatives has been studied by electron paramagnetic resonance and optical techniques [70]. Also, the character of the hyperfine structure, splitting constants and g-values have been determined for free radicals obtained from 1- and 2-naphthol, 1,2- and 1,4-naphthoquinones, 1,5, 1,6- and 2,7 naphthalenediols [71] while α -naphthylamine in molten iodine shows hyperfine structure believed to

be due to the presence of aromatic ions [72].

The phosphorescent molecules of 1-, and 2-fluoronaphthalene have been oriented and diluted in durene single crystals to obtain the zero-field energies, principal values of the g-tensors and hyperfine coupling constants for H and F nuclei in three canonical orientations [73]. A detailed comparative analysis of the results has shown that the presence of F has little effect on the π -electron distribution in the excited state. In another study, the variation of triplet state e.s.r. signal intensities with temperature during constant continuous irradiation of guest-host crystal systems like β -methylnaphthalene in naphthalene, naphthalene- d_8 , naphthalene- d_{10} and β -methylnaphthalene- d_{10} in naphthalene at approximately 5-25K has been interpreted in terms of a model of energy transfer processes in the crystals [74].

The e.s.r. spectra of radical anions of 1,4-, 1,5-, 1,8-dinitronaphthalenes, consisting of 61, 111 and 85 lines respectively have been analyzed in terms of 1N and 3 proton coupling constants, in consistence

with the full symmetry of the species giving rise to them [75,76]. Also, the line-width alternation in the e.s.r. spectra of symmetrical dinitronaphthalene in HCONMe_2 -EtOH and EtOH- H_2O have been attributed to asymmetric solvation in which structural factors govern the rate of equilibration [76].

The nuclear magnetic parameters (n.m.r.) for a series of 1,4 disubstituted naphthalenes have been determined in several solvents [77]. In cyclohexane, the chemical shifts for the various types of protons were found to follow the group dipole moments but there are indications of an interaction with the α -H atom in cases of the nitro and hydroxyl groups.

In n.m.r. studies of α - and β -naphthol [78,79] the 2nd moment and line-width of the spectrum of both compounds have been found to decrease near 312K as the samples warmed up, but below 94K, the lattice of the two compounds appeared to be effectively rigid.

The assignment of ^{13}C -H coupling patterns for some mono-, di- and tri-substituted naphthalenes and substituted nitronaphthalenes has been made

possible by obtaining the ^{13}C chemical shifts of the compounds and also making references to the ^{13}C nmr spectra of some deuterated derivatives [80].

The MINDO/2 method has been employed in calculating the ^{13}C screening tensors and $2p$ electron charge densities to aid an interpretation of the carbon-13 nmr chemical shifts of some 2-substituted naphthalenes and their 6-methoxy derivatives [81]. Also, correlations between substituent-induced shifts, $\Delta\delta$ and INDO MO charge densities have been investigated for all positions in mono-substituted naphthalenes carrying the substituents NO_2 , CHO , CO_2H , CN , OH , NH_2 , F , OMe and Me [82].

The photoelectron spectra of naphthalene has been compared with eigen values obtained by Boschi et al [83] in studies of some polycyclic ring systems using the partial retention of diatomic differential overlap (PRDDO) method [84].

Several authors have also observed the PE spectra of substituted naphthalenes [85,86]. The changes in the π -MO energies of naphthalene caused by

the introduction of a substituent have been found to depend on the position and properties of the substituent. In monosubstituted naphthalenes with an electron-donating group, the individual bands of the PE spectra were apparently shifted to a higher energy compared with those of naphthalene, whereas for monosubstituted naphthalenes with electron-accepting groups, the bands were shifted to a lower energy.

Although the change in the energy and character of molecular orbitals due to the introduction of a substituent into the parent naphthalene has been a very interesting problem for chemists, the origin of such a change in the π -MO character and energy has not been fully understood [85-86]. Thus, "molecular orbital analysis" which is an application of configuration analysis proposed by Baba et al [87] has been applied to the interpretation of the photoelectron spectra of substituted naphthalenes, with particular attention paid to the dependence of the spectra on the position of substitution and on the character of the substituents [88].

The dipole moments and spectral characteristics of α -naphthol, α -naphthylamine, α -chloronaphthalene, α -methoxynaphthalene and α -naphthoic acid dissolved in cyclohexane, heptane, dioxane, water, methanol, benzene, chloroform and carbon tetrachloride have been determined from the spectra shift of the absorption and the fluorescence maximum at the vapour-solution transition [89]. The excited states were found to have larger dipole moments than the ground states. Also, the effect of chemical substitution on molecular electrical properties, dipole moments of some mono- and di-substituted naphthalenes have been calculated by a MO LCAO method and correlated with structure [90]. The variations in dipole moments of ground and excited states of α - and β -naphthol, α - and β -naphthylamine determined by spectrographic methods [91] have been found to be in good agreement with results of Matago [32] obtained by the A.S.M.O.-C.I method from the slope of the difference in wavenumbers of the absorption and fluorescence maxima.

Yoshinaga et al [92], in a comparative study of experimental and calculated oscillator strengths

for condensed ring systems have calculated the oscillator strength of naphthalene by the dipole-length dipole-velocity and mixed dipole methods. The calculated oscillator strengths have been compared with experimental values obtained by means of the dichroism analysis technique. Also, the effect of substituents on ionization potentials and electron affinities of conjugated systems have been calculated using perturbation theory in the framework of the restricted and unrestricted Hartree-Fock methods [93].

1.4 AIMS AND OBJECTIVES OF PROJECT

The main aim of the work presented in this thesis is to study in fuller detail, the ground and excited state properties of naphthalene and some of its derivatives. Naphthalene and its derivatives are some of the hydrocarbon derivatives which in general have a lot of biological and economic significance. Therefore, a systematic understanding of these compounds should lead to a better understanding of the really complex ones which play serious roles in

living organisms or have interactions with them.

The molecular orbitals will be evaluated using the modified HMO theory. The charge densities, electronic transition frequencies and other molecular properties calculated are to be compared with experimental values.

UNIVERSITY OF IBADAN LIBRARY

CHAPTER 2

THEORETICAL BACKGROUNDS

2.1 MOLECULAR ORBITAL CALCULATIONS

2.1.1 Huckel Molecular Orbital Theory

The Huckel Molecular Orbital (HMO) Theory is one of the various theories [1,2,94-97] that have been proposed for the calculation of molecular orbitals and their derivatives.

In the HMO theory [22] we start with the equation

$$\mathcal{H} \psi = E \psi \quad \dots \quad (1)$$

where \mathcal{H} is the electronic Hamiltonian operator, including all electronic and nuclear interaction terms.

Equation 1 cannot be completely solved for any organic molecule containing π -electrons, and therefore the Huckel theory makes use of the basic postulates of quantum mechanics and a few other assumptions.

Some of the assumptions made in the HMO theory are that:

(i) for a polyelectronic system, the total wavefunction can be factored into sets of independent, non-interacting electronic systems ψ , each of which describes a particular set of electrons

i.e.

$$\psi_{\text{polyelec}} = \psi_{\sigma} \psi_{\pi}$$

and

$$E_{\text{tot}} = E_{\sigma} + E_{\pi} \dots \quad (2)$$

where ψ_{σ} is wavefunction due to σ -electron systems and E_{σ} is total σ -electron energy.

(ii) ψ_{σ} is divisible into a set of relatively localized two-center σ -bonds as in saturated molecules. Thus,

$$\psi_{\sigma} = \prod_i \theta_{\sigma_i}$$

and

$$E_{\sigma}^{\text{tot}} = \sum_i \epsilon_{\sigma_i} \dots \quad (3)$$

where

θ_{σ_i} are localized bond functions
 ϵ_{σ_i} are σ -bond energies.

(iii) no corresponding assumptions as in (i) and (ii) can be made for π -electron systems, since these frequently have properties that reflect extensive delocalization. Thus,

$$\Psi_{\pi} = \sum_j \Psi_j \quad \dots \quad (4)$$

where each Ψ_j is of the form

$$\begin{aligned} \Psi_j &= c_{j1} \Psi_1 + c_{j2} \Psi_2 + c_{j3} \Psi_3 \dots c_{jn} \Psi_n \\ &= \sum_{i=1}^n c_{ji} \Psi_i \quad \dots \quad (5) \end{aligned}$$

where

$$j = 1, 2, \dots, n$$

c_{ji} is the coefficient of the i^{th} AO in the j^{th} MO

Ψ_i is a $2p_z$ AO on i^{th} carbon atom in a π -system containing n sp^2 hybridized carbon atoms.

(iv) the Ψ_j 's are eigenfunctions of a Hamiltonian operator (\mathcal{H}_{eff}) that is considered to be effective for the energy and behaviour of the π -system only.

Thus

$$\mathcal{H}_{\text{eff}} \psi_j = E_j \psi_j \quad \dots \quad (6)$$

where \mathcal{H}_{eff} is an approximate 'core' Hamiltonian that is considered effective for the motion of the π -electrons about a "core" consisting of the nuclei, the non-bonding and inner shell electrons and the σ -electronic framework of the molecule.

The problem is to find a set of ψ_j 's (one-electron π -wave functions) such that the expectation values of their energies are a minimum for every member of the set. Thus, for each ψ_j ,

$$\langle E_j \rangle = \frac{\int \psi_j \mathcal{H}_{\text{eff}} \psi_j \, d\tau}{\int \psi_j^2 \, d\tau} \quad \dots \quad (7)$$

and it is required to minimize $\langle E_j \rangle$ for each j in the set.

To find sets of coefficients C_{ji} , for each MO ψ_j that give the lowest possible values for each energy E_j and therefore the lowest value for E_{π}^{tot} , where

$$E^{\text{tot}} = 2 \sum_{j=1}^n (E_j)_{\text{occ}} \quad \dots \quad (8)$$

the variation method is used. The ground state ψ_0 is associated with E_0 , which for any set of electrons is the most stable distribution possible for that set. Any other distribution of these electrons, and hence any other Ψ , must represent a less probable arrangement and hence must correspond to a higher energy. That is, for ψ_j , $\langle E_j \rangle$ is always higher than E_0 .

i.e.

$$\langle E_j \rangle = \frac{\int \psi_j \mathcal{H} \psi_j \delta \tau}{\int \psi_j^2 \delta \tau} > E_0$$

Thus,

$$\langle E_j \rangle = \epsilon_j = \frac{\int \psi_j \mathcal{H} \psi_j \delta \tau}{\int \psi_j^2 \delta \tau} \text{ is to be}$$

minimized with respect to each coefficient c_{ji} for a given value of j (i.e. for one particular MO) and this is to be repeated for each value of j (i.e. for all possible MO's). Thus, for the j^{th} MO ψ_j , the problem would be to find sets of c_{ji} such that

$$\frac{\delta \epsilon_j}{\delta c_{ji}} = 0 \quad \text{for each value of } i \text{ up}$$

to n .

This is then repeated for each of the j MO's up to ψ_n .

For each atomic orbital ψ_i , there is obtained a secular equation

$$\sum c_{ji} \int \psi_i (\mathcal{H} - E) \psi_j \delta\tau = 0 \quad \dots \quad (9)$$

and for an n -carbon system (where each carbon is sp^2 hybridized and contributes one $2p_z$ orbital to the π -system), there are n -such equations, which determinant on setting equal to zero, gives n -roots that yield n -eigenvalues of the n -possible MO's.

$$\begin{vmatrix} H_{11} - \epsilon S_{11} & H_{12} - \epsilon S_{12} & \dots & H_{1n} - \epsilon S_{1n} \\ H_{21} - \epsilon S_{21} & H_{22} - \epsilon S_{22} & & H_{2n} - \epsilon S_{2n} \\ \vdots & & & \vdots \\ H_{n1} - \epsilon S_{n1} & & & H_{nn} - \epsilon S_{nn} \end{vmatrix}$$

Expansion of this determinant gives a secular polynomial of order n , whose roots can be reinserted into the n -secular equations to obtain n sets of coefficients, one set for each of the $n \psi_j$,

where, the matrix elements are defined as

$$\begin{aligned} H_{ii} &= \int \psi_i \mathcal{H} \psi_i \delta\tau \\ H_{ij} &= \int \psi_i \mathcal{H} \psi_j \delta\tau \\ S_{ij} &= \int \psi_i \psi_j \delta\tau \quad \dots \quad (11) \end{aligned}$$

In the basic Huckel method, the secular determinant is solved after making the following approximation and definitions:

(i) the matrix elements H_{ii} :

these are referred to as Coulomb integrals, and for all C-atoms that are part of the π -framework of the molecule, the Coulomb integrals are set equal to some particular numerical value α

i.e.

$$H_{ii} = \int \psi_i \mathcal{H} \psi_i \delta\tau = \alpha$$

α represents the interaction energy of an electron in an isolated $2p_z$ orbital with its own nucleus, a negative term useful in evaluating bond energy terms.

(ii) the matrix elements H_{ij} :

these are off-diagonal terms which are called bond (or resonance) integrals

$$H_{ij} = \int \psi_i^* \mathcal{H} \psi_j \delta\tau = \beta \quad (\text{atom } i \text{ directly bonded to atom } j)$$

$$= 0 \quad (\text{atom } i \text{ and } j \text{ not directly bonded})$$

β term arises from energy of interaction of an electron with two nuclei simultaneously, therefore it is very important in assessing bonding interactions and stabilities.

(iii) the S_{ij} terms:

these are called overlap integrals, and

$$S_{ij} = \int \psi_i^* \psi_j \delta\tau = 1 \quad \text{if } i = j$$

$$= 0 \quad \text{if } i \neq j$$

Now, with the approximations and definitions, for an n-center system, the secular equations are now reduced to the following:

$$C_1(\alpha - \epsilon) + C_2\beta_{12} + C_3\beta_{13} + \dots + C_n\beta_{1n} = 0$$

$$C_1\beta_{21} + C_2(\alpha - \epsilon) + C_3\beta_{23} + \dots + C_n\beta_{2n} = 0$$

$$C_1\beta_{31} + C_2\beta_{32} + C_3(\alpha - \epsilon) + \dots + C_n\beta_{3n} = 0$$

$$\vdots$$

$$\vdots$$

$$C_1\beta_{n1} + \dots + C_n(\alpha - \epsilon) = 0.$$

The secular determinant would be

$$\begin{vmatrix} \alpha - \epsilon & \beta_{12} & \beta_{13} & \dots & \beta_{1n} \\ \beta_{21} & \alpha - \epsilon & \beta_{23} & & \beta_{2n} \\ \beta_{31} & \beta_{32} & \alpha - \epsilon & & \beta_{3n} \\ \vdots & & & \ddots & \vdots \\ \beta_{n1} & & & & \alpha - \epsilon \end{vmatrix} = 0$$

expansion of which yields an n^{th} -order secular polynomial, P_s , that has n real roots of the form $(\alpha - \epsilon) = m_j \beta$ ($j = 1, 2, 3, \dots, n$) and n -associated energy values

$$\epsilon_j = \alpha - m_j \beta \quad \dots \quad (12)$$

which are the allowed energy values for the MO's or the so-called Huckel eigen values.

2.1.2 The Omega (ω) Technique

In the simple Huckel molecular orbital theory, all of the Coulomb integrals, α_i 's are taken to be the same, all of the exchange integrals β_{ij} 's for bonded atoms are taken as equal. β for non-bonded atoms are taken as zero, and all overlap integrals of the S_{ij} ($i \neq j$) are taken as zero.

The modification of the SHMO used in this work is the ω -technique introduced by Wheland and Mann [98] and used extensively by Streitwieser [99,100], which provides for electron repulsion effects in an empirical manner. The effect is to spread the charge density more evenly throughout the molecule. Thus, the off-diagonal elements are left unchanged (β or 0) and the diagonal elements are made electron dependent by including the electron (charge) density (ρ) explicitly.

But since ρ is part of the solution, the calculation becomes an iterative one as in the self-

consistent-field (SCF) method [101].

For the r^{th} iteration,

$$\alpha_i^r = \alpha_i^0 + \omega(1 - q_i^r) \quad \dots \quad (13)$$

where

ω is a scaling constant, determined empirically to be 1.4, q_i is the π -electron density on atom i , α_i^0 and β are the standard coulomb and resonance integrals of carbon, which in a benzene ring are given the values 0.0 and 1.0 respectively.

2.1.3 Calculations Involving Heteroatoms

Because a numerical value is not given to α in the SHMO calculation, heteroatoms, X, may only be incorporated into a π -lattice in the simple LCAO method by the use of appropriate values for the parameters α_X and β_{C-X} [102]. Thus, the heteroatom values α_X , is related to α_C , and the adjustment of α is expressed in units of β_{C-C} . Thus,

$$\alpha_X = \alpha_C + h_X \beta_{C-C} \quad \dots \quad (14)$$

The resonance integrals β_{C-X} associated with

a C-X bond are also expressed in units of β_{C-C} .

$$\beta_{C-X} = k_{C-X} \beta_{C-C} \dots \quad (15)$$

where

h_x and k_{C-X} are optimized proportionality constants.

2.1.4 Bond Orders, Charge Distributions and Free Valence Index

The relative pi-binding between pairs of adjacent nuclei is expected to be related to the coefficients of the atomic orbitals on the atoms between which the bond is formed. This approach has been put on a qualitative basis by Coulson [103] through the mobile π -bond under ρ_{ij} between adjacent atoms i and j . Thus,

$$\rho_{ij} = \sum_k n_k c_{ki} c_{kj} \dots \quad (16)$$

where n_k is the number of electrons in a particular molecular orbital k , and c_{ki} and c_{kj} are the coefficients of the atomic orbitals ψ_i and ψ_j in ψ_k respectively. σ -bonds are taken as 1.0 bonds and the

total bond order, P_{ij} can then be written as

$$P_{ij} = 1 + p_{ij} \quad \dots \quad (17)$$

where

P_{ij} = total bond order between adjacent atoms i and j

p_{ij} = mobile π -bond order between adjacent atoms i and j

One possible approach to the study of chemical reactivity is to determine the degree that the atoms in a molecule are bonded to adjacent atoms relative to their theoretical maximum bonding power. Coulson [103] defines a free valence index, τ_i for atom i as

$$\tau_i = \text{maximum possible binding power of } i^{\text{th}} \text{ atom} \\ - \sum_{ij} P_{ij} \quad \dots \quad \dots \quad (18)$$

where

$\sum_{ij} P_{ij}$ is the sum of the total bond orders of all bonds to the i^{th} atom.

Deviations from the normal electron density at a given π -bonded atom can be calculated by summing the electron probabilities corresponding to the contribution of the particular atomic orbital to the

various occupied orbitals [103,104]. If a carbon atom forms three σ -bonds and is also π -bonded, it will be neutral if there is an average of one electron in its $2p_z$ π -bonded orbital.

Thus, if q_i is taken as the deviation from neutrality of such a carbon, q_i is written as

$$q_i = 1 - \sum_k n_k c_{ki}^2 \dots \quad (19)$$

where

n_k and c_{ki} are as previously defined. The net charge density ρ_{ii} on atom i is then

$$\rho_{ii} = \sum_k n_k c_{ki}^2 \dots \quad (20)$$

2.1.5 Ionization Potentials

The ionization potential, I.P., is the energy required for a neutral molecule to loose an electron from its highest occupied molecular orbital and become a cation [99,105]. Thus,

$$E_{\pi}^{\dagger} - E_{\pi} = \chi \text{ (in units of } \beta \text{)} \quad (21)$$

where

E_{π}^+ is the total pi-electron energy of the cation and E_{π} is total pi-energy of the neutral molecule and χ is the ionization potential in units of β which can be converted to eV.

2.1.6 Dipole Moments

In a neutral molecule consisting of several charged points, the ground state dipole moment, μ , is the vector sum or resultant of the component moments. The dipole moment can simply be written as [106,107]:

$$\mu = \sum e r \quad \dots \quad (22)$$

where r is the vector radius separating two nuclei, and e is charge of an electron.

The dipole moment associated with a delocalized bond can be calculated by demonstrating that the moment associated with a polyelectronic wave function built from several orbitals is the sum of the dipole moments associated with each of the orbitals [107]. Considering

$$\Psi(m_1, m_2) = \frac{1}{\sqrt{2}} \begin{vmatrix} \psi_1(m_1) & \psi_2(m_1) \\ \psi_1(m_2) & \psi_2(m_2) \end{vmatrix} \quad \dots \quad (23)$$

where $\Psi_{(m_1, m_2)}$, the total wave function of two electrons is represented under the form of a single Slater determinant, the contribution to the dipole moment coming from the two electrons is (assuming the φ 's are real)

$$\begin{aligned} \mu &= -e \int |\Psi_{(m_1, m_2)}|^2 (r_{m_1} + r_{m_2}) \delta v_1 \delta v_2 \\ &= -\frac{e}{2} \int (r_{m_1} + r_{m_2}) \left[\varphi_1^2(m_1) \varphi_2^2(m_2) + \varphi_1^2(m_2) \varphi_2^2(m_1) - 2\varphi_1(m_1) \right. \\ &\quad \left. \varphi_2(m_1) \varphi_1(m_2) \varphi_2(m_1) \right] \delta v_1 \delta v_2 \dots \quad (24) \end{aligned}$$

If the φ_i 's form an orthonormal set, equation (24) can be written as

$$\begin{aligned} \mu &= -\frac{e}{2} \int r_{m_1} [\varphi_1^2(m_1) + \varphi_2^2(m_1)] \delta v_1 - \frac{e}{2} \int r_{m_2} [\varphi_1^2(m_2) + \varphi_2^2(m_2)] \delta v_2 \\ &\quad \dots \quad (25) \end{aligned}$$

but since

$$\int r_{m_1} \varphi_i^2(m_1) \delta v_1 = \int r_{m_2} \varphi_i^2(m_2) \delta v_2$$

Equation (25) takes the form

$$\mu = -e \int r_{m_1} \varphi_1^2(m_1) \delta v_1 - e \int r_{m_2} \varphi_2^2(m_2) \delta v_2 \dots \quad (26)$$

thus making it possible to calculate the moment associated with each orbital and then the total dipole moment. This also makes it possible to add the moments of the delocalized bond to the moments of the localized bonds and unshared pair, if the overlap integrals between the orbitals of delocalized and localized bonds are either zero or neglected.

To calculate the moment μ_ϕ to be associated with one orbital ϕ , it is assumed that the orbital is expressed as LCAO function, and the problem is further simplified by assuming that the orbital contains only two atomic functions, thus,

$$\phi = c_1 \psi_1 + c_2 \psi_2$$

∴ the dipole moment μ_ϕ has the form

$$\begin{aligned} \mu_\phi &= -e \int \phi^2 r \delta v \\ &= -e [c_1^2 \int \psi_1^2 r \delta v + c_2^2 \int \psi_2^2 r \delta v + 2c_1 c_2 \int \psi_1 \psi_2 r \delta v] \\ &\dots \quad (27) \end{aligned}$$

Assuming that the ψ_i 's are $2p_z$ functions and are thus symmetrical with respect to an axis

perpendicular to the plane of the molecule,

$$\int \psi_1^2 r dv = r_1 \int \psi_1^2 dv = r_1$$

Equation (27) now takes the form

$$= -e[c_1^2 r_1 + c_2^2 r_2 + 2c_1 c_2 \int \psi_1 \psi_2 r dv] \quad (28)$$

Taking the particular case when ψ_1 and ψ_2 characterize identical nuclei, the formula which gives the center of gravity R of the distribution [107] $\psi_1 \psi_2$ is

$$R = \frac{\int \psi_1 \psi_2 r dv}{\int \psi_1 \psi_2 dv} = \frac{\int \psi_1 \psi_2 r dv}{S} \quad \dots \quad (29)$$

where S is the overlap integral between ψ_1 and ψ_2 .

Geometrically, this center of gravity should be at the midpoint of the bond since ψ_1 and ψ_2 are equivalent. Thus,

$$R = \frac{r_1 + r_2}{2}$$

and

$$\int \psi_1 \psi_2 r dv = S \left(\frac{r_1 + r_2}{2} \right) \quad \dots \quad (30)$$

Equation (28) can now be written as

$$\mu_{\phi} = -e[(c_1^2 + c_1 c_2 S)r_1 + (c_2^2 + c_1 c_2 S)r_2] \quad (31)$$

In the Huckel approximation, equation (31) reduces to

$$\mu_{\phi} = -e(c_1^2 r_1 + c_2^2 r_2) \quad \dots \quad (32)$$

that is the contribution from the orbital ϕ is thus equivalent to a charge c_1^2 at nucleus 1 and a charge c_2^2 at nucleus 2.

The electronic moment associated with a delocalized bond then has the form:

$$\mu_e = -e(\sum_i c_{1i}^2 r_{1i} + \sum_i c_{2i}^2 r_{2i} + \dots) \quad \dots \quad (33)$$

and if the summation is carried out over all occupied orbitals

$$\mu_e = -e(q_1 r_1 + q_2 r_2 + \dots) \quad \dots \quad (34)$$

In a neutral molecule where each atom introduces one electron in the delocalized bond, each core carries one unit of positive charge. Thus, the dipole moment due to the delocalized bond can be calculated from the formula:

$$\mu = e \{ (1-q_1)r_1 + (1-q_2)r_2 + \dots \} \quad (35)$$

The total bond moment of a substituted molecule is obtained by adding vectorially the resulting moments of the substituent groups to the moment contributed by the delocalized bond.

2.2 TRANSITION DIPOLE MOMENT

The transition dipole moment is arrived at as follows [108,109]: If the molecular absorption cross-section is σ , the number of molecules per cm^3 of solution is n' , one can write that

$$\int_{I_0}^I \frac{dI}{I} = -\sigma \ell n' \quad \dots \quad (36)$$

which on integration

$$\begin{aligned} I &= I_0 e^{-\sigma \ell n'} \\ &= I_0 10^{-\sigma n' \ell / 2.303} \end{aligned} \quad (37)$$

where

$$\ell = \text{cell path length.}$$

For uv absorption

$$\log \frac{I_0}{I} = \frac{kc'l}{2.303} = \epsilon c l$$

$$\therefore I = I_0 10^{-\epsilon c l} \quad \dots \quad (38)$$

where

c' = concentration of the absorbing species.

Combining Equations (37) and (38),

$$\sigma = \frac{2.303}{n'} \epsilon c' \quad \dots \quad (39)$$

If 1 cm^3 contains n' molecules, then 1 dm^3 will contain $1000n'$ molecules

$$\text{i.e. } \frac{1000n'}{N} \text{ moles}$$

$$\therefore c' (\text{mol/dm}^3) = \frac{1000n'}{N} \quad \dots \quad (40)$$

$$\text{or } n' = \frac{Nc'}{1000}$$

where N = Avogadro's number.

Substituting for n' in Equation (39)

$$\begin{aligned} \sigma &= \frac{2.303 \epsilon c'}{Nc'} \times 1000 \\ &= \frac{2303}{N} \epsilon \quad \dots \quad (41) \end{aligned}$$

in which the unit of ϵ is $\text{cm}^{-1}\text{mol}^{-1}\text{dm}^3$. The Einstein coefficient of Induced Absorption by light of frequency ν for a transition from a lower state l to an upper state u is given by [110] the equation:

$$B_{lu} = \frac{c}{nh \nu_{lu}} \sigma_{l \rightarrow u} \dots \quad (42a)$$

$$= \frac{c}{nh} \int \sigma(\nu) \nu^{-1} \partial \nu \dots \quad (42b)$$

where

σ is as defined

n is the refractive index of the medium, and

c is the velocity of light.

Equation 42a is applicable to monochromatic radiation or pure electronic transition while Equation 42b applies to spectral bands. Substituting Equation 41 into Equation 42a one obtains:

$$\begin{aligned} B_{lu} &= \frac{c}{nh \nu_{lu}} \cdot \frac{2303}{N} \epsilon_{lu} \\ &= \frac{c \cdot 2303}{n h N} \int \epsilon(\nu) \nu^{-1} \partial \nu \dots \quad (43) \end{aligned}$$

The transition moment integral (M_{lu}) for this transition is related to the Einstein Coefficient of

Induced Absorption by the equation

$$\begin{aligned}
 |M_{lu}|^2 &= \frac{3h^2}{2\pi} B_{l \rightarrow u} \\
 &= \frac{3 \times 2303 \cdot hc}{8 \pi^3 n N} \cdot \epsilon_{lu} \\
 &= \frac{3 \times 2303}{8 \pi^3 n N} \cdot \int \epsilon(\nu) \nu^{-1} d\nu \quad (44)
 \end{aligned}$$

2.3 OSCILLATOR STRENGTH

The oscillator strength, a dimensionless quantity is a measure of the intensity of an electronic transition [108,109]. For pure electronic transitions, the quantum mechanical definition of oscillator strength is

$$f = \frac{8\pi^2}{3he^2} m_e c \nu_{lu} |M_{lu}|^2 \quad \dots \quad (45)$$

Substituting Equation (44) into Equation (45)

$$\begin{aligned}
 f &= \frac{8\pi^2 m_e c}{3 h e^2} \cdot \frac{2303}{nN} \times \frac{3 hc}{8 \pi^3} \epsilon_{lu} \\
 &= \frac{2303 m_e c^2}{n N \pi e^2} \cdot \epsilon_{lu} \quad \dots \quad (46)
 \end{aligned}$$

For vibronic transitions, ϵ_{lu} is replaced by $\int \epsilon(\bar{\nu}) d\bar{\nu}$ in Eqn (46) and

$$f = \frac{2303 \cdot m_e \cdot c^2}{n N \pi e^2} \int \epsilon(\bar{\nu}) d\bar{\nu} \dots \quad (47)$$

where m_e is the mass of electron and e is electronic charge.

2.4 RADIATIVE LIFE-TIME, τ , OF EXCITED STATE

The radiative life-time, τ , of excited state for the transition from state l to state u of the same multiplicity [108,109] is given by

$$\begin{aligned} \frac{1}{\tau} &= \frac{8\pi h \nu_{lu}^3}{c^3} \cdot n^3 \cdot B_{lu} \\ &= 8\pi h \bar{\nu}_{lu}^3 n^3 B_{lu} \dots \quad (48) \end{aligned}$$

Substituting Eqn (43) into Eqn (48),

$$\begin{aligned} \frac{1}{\tau} &= 8 \pi h \bar{\nu}_{lu}^2 \cdot n^3 \cdot \frac{c}{nhN} 2303 \epsilon_{lu} \\ &= \frac{8 \pi n^2 \cdot 2303 c}{N} \int \epsilon(\bar{\nu}) \bar{\nu}^2 d\bar{\nu} \dots \quad (49) \end{aligned}$$

2.5 SOLVENT EFFECTS ON ELECTRONIC SPECTRA

The general theoretical expression derived from perturbation theory of McRae [111] for solvent-induced spectral shifts is

$$\Delta\nu = 2.13 \times 10^{-30} \left[\sum_{j \neq 0} \left(\frac{1}{\nu_{j0}^u} - L_{j0} \right) \frac{f_{j0}^u n_{j0}^2 - 1}{a^3 2n_{j0}^2 + 1} - \sum_{j \neq i} \left(\frac{1}{\nu_{ji}^u} - L_{ji} \right) \frac{f_{ji}^u n_{ji}^2 - 1}{a^3 2n_{ji}^2 + 1} \right] \\ + \frac{1}{hc} \frac{M_{00}^u (M_{00}^u - M_{ii}^u)}{a^3} \cdot \frac{n_0^2 - 1}{2n_0^2 + 1} \\ + \frac{2}{hc} \frac{M_{00}^u (M_{00}^u - M_{ii}^u)}{a^3} \left[\frac{D-1}{D+2} - \frac{n_0^2 - 1}{n_0^2 + 2} \right] \\ + \frac{6}{hc} \frac{(M_{00}^u)^2 (\alpha_0^u - \alpha_i^u)}{a^3 b} \left[\frac{D-1}{D+2} - \frac{n_0^2 - 1}{n_0^2 + 2} \right] \quad \dots \quad (50)$$

where,

$\Delta\nu$ is the spectral shift in the solvent compared to the gaseous state

f_{ji}^u is the oscillator strength for a transition between the i^{th} and j^{th} states of the solute

n_0 is the refractive index of the solvent at the sodium D line

D is the dielectric constant of the solvent

M_{00}^u and M_{ii}^u are the respective dipole moment vectors of the solute molecule in its ground and excited states

" a " is the Onsager's reaction radius of the solute molecule

α_0^u , α_0^i are the respective isotropic polarizabilities of the solute molecules in the ground and excited states

h is Planck's constant, and

c is the speed of light.

McRae's Equation [50] has been shown by Suppan [112,113] to reduce to

$$-\Delta\nu_{1-2} = \frac{\Delta\mu_g \cdot \Delta\mu_{g,e}}{hca^3} \{ \Delta [f(D) - f(n)]_{1-2} \} + \frac{\mu_e^2 - \mu_g^2}{hca^3} \Delta f(n)_{1-2} \quad \dots (51)$$

for two solvents 1 and 2, where

$$f(n) = \frac{(n^2 - 1)}{2n^2 + 1}$$

$$f(D) = \frac{(D - 1)}{2D + 1}$$

μ_g and μ_e represent the ground state and excited state dipole moments.

2.6 GROUP THEORETICAL ANALYSIS OF NAPHTHALENE AND ITS DERIVATIVES

Spectroscopists have realized that the symmetry of a molecule played an important role in what vibrations of the molecule would be permitted and which ones to be excluded [114]. Naphthalene can be considered as possessing the following symmetry elements:

- (1) I - the identity element
- (2) (xy) } planes of symmetry
- (3) (xz) }
- (4) (yz) }
- (5) $C_2(z)$ } 2-fold rotation axis through 180°
- (6) $C_2(y)$ }
- (7) $C_2(x)$ }

The molecule therefore belongs to D_{2h} point group for which the symmetry types and characters are listed in Table 1.

Table 1

Symmetry types and characters of Naphthalene of D_{2h} Point Group

D_{2h}	I	$\sigma_{(xy)}$	$\sigma_{(xz)}$	$\sigma_{(yz)}$	i	$C_2(z)$	$C_2(y)$	$C_2(x)$	
A_g	1	1	1	1	1	1	1	1	$\alpha_{xx}, \alpha_{yy}, \alpha_{zz}$
A_u	1	-1	-1	-1	-1	1	1	1	
B_{1g}	1	1	-1	-1	1	1	-1	-1	R_z, α_{xy}
B_{1u}	1	-1	1	1	-1	1	-1	-1	T_g
B_{2g}	1	-1	1	-1	1	-1	1	-1	R_z, α_{xz}
B_{2u}	1	1	-1	1	-1	-1	1	-1	T_z
B_{3g}	1	-1	-1	1	1	-1	-1	1	R_x, α_{yz}
B_{3u}	1	1	1	-1	-1	-1	-1	1	T_x

The selection rules and distribution of frequencies among the various symmetry species of the D_{2h} point group of naphthalene have been given by O'Reilly et al [115] and are found in Table 2.

Table 2

Selection rules for D_{2h} structure of naphthalene

Species	Number of Vibrations	Activity	Parallel (II) or Perpendicular (I) to plane of Molecule
A_g	9	R	(II)
A_u	4	Inactive	(I)
B_{1g}	8	R	(II)
B_{1u}	4	I,R	(I)
B_{2g}	3	R	(I)
B_{2u}	8	I,R	(II)
B_{3g}	4	R	(I)
B_{3u}	8	I,R	(II)

where

R = Raman-active

I = Infrared-active.

Therefore, of the 48 fundamental vibrations expected for naphthalene, there are only 20 infrared-active fundamentals.

With the introduction of substituents into naphthalene as in Figures 7, 11, 12 and in the compounds (Figure 17)



Fig. 17: 4-bromo-1-naphthylamine, 4-nitro-1-naphthylamine and 2-nitro-1-naphthol

the D_{2h} point group of naphthalene breaks down and there remains only the symmetry elements I and σ_{xy} for the substituted compounds described above.

Thus, these compounds belong to the C_s point group for which the symmetry types and characters are given in Table 3.

Table 3

Symmetry types and characters of C_s point group

C_s	I	$\sigma_{(xy)}$		
A'	1	1	$T_x; T_y; R_z$	$\alpha_{xx}, \alpha_{yy}, \alpha_{zz}, \alpha_{xy}$
A''	1	-1	$T_z; R_x; R_y$	$\alpha_{yz}; \alpha_{zz}$

For these compounds, therefore, all the infrared and Raman vibrations are active.

The infrared vibrational frequencies of simple cases like diatomic molecules can be calculated [116] from

$$\nu = \frac{1}{2\pi c} \sqrt{k \left(\frac{1}{m_1} + \frac{1}{m_2} \right)} \quad \dots \quad (52)$$

where

- ν = the frequency in cm^{-1}
- c = velocity of light
- k = force constant of the bond in dynes per cm, and
- m_1, m_2 = masses of atoms in grams.

To calculate the vibrational frequencies of large molecules, various subparts of the molecule are studied separately.

3.1 PRECURSORS AND SOLVENTS

Naphthalene, 1-naphthol, 2-naphthol and 1-naphthylamine were obtained from the following sources: Naphthalene, 1-naphthol, 2-naphthol, 1-naphthylamine and 2-naphthylamine were prepared.

3.1.1 Preparation and Purification of

Naphthalene, 1-naphthol, 2-naphthol and 1-naphthylamine were

obtained from the following sources: Naphthalene, 1-naphthol, 2-naphthol, 1-naphthylamine and 2-naphthylamine were prepared.

The following procedure was used for the preparation and purification of naphthalene, 1-naphthol, 2-naphthol, 1-naphthylamine and 2-naphthylamine.

Naphthalene was obtained from the following sources: Naphthalene, 1-naphthol, 2-naphthol, 1-naphthylamine and 2-naphthylamine were prepared.

1-naphthol was obtained from the following sources: Naphthalene, 1-naphthol, 2-naphthol, 1-naphthylamine and 2-naphthylamine were prepared.

2-naphthol was obtained from the following sources: Naphthalene, 1-naphthol, 2-naphthol, 1-naphthylamine and 2-naphthylamine were prepared.

1-naphthylamine was obtained from the following sources: Naphthalene, 1-naphthol, 2-naphthol, 1-naphthylamine and 2-naphthylamine were prepared.

2-naphthylamine was obtained from the following sources: Naphthalene, 1-naphthol, 2-naphthol, 1-naphthylamine and 2-naphthylamine were prepared.

UNIVERSITY OF IBADAN LIBRARY

CHAPTER 3

EXPERIMENTAL SECTION

3.1 REAGENTS AND SOLVENTS

Naphthalene, 1-naphthol, 1-naphthylamine and 1-nitronaphthalene were obtained from British Drug Houses (BDH) Limited. 4-bromo-1-naphthylamine, 4-nitro-1-naphthylamine and 2-nitro-1-naphthol were prepared.

3.1.1 Preparation and Purification of Reagents

Naphthalene and 1-nitronaphthalene were recrystallized from alcohol while 1-naphthol and 1-naphthylamine were recrystallized from water-alcohol mixtures. The compounds were dissolved in the solvent at or near the boiling point of the solvent. This was followed by filtration of the hot solution from any insoluble materials, and on cooling, the dissolved substance crystallized out.

4-aceto- α -naphthalide was prepared by [117] mixing 10 grams of α -naphthylamine, 70 cm³ of

glacial acetic acid and 9 cm³ of acetic anhydride (30-40% excess). The mixture was heated at 100°C for five minutes, after which rapid separation of 4-aceto- α -naphthalide was promoted by cooling and stirring. 4-bromo-1-naphthylamine was prepared [118] by mixing 4-aceto- α -naphthalide with a solution of bromine in glacial acetic acid (1:1 mole ratio). The acetyl bromo compound was crystallized from the same solvent and hydrolyzed by boiling with excess of 50% potassium hydroxide solution in an open vessel until the product became quite oily. The 4-bromo-1-naphthylamine was then collected and recrystallized from benzene and petroleum.

4-nitro-1-naphthylamine was prepared [119] by dissolving 2.0 grams of α -nitronaphthalene and 0.5g of powdered hydroxylamine hydrochloride in 120 cm³ of 95% ethanol contained in a 500 ml flask. This was heated on a bath maintained at 50-60°C. A filtered solution of 1.0g of potassium hydroxide in 5.0g of methanol was added gradually with vigorous mechanical stirring over a period of 1 hour. Stirring was continued for an additional hour, and

the warm solution poured slowly into 700 cm³ of ice-water. After the solid had coagulated, it was collected in a filter and washed thoroughly with distilled water. The crude 4-nitro-1-naphthylamine was purified by recrystallization from 50 ml of 95% ethanol.

2-nitro-1-naphthol was prepared from 4-aceto- α -naphthalide. The paste of 4-aceto- α -naphthalide (described in the preparation of 4-bromo-1-naphthylamine) was treated at 14-16° with 7 cm³ of mixed nitric and sulphuric acids in a period of half an hour. The lemon-yellow crystals, after 12 hours were recrystallized from alcohol. The crystals were further hydrolyzed with boiling 5% sodium hydroxide solution. 2-nitro-1-naphthol was recrystallized as yellow leaflets from ethanol [117].

3.1.2 Purification of Solvents

The solvents used for spectroscopic studies are required pure and transparent.

Commercial acetonitrile (140 cm³) was first distilled before 17.5 cm³ of benzoyl chloride was

added. This was refluxed for 1 hour before distilling again into a receiver containing 17.5 ml of distilled water. Anhydrous sodium carbonate (35g) was added and the mixture was again refluxed for two hours before finally distilling into a receiver fitted with a drying tube [120].

200 cm³ of commercial chloroform was shaken three times with 10 cm³ of concentrated sulphuric acid each time. It was then washed thoroughly with distilled water before drying over anhydrous calcium chloride. The solvent was finally distilled into a receiver fitted with a drying tube [121].

250 cm³ of cyclohexane was put in a separatory funnel and 20 cm³ of concentrated sulphuric acid added. The funnel was stoppered and shaken vigorously for about 10 minutes. It was then allowed to stand, settle and the yellowish acid layer run off. This procedure was repeated three times until the acid layer became colourless. The solvent was then washed with water to remove the acid. The sulphur dioxide was extracted by washing with dilute sodium bicarbonate solution before finally distilling the solvent into

a receiver [122].

250 cm³ of methylcyclohexane was put in a separatory funnel, 20 cm³ of concentrated sulphuric acid was added and the stoppered separatory funnel and its contents were shaken vigorously for about ten minutes. It was then allowed to stand and settle. When settled, the yellowish acid layer was run off. Shaking with acid was repeated three times.

Successive portions of a concentrated solution of potassium permanganate in 10% H₂SO₄ were added with vigorous shaking until the colour of the permanganate remained unchanged. The permanganate layer was then run off, the solvent washed thoroughly with water, dried over anhydrous calcium chloride and distilled into a receiver filtered with a drying tube [121].

To purify methanol, 1 gram of clean, dry magnesium turnings and 0.1 gram of resublimed iodine were placed in a 500 ml round-bottomed Pyrex flask which was fitted with a double surface reflux condenser. 10-15 cm³ of methanol was added through the condenser and the mixture warmed on a water-bath until the iodine disappears. After a vigorous evolution of

hydrogen has taken place, a further 0.1g of iodine was added and the mixture heated until all the magnesium has been converted into the methoxide. 180 cm³ of the methanol was then added and the mixture boiled for 30 minutes under reflux. The product was then distilled with exclusion of moisture, the first 10 ml of distillate being discarded [121].

Calcium oxide (50 g) freshly ignited in a furnace for 2 hours was added to 200 cm³ of rectified spirit in a 500 ml round-bottomed flask. The flask was fitted with a double surface condenser carrying a drying tube, refluxed for 6 hours over a heating mantle and allowed to stand overnight. The ethanol was then distilled off into a receiver fitted with a drying tube, the first 10 cm³ of distillate being discarded. To prevent carryover of CaO with the distillate, a splashhead was fitted between the flask and the condenser [121].

200 cm³ of n-heptane was dried over sodium wire for 24 hours. The n-heptane was then distilled off into a receiver fitted with a drying tube.

3.2 SPECTRAL MEASUREMENTS

3.2.1 Ultraviolet Spectra

The absorption spectra were measured with the Pye Unicam SP 6-550 uv-visible spectrophotometer. The solution of the compounds were prepared in the range of 10^{-4} - 10^{-5} M. The absorption spectra were determined using 1 cm path length silica cells at each wavelength from 200 nm to 480 nm. After each run, the cells were washed with soap water, dried, washed with acetone, then with fresh solvent and dried before use.

The instrument was calibrated for wavelength using 0.0400 g/dm^3 (0.0002M) solution of $\text{K}_2\text{Cr}_2\text{O}_4$ prepared in a 0.05 M ($2.8055 \text{ g/100 cm}^3$) solution of potassium hydroxide. The solution which was run between 220 nm and 500 nm at intervals of 5 nm and around the peaks at intervals of 1 nm gave maximum absorption on the instrument used at $\lambda = 379 \text{ nm}$. Potassium chromate (0.002 M) solution in a 0.05 M KOH solution should give maximum absorption at $\lambda = 370 \text{ nm}$ [123]. Therefore, actual λ values reported

in this thesis are the values read from the instrument reduced by 9 nm.

3.2.2 Infrared Spectra

The infrared spectra were recorded in kBr pressed discs containing between 0.5 and 2.0 mg of sample in about 150 mg of dry kBr using Perkin-Elmer double beam infrared spectrophotometer model 577.

The infrared frequencies reported in this thesis have been calibrated with polystyrene film and are believed to be correct to within $\pm 4 \text{ cm}^{-1}$ in the 4000-2000 cm^{-1} region and $\pm 2 \text{ cm}^{-1}$ in the 2000-200 cm^{-1} region.

3.2.3 Physical Data on Reagents and Solvents

Tables 4a and 4b give physical data on reagents and solvents used in this work.

UNIVERSITY OF IBADAN LIBRARY

Table 4 a

Physical Data on Reagents

Compound	Molecular formula	Molar mass	Melting point ($^{\circ}\text{C}$)	Physical State	Solubility
Naphthalene	C_{10}H_8	128	80.3°	Colourless plates from EtOH	Et_2O , C_6H_6 , EtOH, CHCl_3 , toluene, xylene
1-Naphthol	$\text{C}_{10}\text{H}_8\text{O}$	144	94.0°	Needles from aqueous ethanol	EtOH, Et_2O , CHCl_3 , C_6H_6 , H_2O
1-Naphthylamine	$\text{C}_{10}\text{H}_9\text{N}$	143	50.0°	Needles from aqueous ethanol	EtOH, Et_2O
1-Nitronaphthalene	$\text{C}_{10}\text{H}_7\text{O}_2\text{N}$	173	61.5°	Yellow needles from ethanol	CS_2
4-bromo-1-naphthylamine	$\text{C}_{10}\text{H}_8\text{NBr}$	222	102°	Needles from petroleum benzene	-
4-nitro-1-naphthylamine	$\text{C}_{10}\text{H}_8\text{O}_2\text{N}_2$	188	195°	Orange needles from EtOH	EtOH, AcOH
2-nitro-1-naphthol	$\text{C}_{10}\text{H}_7\text{O}_3\text{N}$	189	128°	Yellow leaflets from EtOH	-

Table 4b
Physical Data on Solvents

Solvent	Molecular formula	Molar mass	Boiling point ($^{\circ}\text{C}$)	Density	Refractive index	Viscosities (Cp)
Acetonitrile	$\text{C}_2\text{H}_3\text{N}$	41	81.6°	0.7828	1.34423	0.345
Chloroform	CHCl_3	119.5	62.0°	1.4985	1.44858	0.542
Cyclohexane	C_6H_{12}	84	81.0°	0.7791	1.42623	1.020
Methycyclohexane	C_7H_{14}	98	100.4°	0.7773	1.4253	-
Methanol	CH_4O	32	64.1°	0.7910	1.3276	0.547
Ethanol	$\text{C}_2\text{H}_6\text{O}$	46	78.5°	0.7893	1.35954	1.200
n-Heptane	C_7H_{16}	100	98.4°	0.6796	1.38777	0.386

CHAPTER 4

RESULTS AND DISCUSSIONS

4.1 HUCKEL MOLECULAR ORBITAL CALCULATIONS

The Huckel molecular orbital calculations of pi-energy levels, charge densities, delocalization energies and bond orders were carried out on an IBM 370/135 Computer using the computer programme QCPE 110 from Quantum Chemistry Programme Exchange of Indiana University, Bloomington, Indiana, U.S.A.

The initial input parameters of bondlength [107] were used to modify the Huckel matrix by the bondlength relationship using an iterative procedure until a self-consistent energy was obtained. The resonance integrals, β are modified by [94,124].

$$\beta_{jk} = \beta_0 e^{-(R_{jk} - 1.397)/0.3106}$$

where

R_{jk} is the bondlength between atoms j and k. The various bondlengths used are in Table 5.

Table 5: Bond Lengths and Bond Moments
used in HMO Calculations [106,107]

Bond	Length (Å)	Bond Moment
C-C	1.394	-
C-H	1.084	0.40
C-O	1.364	1.50
O-H	0.956	1.50
C-N	1.426	1.15
N-H	1.038	1.31
C-Cl	1.717	2.30
C-Br	1.879	2.20

The atomic indices for the parent molecules, naphthalene, 1-naphthol and 1-nitronaphthalene and their derivatives for which calculations were done are shown in Figure 18. The aromatic ring carbon atoms were numbered 1 to 10, the element next in substituent X in 1- and 2-monosubstituted naphthalenes 4 and 3

respectively.

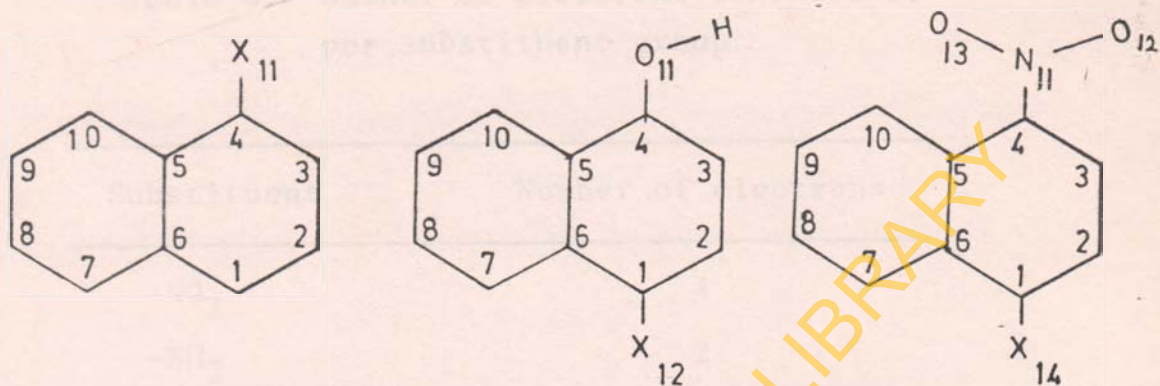


Figure 18: Atomic indices for substituted naphthalenes, substituted naphthols and substituted nitronaphthalenes.

The total number of electrons contributed by each atom or group to the pi-electron system of naphthalene are given in Table 6. Oxygen, nitrogen and the halogens were taken as contributing two electrons each to the pi-electron system in the neutral molecule. The total number of pi-electrons in naphthalene was taken as 10, that in monohydroxynaphthalene as 12, naphthylamine as 12, and for nitronaphthalene as 14.

Table 6: Number of electrons contributed per substituent group

Substituent	Number of electrons
-NO ₂	4
-NH ₂	2
-OH	2
-Br, Cl	2
-CO ₂ H	4
-OCH ₃	2
-CH ₃	2
-NO	2
-CN	4

The calculated pi-energies E_{π} were used to calculate transition frequencies, represented as

$$\bar{\nu} = (E_j^* - E_i) \beta \quad \dots \quad (53)$$

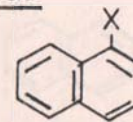
where E_j^* is the energy of the j^{th} unoccupied molecular

orbital and E_1 is the energy of the i^{th} occupied molecular orbital while the dipole moments were evaluated, using the net charge distribution in the atoms, according to equation 22. . The CCC and COH bond angles were taken as 120° and 108° respectively. The bond moments [107] used to correct for the replacements of the C-H bond(s) are given in Table 5.

4.1.1 Molecular Orbital Energies

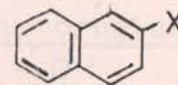
The results of the molecular orbital energies (occupied and lowest unoccupied) $E_1, E_2 \dots$ in β units and those of the total pi-energy E_π , pi-delocalization energy DE_π , bonding energy per electron BEPE and delocalization energy per electron DEPE are listed in Tables 7-12 and Tables 13-18. In general, for the monosubstituted compounds (i.e. 1- and 2- $C_{10}H_7X$), the unsubstituted naphthalene has the largest DEPE, which implies the most stable configuration when compared with those of the substituted compounds. Also, monosubstituted compounds with electron-withdrawing substituents appear to have greater total pi-energies

Table 7: Energies of the occupied and lowest unoccupied molecular orbitals (E_1, E_2, \dots) in β units for

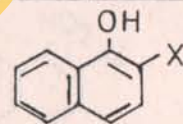


Substituent (X)	E_1	E_2	E_3	E_4	E_5	E_6	E_7	E_8	E_9
H	2.2132	1.6244	1.2757	0.9378	0.6861	-0.6861			
Br	2.3330	1.7784	1.5205	1.0694	0.9530	0.2429	-0.7222		
CN	2.2523	1.7084	1.4522	1.0688	0.9431	0.5969	-0.5969		
NO	2.3154	1.9707	1.5804	1.2142	0.9431	0.6545	-0.6545		
CH ₃	2.3330	1.7783	1.5204	1.0693	0.9532	0.2430	-0.7226		
OCH ₃	2.3330	1.7785	1.5203	1.0691	0.9533	0.2433	-0.7228		
CO ₂ H	2.3035	1.9359	1.5859	1.2245	0.9533	0.6711	0.5757	-0.5420	
NH ₂	2.3330	1.7784	1.5204	1.0692	0.9532	0.2431	-0.7226		
NO ₂	2.8215	2.1809	1.6158	1.2596	0.9458	0.6780	0.6168	-0.6414	
OH	2.333	1.7784	1.5204	1.0693	0.9532	0.2430	-0.7227		

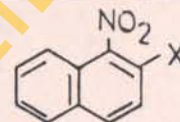
Table 8: Energies of the occupied and lowest unoccupied molecular orbitals (E_1, E_2, \dots) in β units for



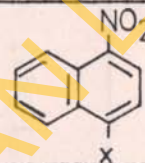
Sub tituent (X)	E_1	E_2	E_3	E_4	E_5	E_6	E_7	E_8	E_9
H	2.2132	1.6244	1.2757	0.9378	0.6861	0.6861			
Br	2.3255	1.8263	1.4247	1.2005	0.8553	0.2611	-0.6564		
CH ₃	2.3255	1.8263	1.4247	1.2006	0.8555	0.2611	-0.6567		
OCH ₃	2.3256	1.8263	1.4246	1.2005	0.8555	0.2613	-0.6568		
CO ₂ H	2.2855	1.9884	1.5240	1.2710	0.9217	0.6827	0.5772	-0.5870	
NH ₂	2.3256	1.8263	1.4246	1.2005	0.8555	0.2613	-0.6567		
NO ₂	2.8196	2.1923	1.5976	1.2751	0.9339	0.6831	0.6171	-0.6608	
OH	2.3255	1.8263	1.4246	1.2005	0.8555	0.2612	-0.6568		

Table 9: Energies of the occupied and lowest unoccupied molecular orbitals(E_1, E_2, \dots) in β units for

Substituent (X)	E_1	E_2	E_3	E_4	E_5	E_6	E_7	E_8	E_9
NH ₂	2.4304	2.0208	1.7647	1.3662	1.1731	0.8359	0.2412	-0.6486	
OH	2.3817	2.0221	1.9639	1.5047	1.1990	0.9664	0.6406	-0.6405	
CO ₂ H	2.3678	2.1131	1.9690	1.6268	1.2784	1.1231	0.8238	0.5986	-0.5985
NO ₂	2.8244	2.2842	1.9717	1.5606	1.2132	0.9355	0.6529	0.6169	-0.6294
Br	2.4306	2.0209	1.7646	1.3661	1.1730	0.8356	0.2411	-0.6486	
CH ₃	2.2142	1.8926	1.5626	1.1618	0.9524	0.6487	-0.2413		

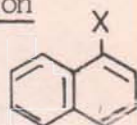
Table 11: Energies of the occupied and lowest unoccupied molecular orbitals(E₁, E₂) in β units for

Substituent (X)	E ₁	E ₂	E ₃	E ₄	E ₅	E ₆	E ₇	E ₈	E ₉	E ₁₀
NH ₂	2.8588	2.2707	1.8148	1.4085	1.1948	0.8510	0.6380	0.2682	-0.6422	
OH	2.8262	2.2537	2.0233	1.5196	1.2446	0.9105	0.6652	0.6165	-0.6272	
CO ₂ H	2.8216	2.2486	2.0986	1.6614	1.3027	1.1400	0.8284	0.6231	0.6130	-0.5838
NO ₂	2.8601	2.6239	2.2067	1.6643	1.3446	1.0697	0.7926	0.6325	0.2554	-0.6145
Br	2.8586	2.2707	1.8148	1.4085	1.1948	0.8508	0.6380	0.2682	-0.6420	
CH ₃	2.4829	2.1183	1.7092	1.2981	1.0898	0.7623	0.1611	-0.2415		

Table 12: Energies of the occupied and lowest unoccupied molecular orbitals(E₁, E₂,.....) in β units for

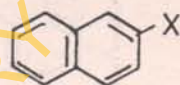
Substituent (X)	E ₁	E ₂	E ₃	E ₄	E ₅	E ₆	E ₇	E ₈	E ₉	E ₁₀
NH ₂	2.8551	2.2888	1.7755	1.4809	1.0698	0.9502	0.6374	0.2496	-0.7092	
OH	2.8218	2.2934	1.9626	1.5616	1.2070	0.9478	0.6480	0.6166	-0.6118	
CO ₂ H	2.8551	2.2888	1.7755	1.4809	1.0698	0.9502	0.6374	0.2496	-0.7092	
NO ₂	2.8468	2.6340	2.1880	1.6852	1.3511	1.0318	0.8410	0.6319	0.2314	-0.6230
Br	2.8550	2.2887	1.7755	1.4810	1.0699	0.9500	0.6374	0.2494	-0.7089	
CH ₃	2.4735	2.1441	1.6883	1.3323	0.9866	0.8677	0.1390	-0.2424		

Table 13: Total Energies (E_{π}), Delocalization Energies (DE_{π}),
Bonding Energies per Electron (BEPE) and Delocalization
Energies per Electron (DEPE) in β units for



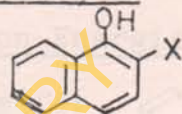
Substituent (X)	E_{π}	DE_{π}	BEPE	DEPE
H	13.4740	3.4740	1.3474	0.3474
NH ₂	12.5081	2.5081	1.0423	0.2090
CO ₂ H	14.5476	2.5476	1.0391	0.1819
OH	12.5083	2.5083	1.0423	0.2090
NO ₂	16.2031	4.2031	1.1573	0.3021
CH ₃	12.5084	2.5084	1.0424	0.2090
OCH ₃	12.5080	2.5080	1.0423	0.2090
Br	12.5082	2.5082	1.0423	0.2090

Table 14: Total Energies (E_{π}), Delocalization Energies (DE_{π}), Bonding Energies per Electron and (DEPE) in β units for



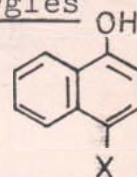
Substituent (X)	E_{π}	DE_{π}	BEPE	DEPE
H	13.4740	3.4740	1.3474	0.3474
NH ₂	12.4644	2.4644	1.0387	0.2054
CO ₂ H	14.5463	2.5463	1.0390	0.1818
OH	12.4646	2.4646	1.0387	0.2054
NO ₂	16.2029	4.2029	1.1574	0.3002
CH ₃	12.4646	2.4646	1.0387	0.2053
OCH ₃	12.4664	2.4644	1.0387	0.2053
Br	12.4643	2.4643	1.0387	0.2054

Table 15: Total Energies (E_{π}), Delocalization Energies (DE_{π}), Bonding Energies per Electron (BEPE) and Delocalization Energies per Electron (DEPE) in β units for



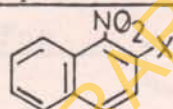
Substituent (X)	E_{π}	DE_{π}	BEPE	DEPE
NH ₂	16.3819	4.3819	1.1701	0.3129
OH	21.2366	7.2366	1.5169	0.5169
CO ₂ H	23.8009	7.8009	1.4875	0.4875
NO ₂	20.0849	6.0849	1.2553	0.3803
Br	16.3814	4.3814	1.1701	0.3129
CH ₃	19.1822	7.1822	1.5985	0.5985
CN	19.9274	5.9274	1.4233	0.4233

Table 16: Total Energies (E_{π}), Delocalization Energies (DE_{π}), Bonding Energies per Electron (BEPE) and Delocalization Energies Per Electron (DEPE) in β units for



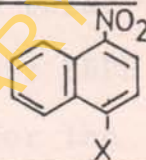
Substituent (X)	E_{π}	DE_{π}	BEPE	DEPE
NH ₂	16.4272	4.4272	1.1734	0.3162
OH	21.2352	7.2352	1.5168	0.5168
CO ₂ H	23.7984	7.7984	1.4874	0.5570
NO ₂	20.0845	6.0845	1.2552	0.3802
Br	16.4271	4.4271	1.1733	0.3162
CH ₃	19.2272	7.2272	1.6023	0.6023
CN	19.9241	5.9241	1.4231	0.4232

Table 17: Total Energies (E_{π}), Delocalization Energies (DE_{π}), Bonding Energies per Electron (BEPE) and Delocalization Energies per Electron (DEPE) in β units for



Substituent (X)	E_{π}	DE_{π}	BEPE	DEPE
NH ₂	15.1971	1.1971	0.9498	0.0748
OH	20.0862	6.0862	1.2553	0.3803
CO ₂ H	22.6488	6.6488	1.2582	0.3694
NO ₂	19.5235	3.5235	1.0846	0.1957
Br	15.1967	1.1967	0.9498	0.0748
CH ₃	19.2433	5.2433	1.3745	0.3745
CN	18.7761	4.7761	1.1735	0.2985

Table 18: Total Energies (E_{π}), Delocalization Energies (DE_{π}), Bonding Energies per Electron (BEPE) and Delocalization Energies per Electron (DEPE) in β units for



Substituent (X)	E_{π}	DE_{π}	BEPE	DEPE
NH ₂	15.2400	1.2400	0.9525	0.0775
OH	20.0845	6.0845	1.2552	0.3802
CO ₂ H	22.6635	6.6635	1.2590	0.3702
NO ₂	19.5552	3.5552	1.0864	0.1975
Br	15.2400	1.2400	0.9525	0.0775
CH ₃	19.2627	5.2627	1.3759	0.3759
CN	18.7803	4.7803	1.1738	0.2987

than compounds with electron-donating substituents, even though this is not obvious on mere comparison of the BEPE values.

For the 1,2 disubstituted compounds, the total pi-energies of the hydroxyl-compounds and their BEPE and DEPE are greater than the same energies for the corresponding nitro-substituted analogues for the same substituent X, suggesting that the -OH group donates electrons into the π -system while the -NO₂ group is electron withdrawing. This is consistent with the known behaviour of these substituents. In the case of the 1,4 disubstituted compounds, a similar pattern is observed as with 1,2 disubstituted compounds.

Generally, however, for the same substituent X, the 1,4 disubstituted compounds have greater total pi-energies than the 1,2 disubstituted compounds excepting the 1,2 hydroxy compounds with electron-withdrawing substituents which have slightly greater energies than their 1,4 counterparts. With electron-withdrawing substituents like -CO₂H, -NO₂, the total pi-energies in both the hydroxy- and the nitro-compounds appear to follow the sizes of such substituents. This trend is

not obvious for the electron-donating substituents. Thus, it is not possible to predict substituent effects on the total energies of these compounds.

4.1.2 Charge Distributions and Bond Orders

The molecular diagrams giving the calculated π -electron populations and bond orders of naphthalene and its 1- and 2-monoderivatives are indicated in Figures 19-20. Figures 21-24 give the diagrams for the 1, 2 and 1,4 disubstituted compounds. The charge distribution on naphthalene is unity at all carbon atoms, but for the 1- and 2- $C_{10}H_7X$ compounds, where X is electron-donating, there is an increase in the electronic charges of the aromatic ring carbon atoms.

Table 19 gives the positions of substitution and correlation coefficients between charge densities and Hammett's substituent constant. The table shows that the charge densities of the predicted reaction centers which are farthest away from the substituents correlate fairly well with the substituent constants. The better correlation between charge densities and the

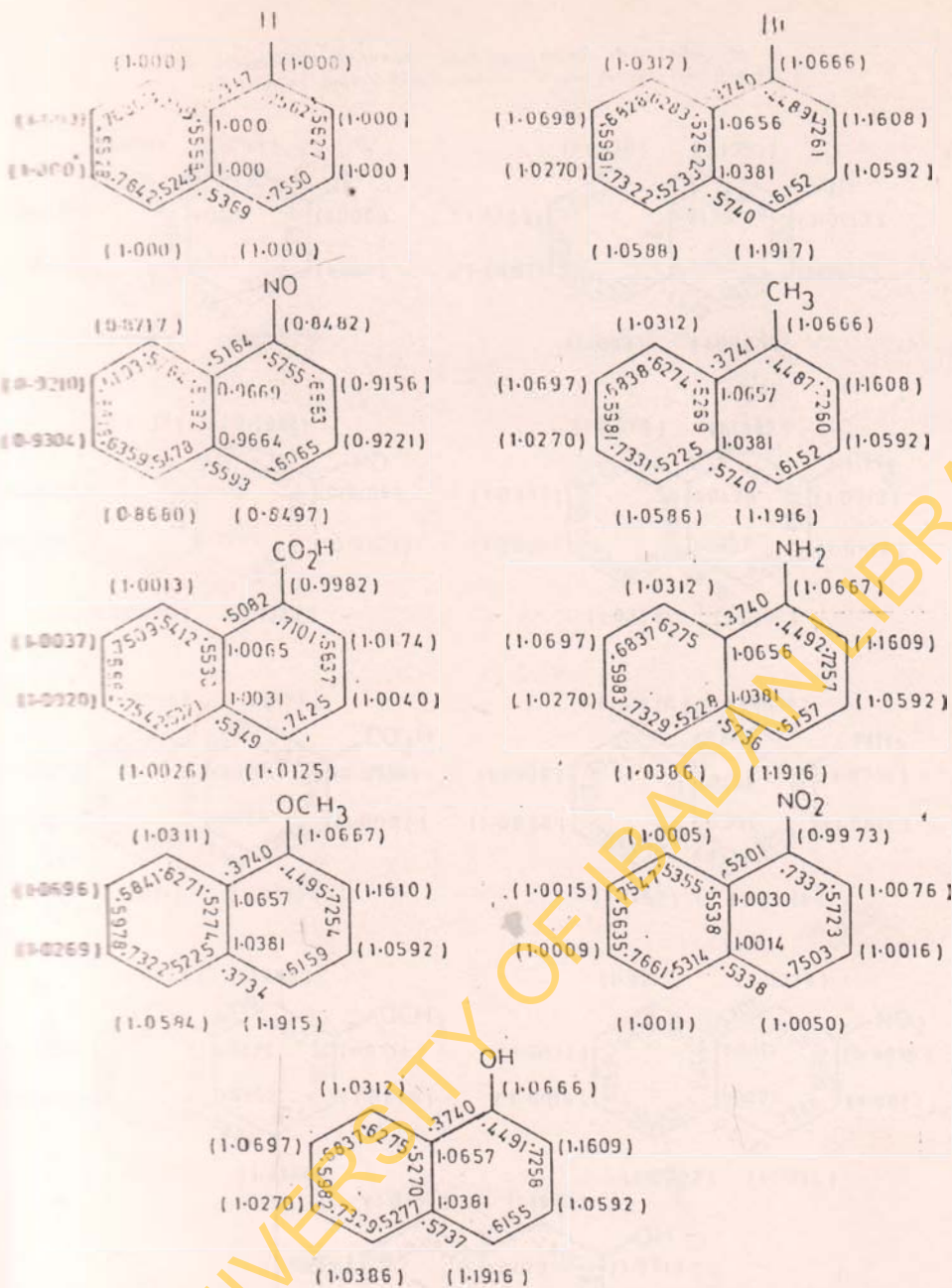


Fig. 10: Molecular diagrams showing charge densities in brackets and π -bond orders along bonds for $1-C_6H_7X$.

Fig. 20: Molecular diagrams showing charge densities in brackets and a bond order (long bond) for 2 C_6H_5X

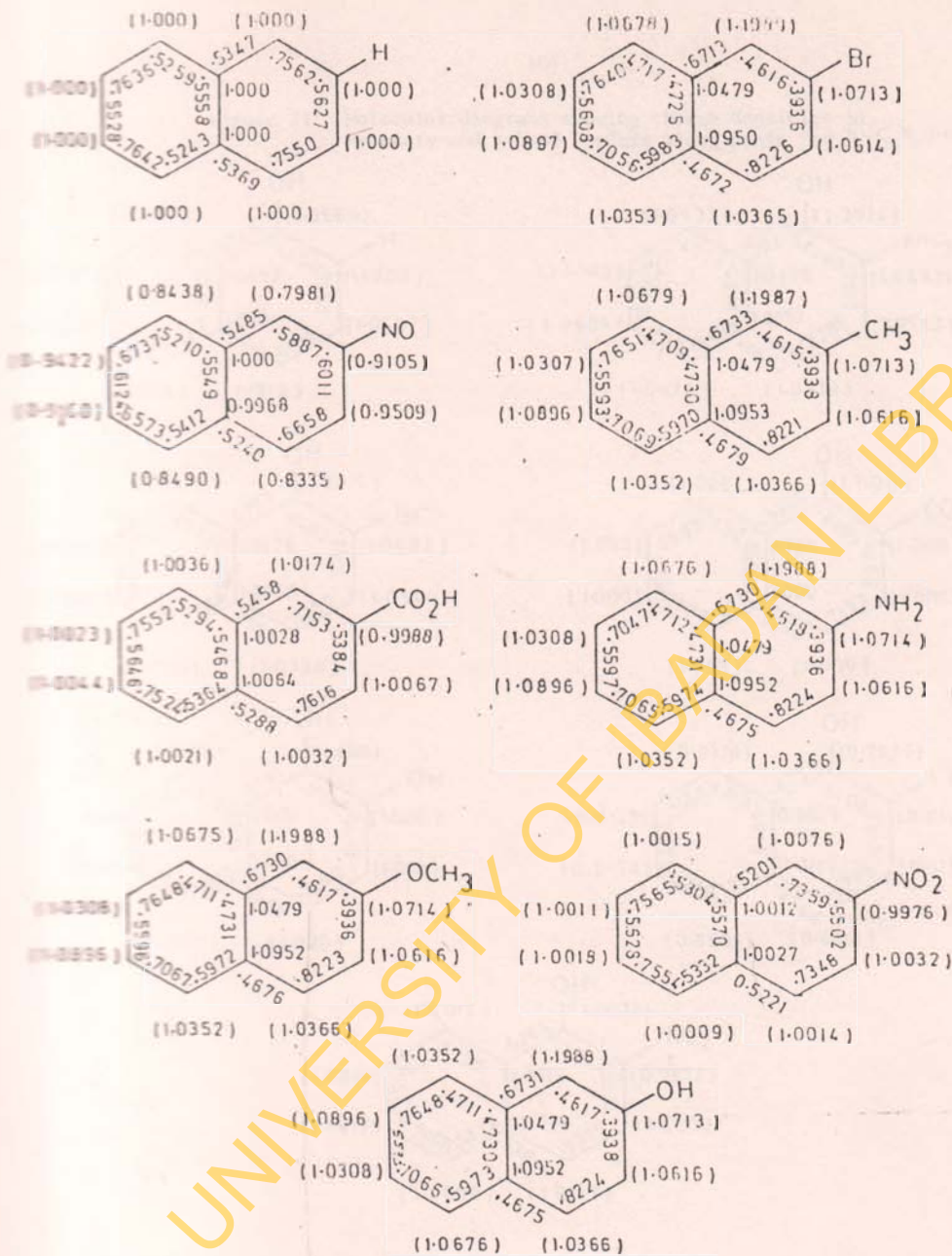


Figure 21: Molecular diagrams showing charge densities in brackets and π -bond orders along bonds for 2-C₆H₆-1-OH

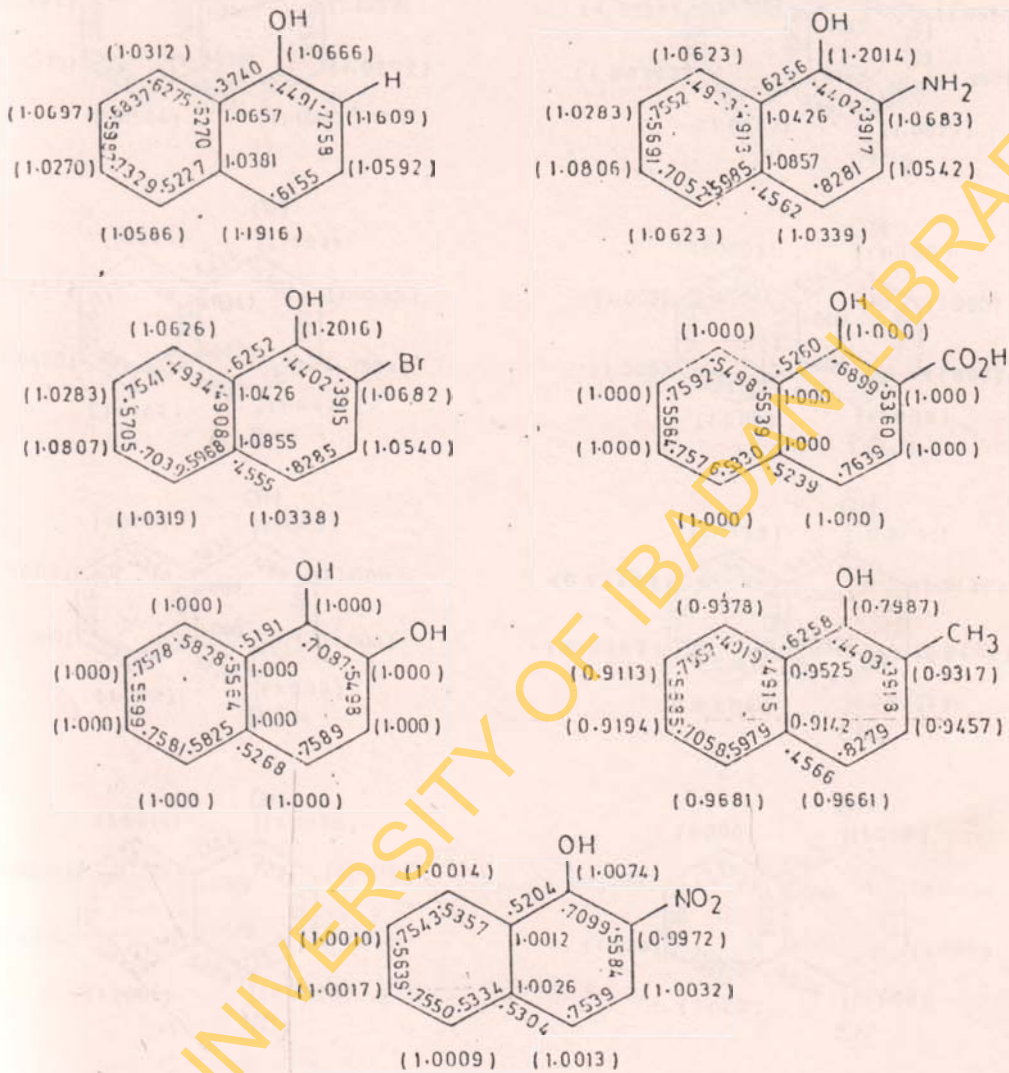


Figure 22: Molecular diagrams showing charge densities in brackets and π -bond orders along bonds for 4- $C_{10}H_6$ -1-OH

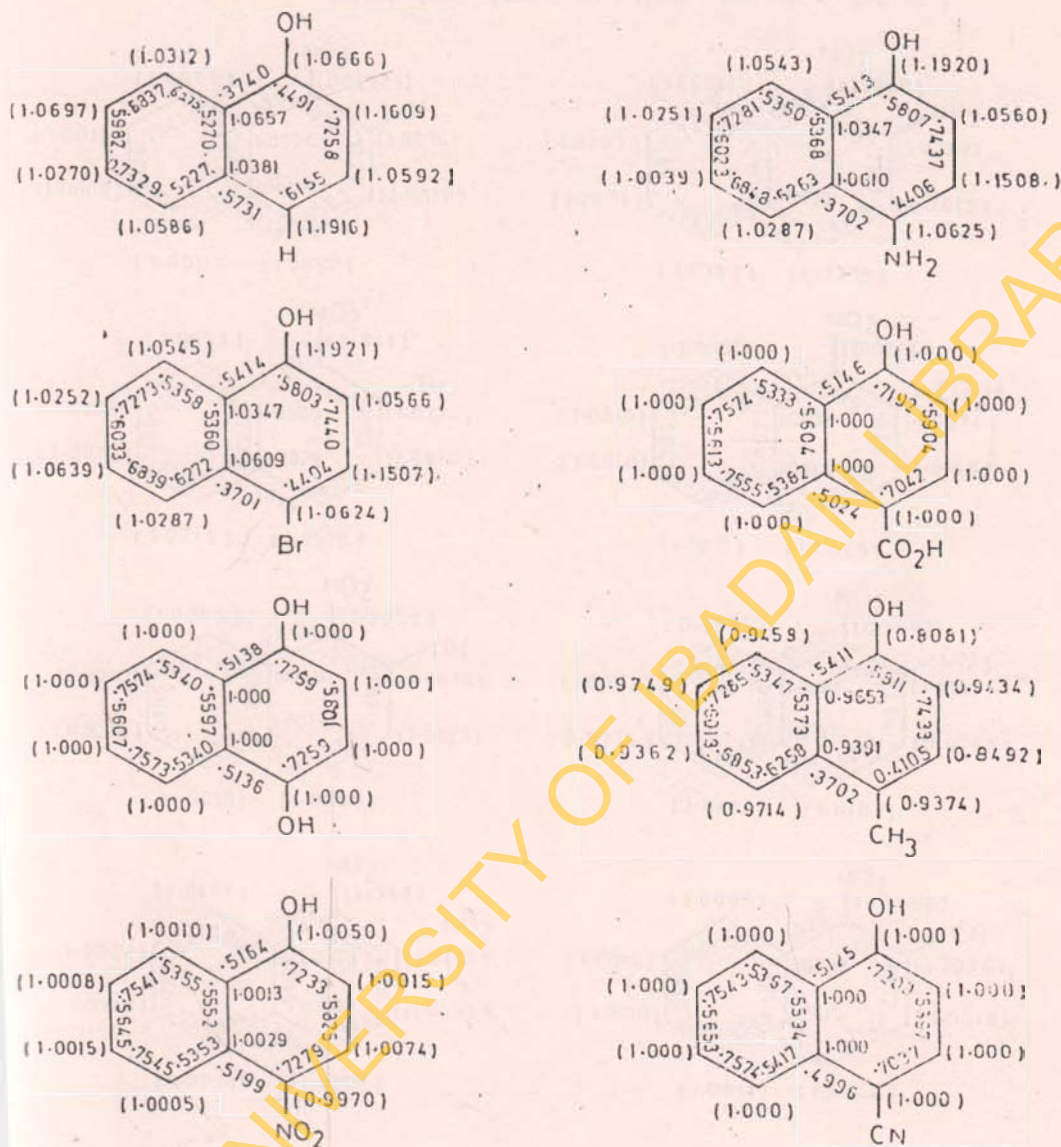


Figure 23: Molecular diagrams showing charge densities in brackets and π -bond orders along bonds for 2- $C_{10}H_6-INO_2$

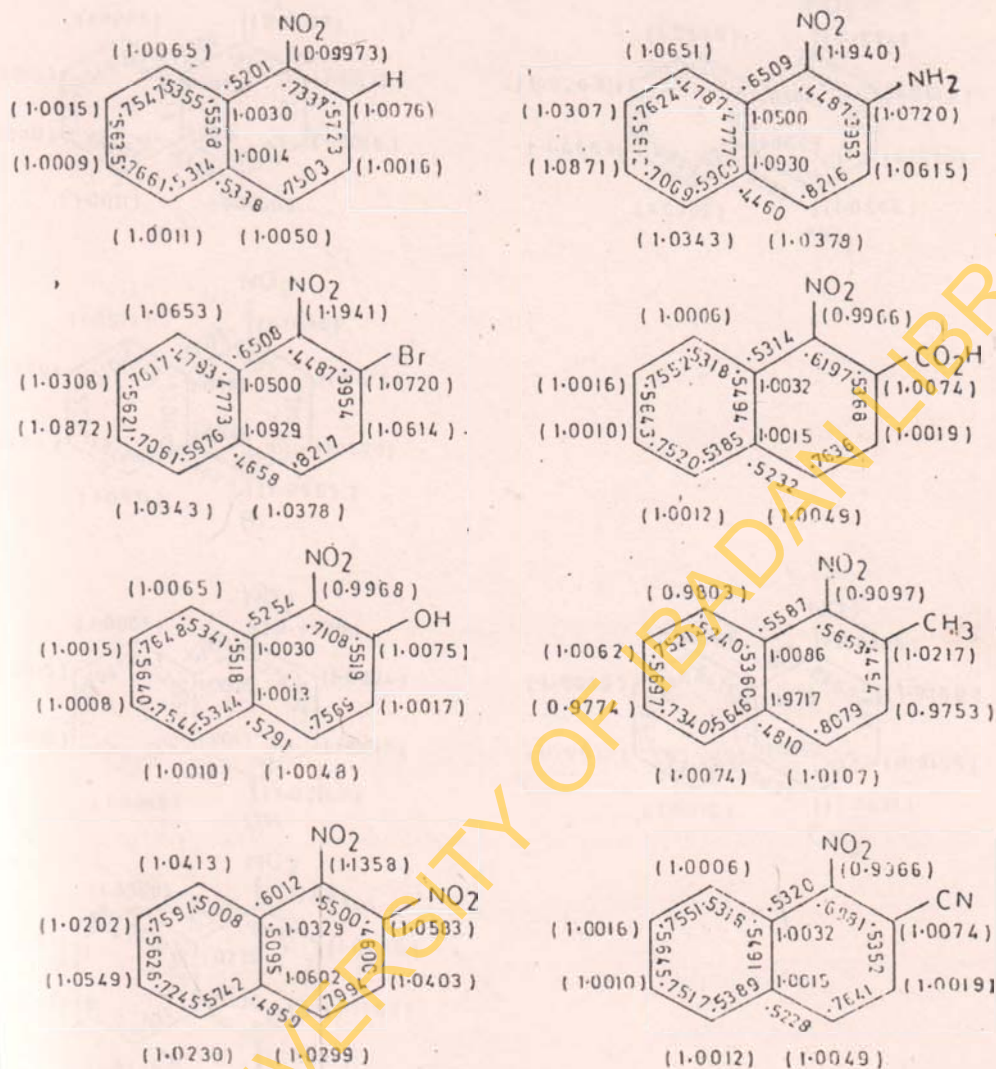
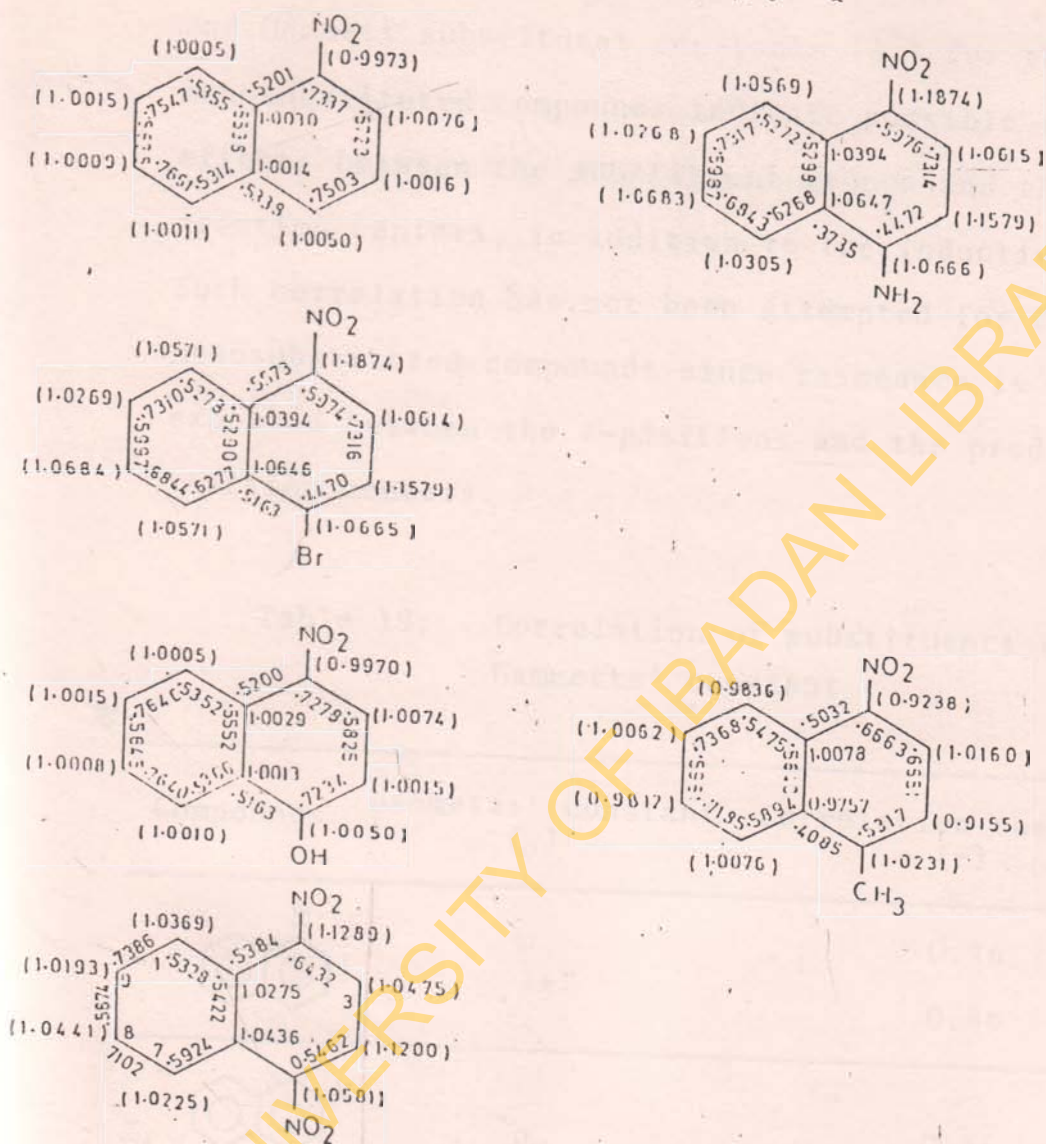
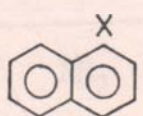
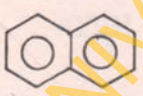


Figure 24: Molecular diagrams showing charge densities in brackets and π -bond orders along bonds for 4- $C_{10}H_6-INO_2$



2nd Hammett substituent constants (ρ^+) for the 1-monosubstituted compounds indicate possible resonance effects between the substituent groups and the reaction centers, in addition to the inductive effects. Such correlation has not been attempted for 2-monosubstituted compounds since resonance is not expected between the 2-positions and the predicted reaction centers.

Table 19: Correlation of substituents with Hammetts' constant

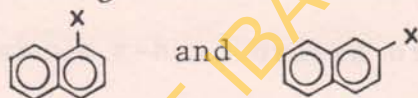
Compounds	Hammetts' constant (ρ)	Correlation coefficient (r)
1. 	ρ ρ^+	0.46 0.86
2. 	ρ_m	0.65

X = -H, -Br, -CH₃, -OCH₃, -NH₂, -NO₂ and -OH.

In electrophilic substitution reactions, π -electron

density at the positions which are attacked by the reagent is a measure of reactivity. Also, it is well-known that in all naphthalene derivatives with substituents in α -positions, the 3 positions become less active, whereas for the β -derivatives, the 1-position is found to be reactive and the 3-position to be inert [125]. Table 20 shows calculated charge distribution for selected 1- and 2- $C_{10}H_7X$ compounds.

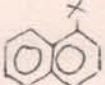

Table 20: Charge Distributions for some



Substituent X	Position	q_1	q_2	q_3	q_4
NH ₂	1	1.0667	1.1609	1.0592	1.1916
	2	1.1988	1.0714	1.0616	1.0366
CO ₂ H	1	0.9982	1.0174	1.0040	1.0125
	2	1.0174	0.9988	1.0067	1.0032
NO ₂	1	0.9973	1.0076	1.0016	1.0050
	2	1.0076	0.9976	1.0032	1.0014

Thus, the charge distributions predict that the ortho- (q_2) and the para- (q_4) positions of 1- $C_{10}H_7X$ (X electron donating) would be susceptible to electrophilic attack whereas for 2- $C_{10}H_7X$ where X is also electron donating, the q_1 (ortho) positions would be most susceptible. For 1- and 2- $C_{10}H_7X$ (X is electron-withdrawing) there is a decrease from unity at the centers of attachment of the substituents while substitution favours most strongly electrophilic attack at the ortho positions only.

Table 21 shows π -bond orders of some bonds in 1- and 2- $C_{10}H_7X$ compounds. A comparison of the molecular diagrams of the naphthalene ring with those of the 1-X and 2-X substituted compounds make it possible to say that the introduction of the substituent into 1-position (α) leads to increases in the bond orders of the 2-3 bonds (where X could be electron withdrawing or donating) and to decreases in those of the 1-2, 1-9 and 3-4 bonds. That is, 1-substitution has a tendency to unify the bond orders along the direction of the short molecular axis. Contrary to this, substitution in the 2-position (β) cause decreases in

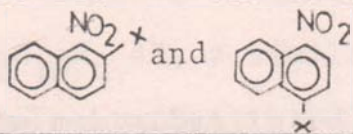
Table 21: $\bar{\lambda}$ -Bond Orders for Some  and 

Bond	NH ₂	CO ₂ H	NO ₂	H
1-C₁₀H₇X				
1-2	0.4492	0.7101	0.7337	0.7550
2-3	0.7257	0.5837	0.5723	0.5621
9-10	0.5270	0.5523	0.5538	0.5558
1-9	0.3740	0.5082	0.5355	0.5369
3-4	0.6157	0.7425	0.7503	0.7562
2-C₁₀H₇X				
1-2	0.4618	0.7153	0.7395	0.7550
2-3	0.3936	0.5384	0.5562	0.5627
9-10	0.4731	0.5468	0.5510	0.5558
1-9	0.6730	0.5458	0.5201	0.5369
3-4	0.8224	0.7516	0.7585	0.7562

the bond orders of the 1-2, 2-3 and 9-10 bonds and increases in those of 1-9 and 3-4 bonds. In other words, substitution in 1-positions cause an increase in the mobilities of π -electrons in the direction of the short molecular axis, whereas those in 2-positions lead to decreased π -electron mobilities in this direction and to an increase of mobilities in the direction of the long molecular axis.

In another comparison of molecular diagrams of $1\text{-C}_{10}\text{H}_7\text{NO}_2$ with $1\text{-NO}_2\text{C}_{10}\text{H}_6\text{ 2X}$ and $1\text{-NO}_2\text{C}_{10}\text{H}_6\text{ 4X}$ compounds it is revealed that substituents may have no significant influence on charge redistribution of the unsubstituted ring carbon atoms [126]. However, for auxochromic substituents at the 2-position, there is a greater π -electron density at the 6 and 8-positions, thus such carbon atoms have higher affinity for electrophilic attack. In the cases of $1\text{-OHC}_{10}\text{H}_7$ and $1\text{-OHC}_{10}\text{H}_6\text{ 2X}$ (or 4X), a similar situation is found for auxochromic substitution at the 2-position.

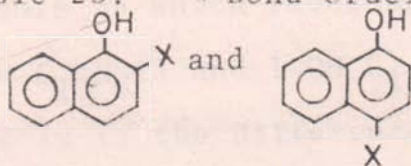
Table 22 shows π -bond orders of some bonds in $1\text{-NO}_2\text{C}_{10}\text{H}_6\text{ 2X}$ and $1\text{-NO}_2\text{C}_{10}\text{H}_6\text{ 4X}$ compounds.

Table 22: π -Bond orders for Some

Bond		NH ₂	NO ₂	OH	H
1-2	2X	0.4487	0.5500	0.7108	0.7337
	4X	0.5976	0.6432	0.7278	0.7337
2-3	2X	0.3953	0.4600	0.5825	0.5723
	4X	0.7314	0.6817	0.5519	0.5723
9-10	2X	0.4777	0.5095	0.5518	0.5538
	4X	0.5298	0.5422	0.5552	0.5538
1-9	2X	0.6509	0.6012	0.5254	0.5201
	4X	0.3755	0.4316	0.5200	0.5201
3-4	2X	0.8216	0.7994	0.7569	0.7503
	4X	0.4472	0.5462	0.7234	0.7503

Again, considering π -bond orders of 1-NO₂C₁₀H₆ 2X and 1-NO₂C₁₀H₆ 4X, a similar explanation can be given as for the monosubstituted derivatives. It would be reasonable, again, to say that the introduction of another substituent into the 4-position leads to increases in the bond orders of the 2-3 bond and to decreases for the 1-2, 1-9 and 3-4 bonds. The effect of substitution at the 4-position in 1-C₁₀H₇NO₂ on the 9-10 bond is ambiguous. However, a look at the 6-7 bond which is parallel to the 9-10 and 2-3 bonds reveals that there are great increases of bond orders with 4-substitution. Contrary to this, substitution in the 2-positions cause decreases in the bond orders of 1-2, 2-3 and 9-10 bonds while there are increases in the 1-9 bond orders.

Table 23 shows the bond orders of some bonds in 1-OH C₁₀H₆ 2X and 1-OH C₁₀H₆ 4X compounds.

Table 23: π -Bond Orders for Some

Bond		NH ₂	NO ₂	CO ₂ H	H
1-2	2X	0.4402	0.7099	0.6899	0.4491
	4X	0.5807	0.7233	0.7192	0.4491
2-3	2X	0.3917	0.5584	0.5360	0.7258
	4X	0.7437	0.5825	0.5904	0.7258
9-10	2X	0.4913	0.5526	0.5539	0.5270
	4X	0.5368	0.5552	0.5604	0.5270
1-9	2X	0.6256	0.5357	0.5260	0.3740
	4X	0.3702	0.5199	0.5024	0.3740
3-4	2X	0.8281	0.7539	0.7039	0.6155
	4X	0.4406	0.7279	0.7042	0.6155

From Table 23 which shows bond orders of some bonds in 1-OH $C_{10}H_62X$ and 1-OH $C_{10}H_64X$ compounds, it appears as if the differences of the bond orders from those of the parent compound depend on whether X, the substituent, is electron donating or withdrawing. Thus, for electron withdrawing X in 4-position, there are increases in the bond orders of 1-9 and 3-4 bonds, while the bond order of the 2-3 bond is decreased. This same kind of result has been reported for α , α' naphthalenediols and β , β' naphthalenediols by Kichisuke Nishimoto et al [127]. This is unlike what happens with 1-NO₂ $C_{10}H_7X$. However, when it is an electron donating group the opposite, that is decreases in bond orders of 1-9 and 3-4 bonds with accompanying increases in the 2-3 bond is true. For the 1-2 and 9-10 bonds, there are increases in the bond orders, though the increases appear to be much greater for electron-withdrawing substituents.

It can be said that substitutions in the 4-position of 1-NO₂ $C_{10}H_7$ cause an increase in the mobilities of π -electrons in the direction of the short molecular axis, whereas those in 2-position

lead to decreases in π -electrons in this direction and to increases of mobilities in the direction of the long molecular axis. This is in agreement with what is obtained for 1- and 2-monosubstitution in the naphthalene ring. However, one cannot easily explain the effects of 4- and 2-substitution in 1-C₁₀H₇OH and this may very much be the basis for the differences between 1-C₁₀H₇NO₂ and 1-C₁₀H₇OH in most of their chemical behaviour.

4.2 THE ELECTRONIC SPECTRA

The electronic spectra calculated by the Huckel Molecular Orbital Method have been compared with observed or literature-value [44,46,128] electronic transition wavelengths and are given in Tables 24-29. The following equations,

$$\lambda (^1L_a) = 474(\Delta m_1)^{-\frac{1}{2}} - 145 \text{ m}\mu \quad \dots \quad (54)$$

$$\lambda (^1L_b) = 428(\Delta m_2)^{-1} + 50 \text{ m}\mu \quad \dots \quad (55)$$

$$\lambda (^1B_b) = 358(\Delta m_2)^{-1} \text{ m}\mu \quad \dots \quad (56)$$

[where

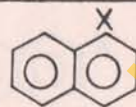
$$\Delta m_1 = m_1 - m_{1'},$$

$$\Delta m_2 = \sqrt{(m_1 - m_{2'}) (m_2 - m_{1'})}$$

the m_j 's are as defined in Equation (12) for the calculation of HMO energy levels, and the subscript 1 indicates the highest occupied molecular orbital (HOMO) while 1' indicates LUMO (lowest unoccupied molecular orbital) prescribed by Kichisuke Nishimoto [129] for the calculation of the three absorption wavelength of α -substituted hydrocarbons have been used in this work. It is therefore expected that results obtained would fit best for the 1-monosubstituted naphthalenes. In this calculation, transition from the upper occupied to the first vacant orbital of naphthalene gives a λ_{\max} at 260 nm. It is expected that first-order configurational interaction of the excited states would lead to the two levels B_{3u}^- and B_{3u}^+ , transitions to which will give λ_{\max} at 314 nm and λ_{\max} at 221 nm respectively.

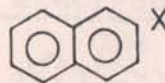
From the data calculated and presented in Tables

Table 24: Calculated (HMO) and observed electronic transition
wavelengths (nm) of

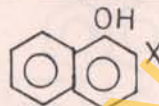


X	'L _b				'L _a				'B _b			
	$\lambda_{\text{calc.}}$	f	λ_{obs}	f	$\lambda_{\text{calc.}}$	f	λ_{obs}	f	$\lambda_{\text{calc.}}$	f	λ_{obs}	f
H	314	1.036	309	0.02	260	1.252	290	0.02	221	1.472	240	-
CO ₂ H	317	1.027	-	-	303	1.074	302	-	232	1.403	230	-
NO ₂	349	0.932	380	0.23	326	0.998	290	0.05	250	1.302	239	-
OCH ₃	313	1.039	-	-	288	1.130	290	-	220	1.479	238	-
CN	328	0.992	321	-	291	1.118	295	-	232	1.403	219	-
CH ₃	322	1.011	312	-	288	1.130	281	-	221	1.479	224	-
NH ₂	337	0.965	316	0.15	313	1.039	290	0.03	227	1.434	239	-
OH	322	1.011	316	0.12	288	1.130	290	0.08	227	1.434	240	-

Table 25: Calculated (HMO) and observed electronic transition
wavelengths (nm) of

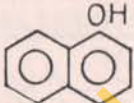


X	'L _b				'L _a				'B _b			
	$\lambda_{\text{calc.}}$	f	λ_{obs}	f	$\lambda_{\text{calc.}}$	f	λ_{obs}	f	$\lambda_{\text{calc.}}$	f	λ_{obs}	f
H	314	1.036	309	0.02	260	1.252	290	0.02	221	1.472	240	-
CO ₂ H	338	0.96	335	-	276	1.18	280	-	240	1.36	240	-
NO ₂	350	0.93	353	-	298	1.09	329	-	264	1.23	260	-
OCH ₃	313	1.039	319	-	265	1.22	267	-	241	1.35	240	-
CH ₃	309	1.05	305	-	265	1.22	275	-	220	1.48	224	-
NH ₂	350	0.93	340	-	296	1.10	281	-	240	1.36	237	-
OH	313	1.039	318	-	265	1.22	274	-	240	1.36	226	-

Table 26: Calculated (HMO) and observed electronic transitionwavelengths (nm) of

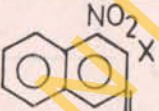
X	'L _b				'L _a				'B _b			
	$\lambda_{\text{calc.}}$	f	λ_{obs}	f	$\lambda_{\text{calc.}}$	f	λ_{obs}	f	$\lambda_{\text{calc.}}$	f	λ_{obs}	f
H	322	1.01	316	0.12	288	1.13	290	0.08	227	1.43	240	-
CO ₂ H	351	0.92	-	-	288	1.13	-	-	229	1.42	-	-
NO ₂	373	0.87	-	-	295	1.10	-	-	226	1.44	-	-
Br	320	1.02	-	-	269	1.21	-	-	224	1.45	-	-
CN	347	0.94	-	-	287	1.13	-	-	248	1.31	-	-
CH ₃	318	1.02	-	-	269	1.21	-	-	224	1.45	-	-
NH ₂	347	0.94	-	-	306	1.06	-	-	267	1.22	-	-
OH	326	0.99	335	-	284	1.15	296	-	231	1.40	235	-

Table 27: Calculated (HMO) and observed electronic transition

wavelengths (nm) of 

X	¹ L _b				¹ L _a				¹ B _b			
	$\lambda_{\text{calc.}}$	f	λ_{obs}	f	$\lambda_{\text{calc.}}$	f	λ_{obs}	f ×	$\lambda_{\text{calc.}}$	f	λ_{obs}	f
H	322	1.01	316	0.12	288	1.13	290	0.08	227	1.43	240	-
CO ₂ H	333	0.98	-	-	301	1.08	-	-	237	1.37	-	-
NO ₂	368	0.88	-	-	278	1.17	-	-	228	1.43	-	-
Br	319	1.02	-	-	264	1.23	-	-	225	1.45	-	-
CN	332	0.98	-	-	286	1.14	-	-	236	1.38	-	-
CH ₃	322	1.01	-	-	264	1.23	-	-	223	1.46	- ^d	-
NH ₂	344	0.95	-	-	305	1.07	-	-	264	1.23	-	-
OH	325	1.01	355	-	279	1.17	-	-	233	1.44	245	-

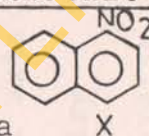
Table 28: Calculated (HMO) and observed electronic transition

wavelengths (nm) of 

X	¹ L _b				¹ L _a				¹ B _b			
	λ _{calc.}	f	λ _{obs}	f	λ _{calc.}	f	λ _{obs}	f	λ _{calc.}	f	λ _{obs}	f
H	326	1.00	380	0.23	250	1.30	290	0.05	210	1.55	239	-
CO ₂ H	346	0.94	-	-	286	1.14	-	-	248	1.31	-	-
NO ₂	373	0.81	-	-	298	1.09	-	-	243	1.34	-	-
Br	352	0.92	-	-	274	1.19	-	-	238	1.37	-	-
CN	342	0.95	-	-	270	1.21	-	-	247	1.32	-	-
CH ₃	344	0.95	-	-	271	1.20	-	-	245	1.33	-	-
NH ₂	394	0.83	-	-	288	1.13	-	-	232	1.40	-	-
OH	355	0.91	-	-	272	1.20	-	-	240	1.36	-	-

Table 29: Calculated (HMO) and observed electronic transition

wavelengths of



X	¹ L _b				¹ L _a				¹ E _b			
	$\lambda_{\text{calc.}}$	f	λ_{obs}	f	$\lambda_{\text{calc.}}$	f	λ_{obs}	f	$\lambda_{\text{calc.}}$	f	λ_{obs}	f
H	326	1.00	380	0.23	250	1.30	290	0.05	210	1.55	239	-
CO ₂ H	346	0.94	-	-	286	1.14	-	-	248	1.31	-	-
NO ₂	375	0.88	-	-	278	1.17	-	-	246	1.31	-	-
Br	342	0.95	-	-	302	1.08	-	-	233	1.40	-	-
CN	342	0.95	-	-	270	1.21	-	-	247	1.32	-	-
CH ₃	327	0.99	-	-	267	1.22	-	-	223	1.46	-	-
NH ₂	398	0.82	380	0.22	291	1.12	290	0.06	240	1.36	240	-
OH	356	0.91	-	-	304	1.07	-	-	235	1.39	-	-

24-29, it is very clear that the electronic spectra for $C_{10}H_7X$ and $X C_{10}H_6Y$ are similar to that of naphthalene. The effect of a substituent X in $C_{10}H_7X$ on $\pi-\pi^*$ transitions in naphthalene has been noted repeatedly [45,130-133] to depend on whether X is located in position 1 or 2. However, in this calculation, there has been greater shift to longer wavelength in the $'L_a$ bands of the 1-derivatives and in the $'L_b$ and $'B_b$ bands of the 2-derivatives. Although the experimental determination of direction of polarisation has been known to be a very difficult problem, it has been asserted [107] in conformity with LCAO calculations, that an electronic transition in $C_{10}H_8$ to an excited state of symmetry B_{3u}^- is polarised in the direction of the longitudinal axis and a transition to an excited state of symmetry B_{2u} is polarised in the direction of the transverse axis of the molecule. This assertion has thus been used to explain the differences in the effect of X on position 1 and 2 in naphthalene.

It has been noted in this work that insertion of X into naphthalene generally produces a shift of the

electronic transition (except for the 1L_a transition of some 2-substituted derivatives) towards longer wavelengths. It can, therefore be assumed that, on introduction of X in naphthalene derivatives, the electrons on the various ring carbon atoms undergo different degrees of perturbation. In conformity with the direction of the moment of conjugation of X relative to the ring, the electron densities on carbon atoms in positions 4 and 5 are expected to change to appreciably greater extents in the 1-derivatives in both ground and excited states, but in the ~~2~~ derivatives those on carbon atoms 6 and 7. Even though our own calculations of charge densities have not clearly indicated this, previous theoretical studies of the energy levels in naphthalene derivatives having X = OH, NH₂ [32, 35, 134] have shown that substitution in position 1 affects the wavefunctions of symmetry B_{2u} through the atomic orbitals of the ring carbon atoms in positions 1, 4, 5 and 8; and the wavefunctions of symmetry B_{3u}^- through the atomic orbitals of the ring carbon atoms 2, 3, 6 and 7. Since the $A_{1g} \rightarrow B_{3u}^+$ transitions, from

data in Tables 24-29 usually vary in the same direction as the $A_{1g} \rightarrow B_{3u}^-$ transitions, it can be said that the electronic transitions of the $A_{1g} \rightarrow B_{3u}^+$ are also polarised parallel to the long axis of the molecule.

A comparison of the values of λ_{\max} for each of the transitions, of the di- and mono-substituted naphthalene derivatives reveals that the electronic spectra for the disubstituted derivatives are identical with those of the monosubstituted derivatives. It can be noticed that in disubstituted naphthalene derivatives, the effect of the substituents on the position of the $\pi-\pi^*$ transitions is not additive. This is contrary to what is expected from perturbation theory, where the effect of weak substituents on the position of $\pi-\pi^*$ transitions in the ring in polysubstituted derivatives are expected to be additive [107]. This appreciable deviation from additivity is particularly pronounced for substituents such as nitro- and amino-groups which are known to cause strong perturbation of the π -electron systems in the ring.

4.3 SOLVENT EFFECT ON ELECTRONIC SPECTRA

Some of the substituted naphthalene compounds for which HMO calculations have been done have also been examined as to their electronic absorption spectra, in various solvents between 200 nm - 480 nm.

Figures 25-30 show the effect of solvent on the absorption spectra of naphthalene, 1-naphthol, 1-naphthylamine, 1-nitronaphthalene, 4-nitro-1-naphthylamine and 4-bromo-1-naphthylamine. The detailed characterization of the spectral properties of the compounds are found in Table 30. In general, three major bands which have been designated ' L_b ', ' L_a ', ' B_b ' in the order of increasing energy are observable in these compounds. The presence of these three regions in the curves of the simple derivatives of naphthalene examined suggests that the absorptions were due, in each case, to the naphthalene molecule. This reason, and the observations from Table 30 that each transition in each of the compounds examined is red shifted in polar relative to non-polar solvents should allow the classification of all the transitions as $\pi-\pi^*$.

For most of the compounds, the shortest wavelength

Figure 25. The electronic absorption spectra of naphthalene in

- (a) Acetonitrile (b) Chloroform (c) Methanol
 (d) n-Heptane (e) Cyclohexane (f) Ethanol
 (g) Methylcyclohexane

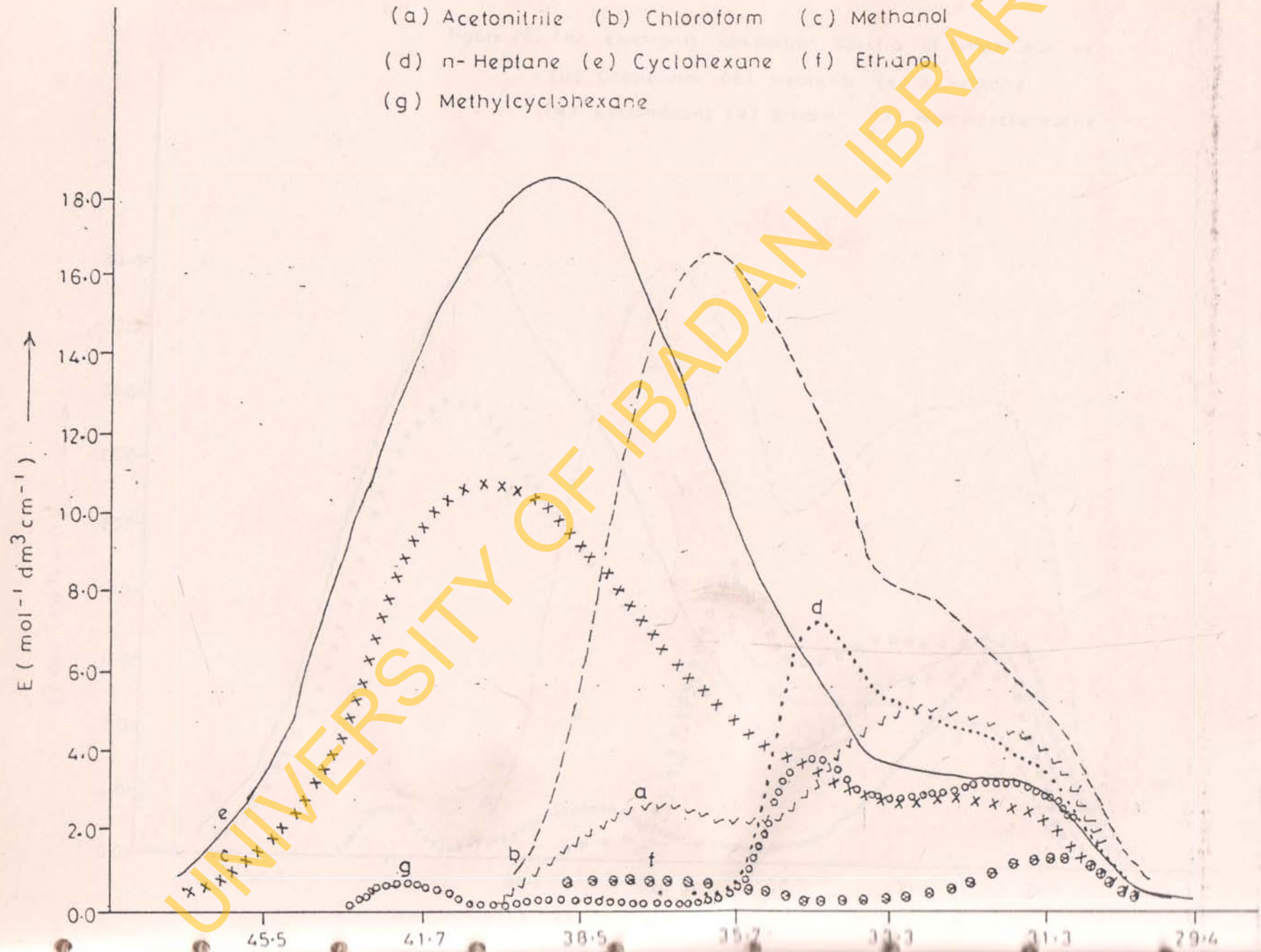


Figure 26. The electronic absorption spectra of 1-naphthol in
 (a) Chloroform (b) Methanol (c) n-Heptane
 (d) Cyclohexane (e) Ethanol (f) Methylcyclohexane

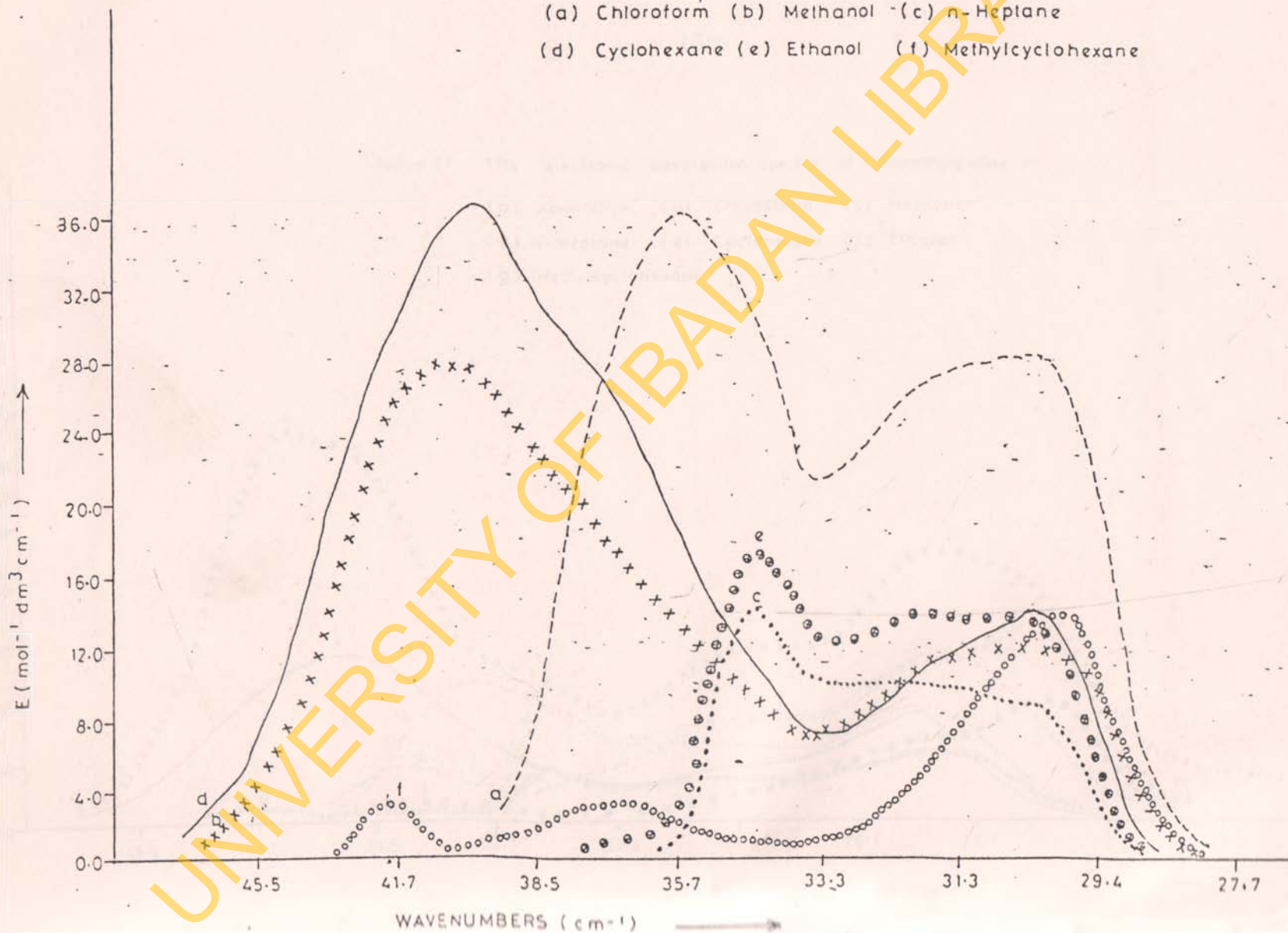


Figure 27. The electronic absorption spectra of 1-naphthylamine in

- (a) Acetonitrile (b) Chloroform (c) Methanol
 (d) n-Heptane (e) Cyclohexane (f) Ethanol
 (g) Methylcyclohexane

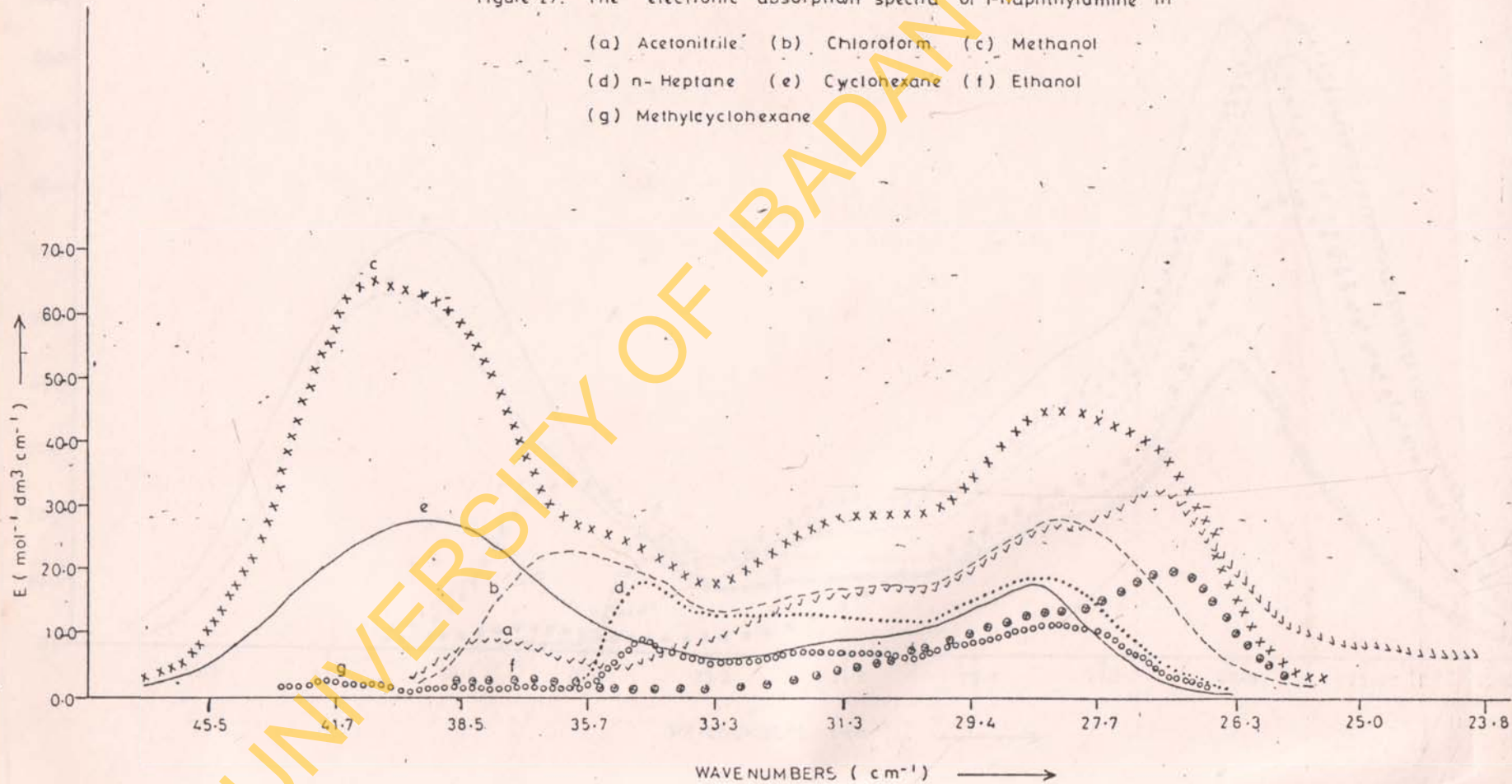


Figure 28. The electronic absorption spectra of 1-nitronaphthalene in
 (a) Acetonitrile (b) Chloroform (c) Methanol
 (d) n-Heptane (e) Cyclohexane (f) Ethanol
 (g) Methylcyclohexane

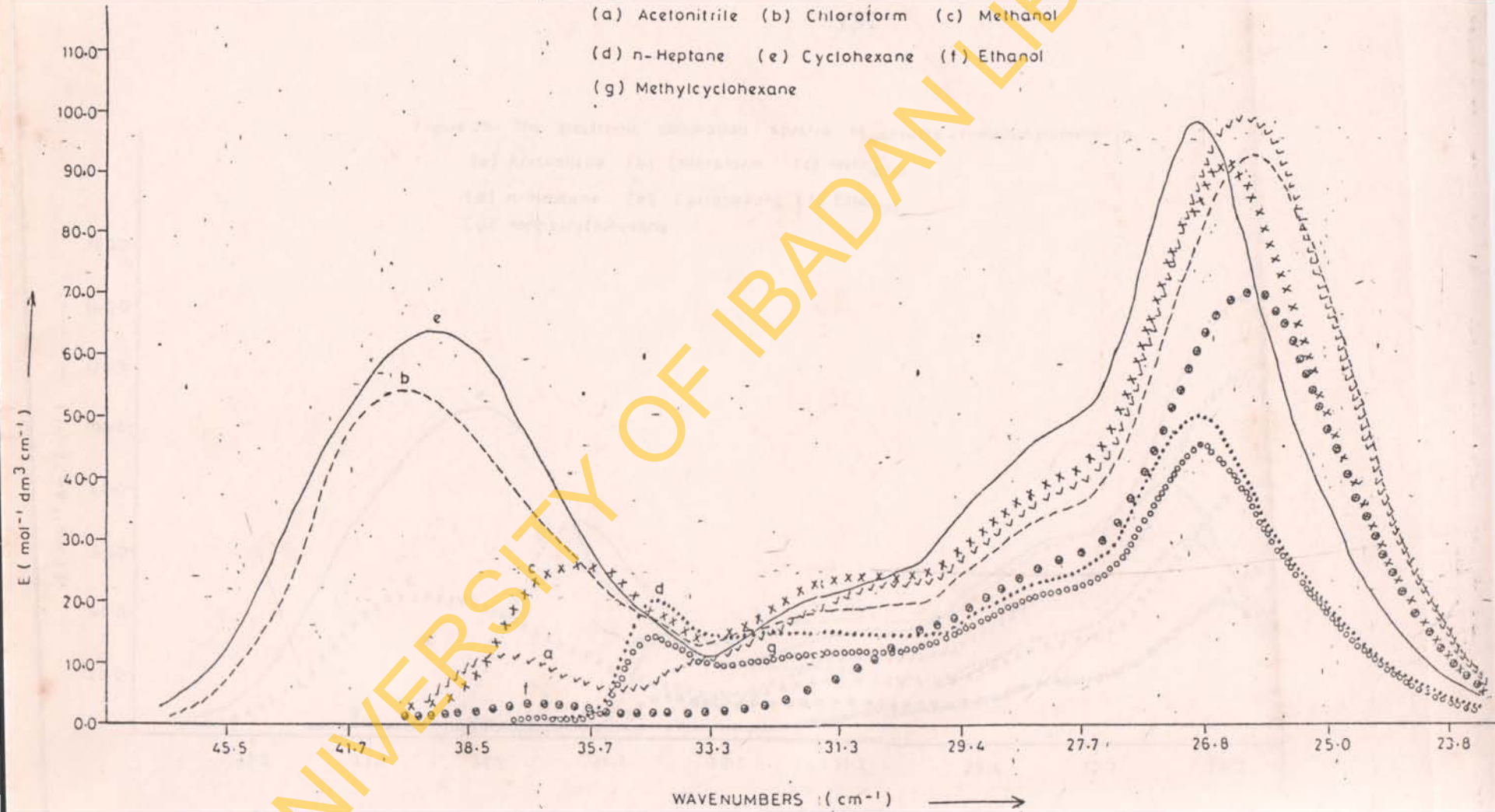


Figure 29. The electronic absorption spectra of 4-nitro-1-naphthylamine in
 (a) Acetonitrile (b) Chloroform (c) Methanol
 (d) n-Heptane (e) Cyclohexane (f) Ethanol
 (g) Methylcyclohexane

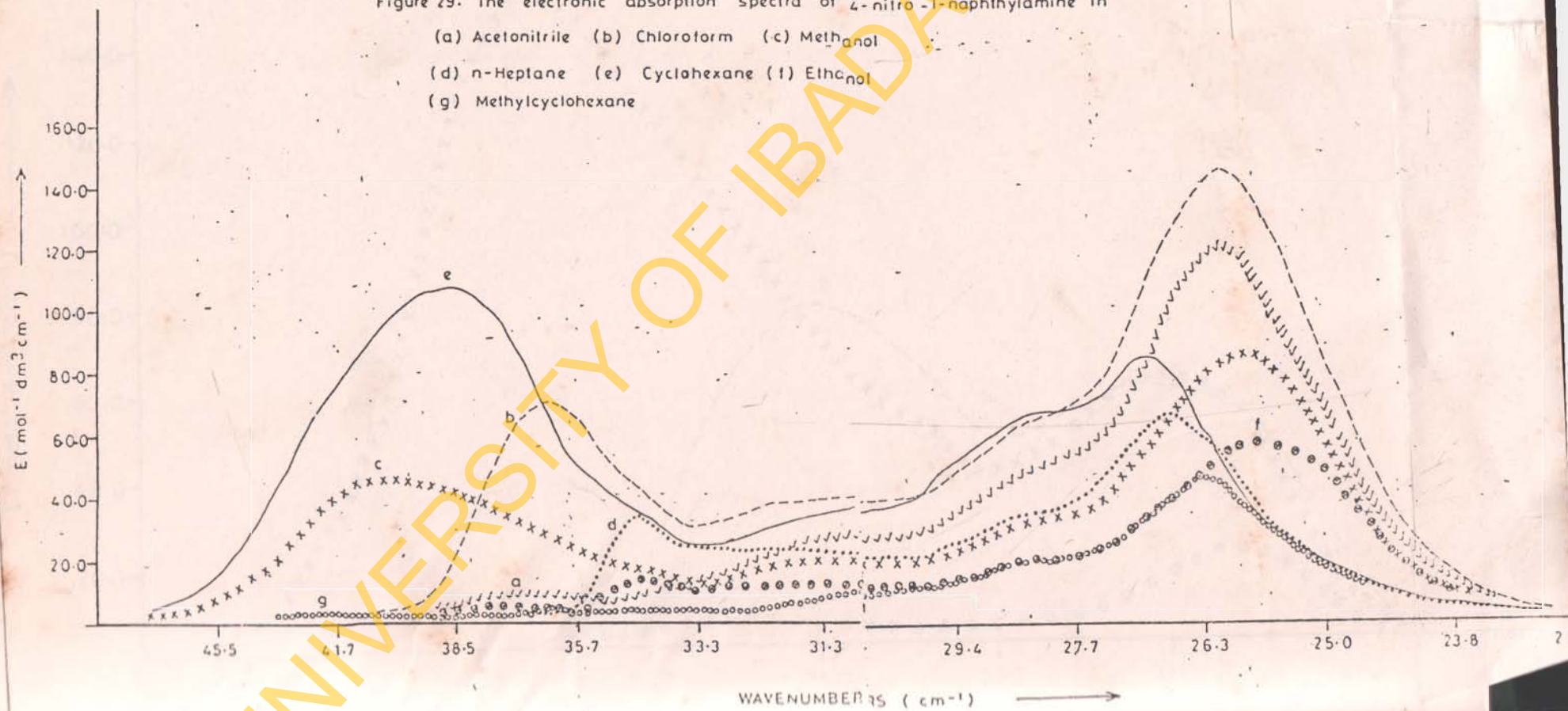


Figure 30. The electronic absorption spectra of 4-bromo-1-naphthylamine in (a) Methanol (b) Chloroform (c) Ethanol

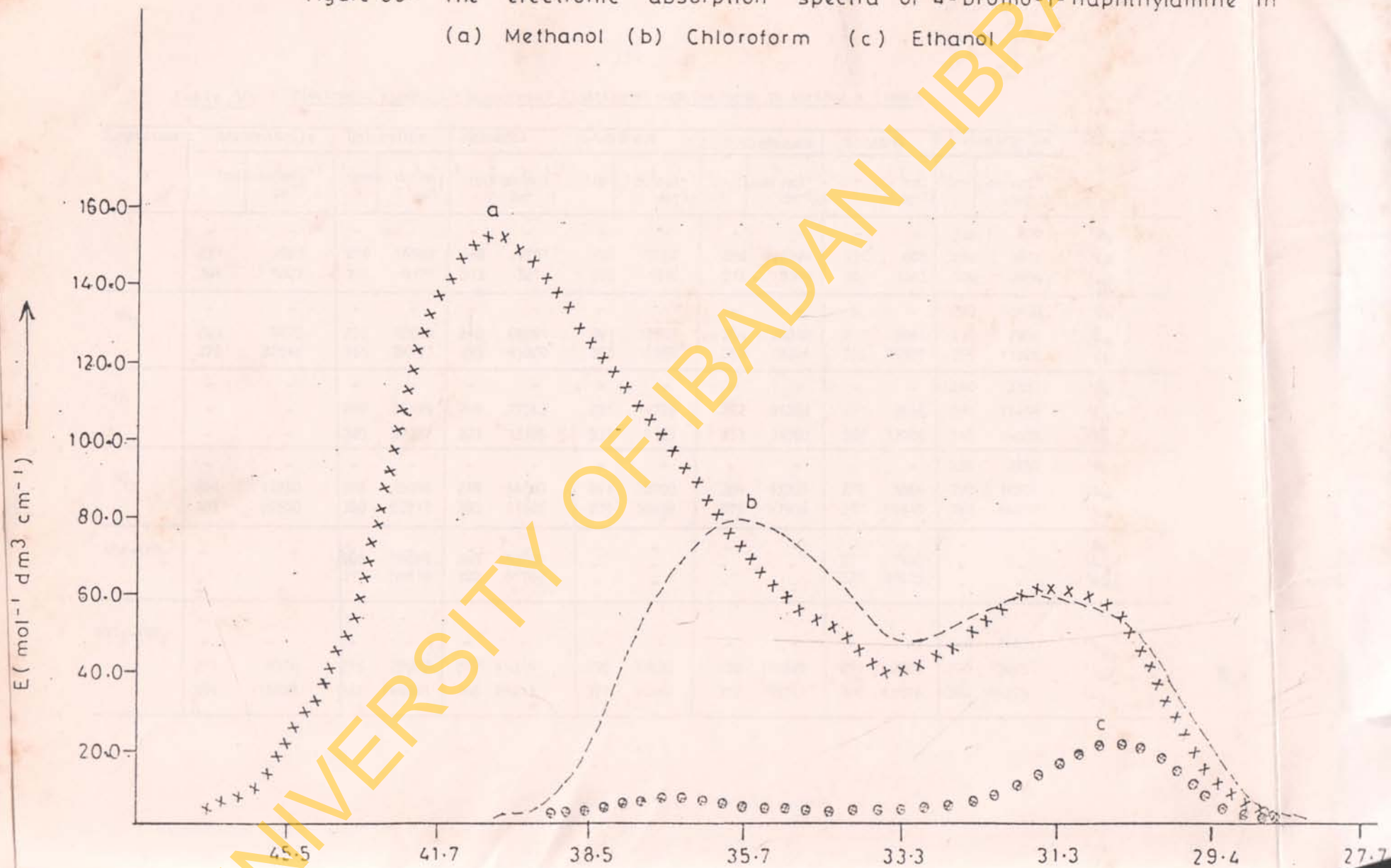


Table 30: Electronic Absorption spectra of Substituted naphthalenes in various solvents

Substituent X	Acetonitrile		Chloroform		Methanol		n-heptane		Cyclohexane		Ethanol		Methylcyclohexane		Assignment
	λ (nm)	ϵ (dm ³ mol ⁻¹ cm ⁻¹)	λ (nm)	ϵ (dm ³ mol ⁻¹ cm ⁻¹)	λ (nm)	ϵ (dm ³ mol ⁻¹ cm ⁻¹)	λ (nm)	ϵ (dm ³ mol ⁻¹ cm ⁻¹)	λ (nm)	ϵ (dm ³ mol ⁻¹ cm ⁻¹)	λ (nm)	ϵ (dm ³ mol ⁻¹ cm ⁻¹)	λ (nm)	ϵ (dm ³ mol ⁻¹ cm ⁻¹)	
H	-	-	-	-	-	-	-	-	-	-	-	-	240	670	'B _b
	271	2681	276	16502	248	10701	291	7262	256	18394	270	805	290	3871	'L _a
	304	5027	301	8177	313	3274	305	4916	310	3394	32	1363	309	2804	'L _b
NH ₂	-	-	-	-	-	-	-	-	-	-	-	-	239	1400	'B _b
	265	8475	276	22500	248	65294	291	17895	254	26842	27	2061	290	7900	'L _a
	370	32542	355	28173	355	45000	353	18158	353	18224	380	19587	355	11320	'L _b
OH	-	-	-	-	-	-	-	-	-	-	-	-	240	3181	'B _b
	-	-	280	36129	248	27763	291	14329	252	36363	27	3545	290	17454	'L _a
	-	-	325	28387	321	12105	331	9123	331	14090	380	13909	316	14000	'L _b
NO ₂	-	-	-	-	-	-	-	-	-	-	-	-	239	2536	'B _b
	266	11250	276	26086	248	54250	291	20000	254	63333	27	3684	290	14202	'L _a
	387	99500	388	92717	383	91125	379	50438	379	97936	38	69649	380	44637	'L _b
4Br-1NH ₂	-	-	280	78889	248	150769	-	-	-	-	-	-	-	-	'B _b
	-	-	317	58518	320	60769	-	-	-	-	27	7592	-	-	'L _a
	-	-	-	-	-	-	-	-	-	-	320	20925	-	-	'L _b
4NO ₂ -1NH ₂	-	-	-	-	-	-	-	-	-	-	-	-	240	2463	'E _b
	271	8276	275	70000	247	45319	290	33690	260	105920	271	2885	290	13695	'L _a
	384	119828	382	144043	386	85213	377	66667	372	85761	390	57576	380	44275	'L _b

absorption band $'B_b$ is very well separated from the other two, $'L_a$ and $'L_b$ bands which overlap to different extents in various solvents, the overlap being minimal in methylcyclohexane. Thus, it can be said that the relative transition energies of the $'L_a$ and $'L_b$ transitions in the substituted naphthalene compounds examined, and hence the degree of overlap of the corresponding bands are influenced not only by the type of substituent in the ring but also by the solvent. For most of the compounds, it should be reasonable to interpret that the vibronic states of the $'L_a$ and $'L_b$ transitions are so close that the absorption bands corresponding to these transitions are merged into broad and unsymmetrical bands such that the solvent has little or no effect on the separation of these bands.

The transition intensities recorded in different solvents (Table 30) reveal that for naphthalene the intensities are of the order $'L_a > 'L_b > 'B_b$. Table 30 shows that the $'L_a$ transition is much more sensitive to solvent perturbation than the $'B_b$ or $'L_b$ as regards changes in transition intensity and

energy.

In comparison to other solvents, the spectra of the examined compounds in heptane is unique. Apart from the relatively low transition intensities, for most of the compounds, one cannot make out any meaningful change in the transition energies of the $'L_a$ band in the spectra. Thus, on this basis alone, one tends to believe that the perturbation by heptane of the $'L_a$ band in the series of compounds examined, if at all, can only be very minimal.

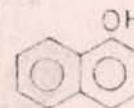
The symmetrical nature of the Franck-Condon envelope of the $'B_b$ and $'L_a$ bands in naphthalene, 1-naphthol, 1-naphthylamine, 4-bromo-1-naphthylamine and also of both the $'L_a$ and $'L_b$ bands in 1-nitronaphthalene and 4-nitro-1-naphthylamine give indication that the most intense vibrational transitions in these compounds are those in which the electron oscillates in an excited state vibrational level other than the zero-point one, and suggests that the $'L_a$ transition is accompanied by changes in the equilibrium nuclear coordinate of the substituted naphthalene compounds. Tables 31-36 also give the

Table 31: Calculated Oscillator strengths (f), half-band widths ($\nu_{1/2}$), dipole moments (μ) in various solvents for naphthalene



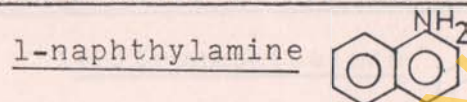
Solvents	λ (nm)	$\nu_{1/2}$ (cm ⁻¹)	f	μ (D)	λ (nm)	$\nu_{1/2}$ (cm ⁻¹)	f	μ (D)
Acetonitrile	271	4428	0.03	1.2	304	4442	0.05	1.7
Chloroform	276	4689	0.17	3.2	301	4196	0.07	2.2
Methanol	248	7189	0.17	3.0	313	2883	0.02	1.2
n-heptane	291	2099	0.001	0.7	305	4156	0.04	1.7
Cyclohexane	256	7891	0.31	4.2	310	3256	0.05	1.8
Ethanol	270	3250	0.006	0.6	321	2292	0.005	0.6
Methylcyclohexane	290	2099	0.018	1.1	309	2843	0.017	1.1

Table 32: Calculated oscillator strengths (f), half-band widths ($\nu_{1/2}$)
dipole moments (μ) in various solvents for 1-naphthol



Solvents	λ (nm)	$\nu_{1/2}$ (cm^{-1})	f	μ (D)	λ (nm)	$\nu_{1/2}$ (cm^{-1})	f	μ (D)
Acetonitrile	-	-	-	-	-	-	-	-
Chloroform	280	4545	0.35	4.6	325	4544	0.28	4.4
Methanol	248	7319	0.44	4.9	321	2234	0.11	2.8
n-heptane	291	2099	0.06	2.0	331	1741	0.03	1.6
Cyclohexane	252	7764	0.61	5.8	331	3268	0.10	2.7
Ethanol	271	3250	0.02	1.2	386	2292	0.06	2.4
Methylcyclohexane	290	2113	0.08	2.2	316	3835	0.12	2.8

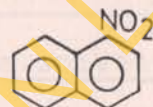
Table 33: Calculated oscillator strengths (f), half-band width ($\nu_{1/2}$)
dipole moments (μ) in various solvents for



Solvents	$\lambda(\text{nm})$	$\nu_{1/2}(\text{cm}^{-1})$	f	$\mu(\text{D})$	$\lambda(\text{nm})$	$\nu_{1/2}(\text{cm}^{-1})$	f	$\mu(\text{D})$
Acetonitrile	265	3501	0.06	1.9	370	2777	0.19	3.9
Chloroform	276	4689	0.23	3.7	355	3330	0.20	3.9
Methanol	248	6660	0.94	7.1	355	3870	0.31	5.4
n-heptane	291	2099	0.08	2.3	353	2648	0.10	2.8
Cyclohexane	254	7507	0.44	4.9	353	2981	0.12	3.0
Ethanol	271	3548	0.02	1.2	370	3659	0.15	3.5
Methylcyclohexane	290	1654	0.03	1.3	355	2164	0.05	2.0

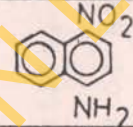
Table 34: Calculated Oscillator strengths (f), half-band widths ($\nu_{\frac{1}{2}}$), dipole moments (μ), in various solvents for

1-nitronaphthalene



Solvents	λ (nm)	$\nu_{\frac{1}{2}}$ (cm^{-1})	f	μ (D)	λ (nm)	$\nu_{\frac{1}{2}}$ (cm^{-1})	f	μ (D)
Acetonitrile	258	3832	0.09	2.3	387	2617	0.56	6.8
Chloroform	276	4689	0.26	6.7	388	2677	0.54	6.7
Methanol	248	7261	0.85	6.8	383	2673	0.53	6.6
n-heptane	291	2113	0.09	2.4	379	2525	0.27	4.7
Cyclohexane	254	7698	1.05	7.6	379	2652	0.56	6.8
Ethanol	271	3399	0.03	1.3	387	2617	0.39	5.8
Methylcyclohexane	290	1767	0.05	1.8	380	2372	0.23	4.3

Table 36: Calculated oscillator strength (f) half-band widths ($\nu_{\frac{1}{2}}$)
dipole moments (μ) in various solvents for
4-nitro-1-naphthylamine



solvents	λ (nm)	$\nu_{\frac{1}{2}}$ (cm ⁻¹)	f	μ (D)	λ (nm)	$\nu_{\frac{1}{2}}$ (cm ⁻¹)	f	μ (D)
Acetonitrile	271	3548	0.06	1.9	384	2675	0.69	7.5
Chloroform	275	4009	0.61	6.0	382	2749	0.86	8.4
Methanol	247	7319	0.72	6.2	386	2570	0.47	6.3
n- heptane	290	2099	0.15	3.1	377	2267	0.32	5.2
Cyclohexane	260	6947	1.58	9.5	372	2342	0.43	5.9
Ethanol	271	3548	0.02	1.1	390	2724	0.34	5.4
Methylcyclo- hexane	290	1878	0.06	1.9	380	2284	0.22	4.2

solvents and the half-bandwidths of electronic transitions. The more polar solvents have greater half-bandwidths for the 1L_a transitions than in methylcyclohexane, which suggests that solute-solvent interaction may be the origin of perturbation for this band.

To know which solvent effects [135-137] predominate in the examined compounds, solvent polarity effects on the electronic transition of each compound, as a function of different solvent physical properties and empirical parameters are summarized in Table 37 (a-f). Figures 31-33 show typical plots. The results in row 1 of each table show that there is no meaningful correlation between solvent dielectric constant (ϵ) and the solvent induced shifts. Solvent ϵ has been shown to be a useful measure of solvent polarity effects on electronic transitions in the absence of solvent-solute interactions [138,139]. Therefore, the poor correlation may indicate the presence of other solvent-solute forces [138]. This is particularly noticeable for naphthalene in the ground state solvent configuration ($r = -0.0769$,

Table 37: Linear regression parameters obtained from plots of the ν_{lb} band maxima (ν_{obs}) vs solvent physical properties and solvent empirical parameters for:

	y	m	r
<u>a: Naphthalene</u>			
1. $\epsilon - 1/2\epsilon + 1$	3.2505	-0.0546	-0.0769
2. $n^2 - 1/n^2 + 2$	2.9456	1.2057	0.4499
3. π^*	2.6511	0.8915	0.9951
<u>b: 1-naphthol</u>			
1. $\epsilon - 1/2\epsilon + 1$	3.3088	-1.0187	-0.5410
2. $n^2 - 1/n^2 + 2$	2.6767	1.1758	0.0055
3. π^*	1.1881	2.6407	0.1679
<u>c: 1-naphthylamine</u>			
1. $\epsilon - 1/2\epsilon + 1$	3.0562	-0.7523	-0.6736
2. $n^2 - 1/n^2 + 2$	2.4752	1.2961	-0.2467
3. π^*	2.6522	0.1659	1.4637

Table 37 (Contd.)

<u>d: 1-nitronaphthalene</u>			
	y	m	r
1. $\epsilon - 1/2\epsilon + 1$	2.7388	-0.3684	-0.7647
2. $n^2 - 1/n^2 + 2$	2.5418	0.2643	0.0075
3. π^*	2.5396	0.0759	-0.5154
<u>e: 4-nitro-1-naphthylamine</u>			
1. $\epsilon - 1/2\epsilon + 1$	2.8532	-0.6499	0.6619
2. $n^2 - 1/n^2 + 2$	2.3754	1.0184	0.6461
3. π^*	2.4579	0.2095	0.9219
<u>f: 4-bromo-1-naphthylamine</u>			
1. $\epsilon - 1/2\epsilon + 1$	4.3050	-3.1037	-1.147
2. $n^2 - 1/n^2 + 2$	2.2554	3.0223	0.0076
3. π^*	1.7440	1.9253	0.6945

Figure 31: Plots of ν_{\max} vs $\epsilon^{-1/2\epsilon+1}$ for (a) 1-naphthol (b) 4-nitro-1-naphthylamine (c) naphthalene (d) 1-naphthylamine (e) 1-nitronaphthalene from different solvents: (1) cyclohexane (2) methylcyclohexane (3) chloroform (4) ethanol (5) methanol (6) acetonitrile

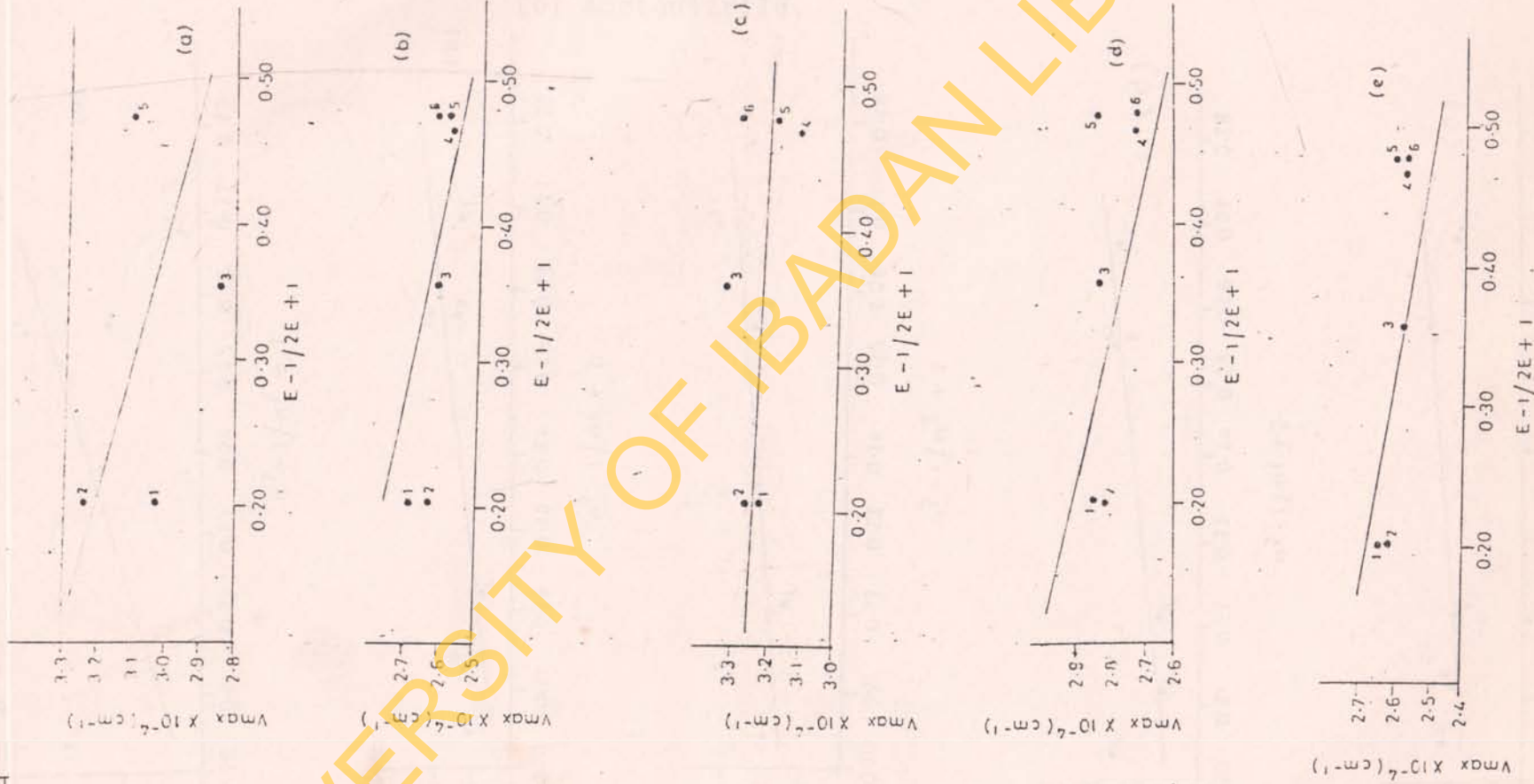


Fig. 32: Plots of v_{\max} vs $n^2 - 1/n^2 + 2$ for (a) 1-naphthol (b) 4-nitro-1-naphthylamine (c) naphthalene (d) 1-naphthylamine. (e) 1-nitronaphthalene from different solvens: (1) cyclohexane (2) methylcyclohexane (3) chloroform (4) ethanol (5) methanol (6) acetonitrile.

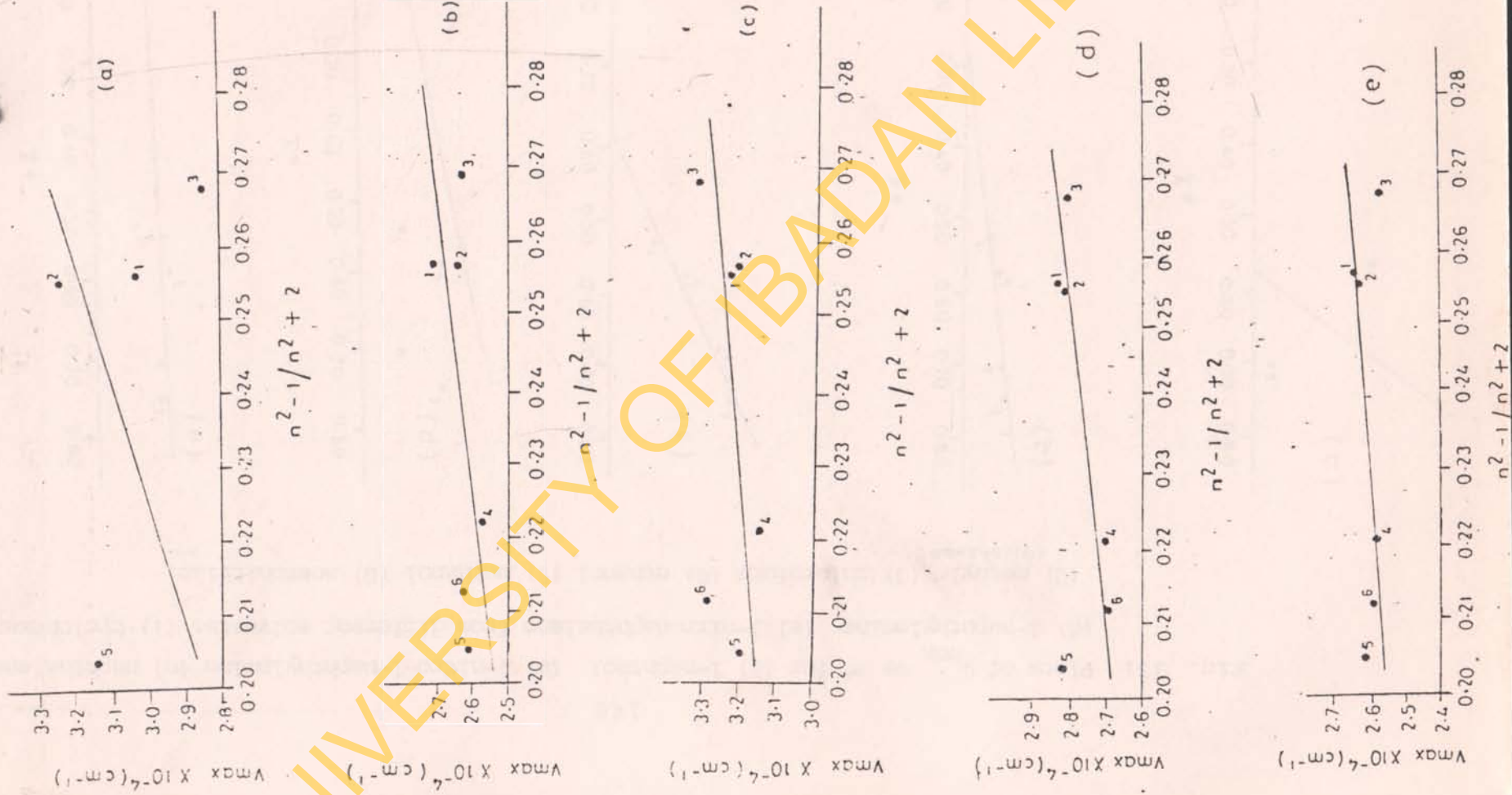


Fig. 33: Plots of ν_{\max} vs π^* for (a) 1-naphthol (b) 4-nitro-1-naphthylamine (c) naphthalene (d) 1-naphthylamine (e) 1-nitronaphthalene from different solvents: (1) cyclohexane (2) methyl- (3) chloroform (4) ethanol (5) methanol (6) acetonitrile.

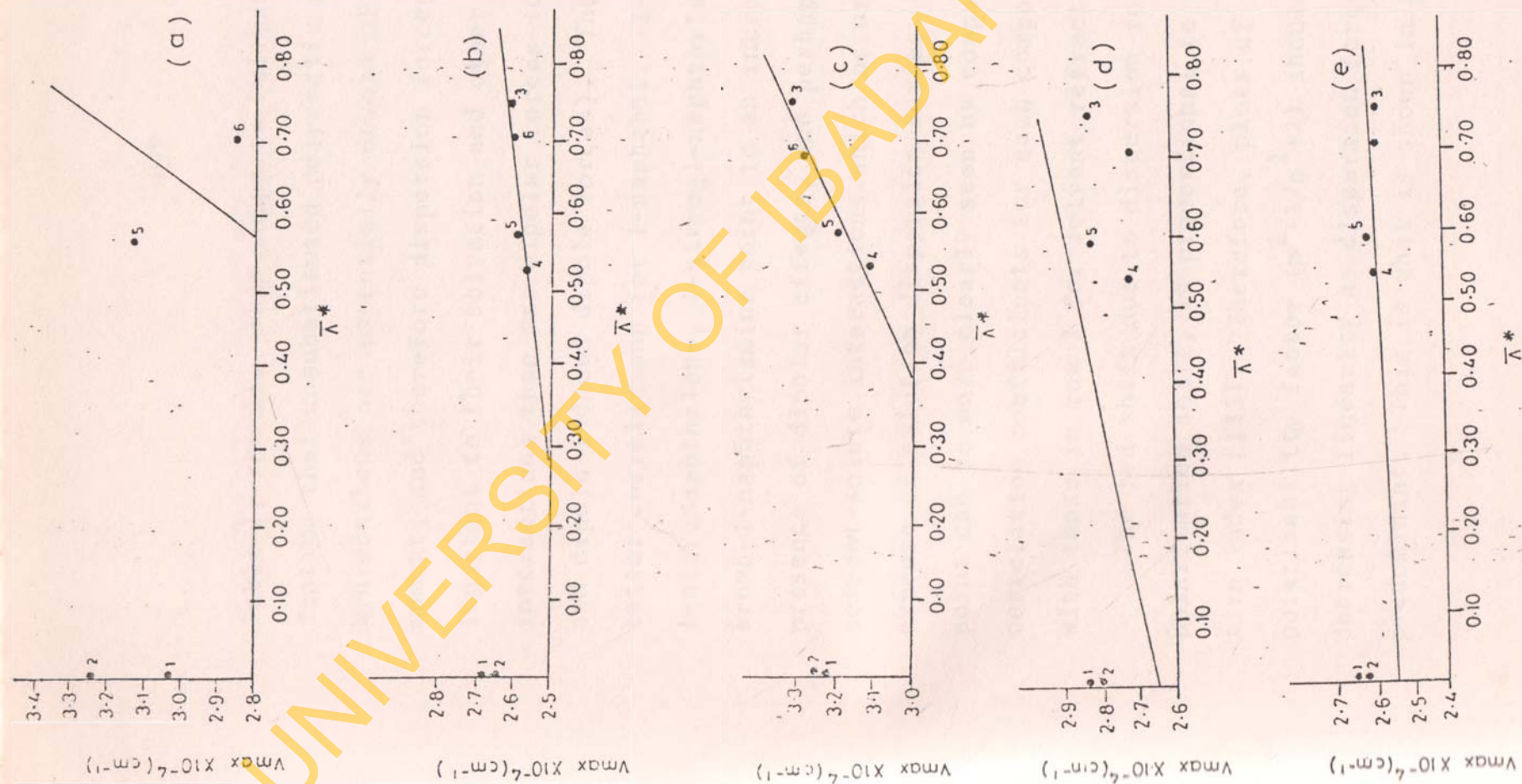


Table 1, row 1). This supports Pullmans [139] contention that unsubstituted polycyclic aromatic hydrocarbons are essentially devoid of dipole moment, and therefore dispersion forces are more important to their solvation and other physical interactions than are dipolar forces (dipole-dipole and dipole-induced dipole forces). The relatively better correlations for 1-naphthol, 1-naphthylamine, 1-nitronaphthalene, 4-nitro-1-naphthylamine and 4-bromo-1-naphthylamine point to an increase in the presence of dipolar effects, and perhaps other solvent-solute interactions which occur at the expense of solution dispersion forces. This latter point can be more clearly seen by comparing the correlation coefficients for each compound in row 1 with those in row 2 for solvent refractive index.

The red shift due to dispersion forces, the polarization shift, is proportional to solvent refractive index [135]. Therefore, plots of ν_{obs} vs the polarizability factor $(n^2 - 1/n^2 + 2)$ should demonstrate decreasing linearity as dispersion forces become less predominant. This is what is shown in row 2 of the

tables for these compounds in the ground state solvent configuration, the correlation coefficients coming in about the reverse order of that shown in row 1 for solvent ϵ .

The π^* scale of solvent polarity-polarizability devised by Kamlet and Taft [140] combines solvent polarity (proportional to ϵ or μ) and solvent polarizability (proportional to n) into a single term. The correlation coefficient ^{plots} of ν_{obs} vs π^* for all the solvents are given in row 3 of the tables for each of the compounds. Tables 37 (a-f) give excellent correlation for naphthalene, 1-naphthylamine, 4-nitro-1-naphthylamine and 4-bromo-1-naphthylamine in the ground state solvent configuration. The unappreciable increase in correlation coefficients going from row 2 to row 3 in 1-naphthol may indicate the presence of hydrogen bonding effects.

Generally, solvent medium effects on 1-naphthol and 1-naphthylamine are expected to be quite pronounced in the relatively polar hydrogen-bonding solvents. Therefore, the emergence of, and or increase in intensity of the L_a band only in hydrogen

bonding solvents with fairly high dielectric constant (excepting the case of cyclohexane) may be due to the fact that hydrogen bonding lowers the energy of the ground state more than that of the excited state with a consequent increase in excitation energy and a blue shift. Also, the high dielectric constant of solvents such as methanol, will favour the production of polar structures. The dipolar excited states are expected to be stabilized by an increase in the dielectric constant more than the non-polar ground state [136]. Therefore, a solvent possessing the two properties of being hydrogen bonding and having high dielectric constant such as methanol will combine these two effects. This will consequently lead to a higher transition energy than would have been otherwise in a solvent not combining these two properties, and the emergence of a short wavelength band as expected.

4.4 GROUND AND EXCITED STATE DIPOLE MOMENTS

The ground state dipole moments of 1- and 2- $C_{10}H_7X$, 1-OH $C_{10}H_6$ 2X (and 4X) have been estimated using the calculated charge density distribution in

Figures 19-24 and are tabulated in Table 38. The dipole moments in each case are calculated in the direction of polarization and have been compared with experimental values. The calculated dipole moments in these molecules show a number of significant features. The 1-methylnaphthalene calculated to have a small dipole moment (0.74D) is in agreement with experimental data (0.28D) [137] in the direction of $\text{Me}^+ - \text{C}_{10}\text{H}_7^-$. This should arise primarily from a polarization of the π -electrons leading to an alternating π -charge in the ring with negative charges at the ortho- and para-positions (Figure 34).

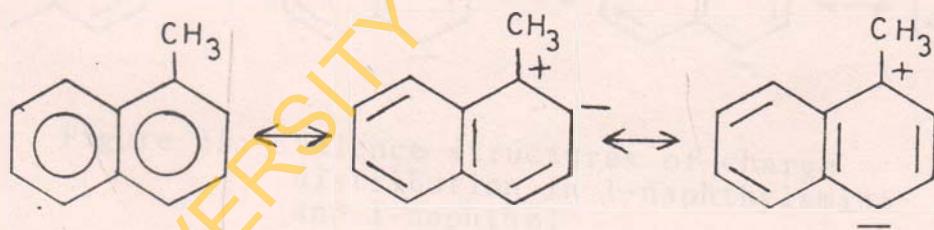


Figure 34: Alternating π -charges in the ring of 1-methylnaphthalene

The charge densities in 1-naphthylamine, 1-naphthol and 1-methoxynaphthalene show substantial π -charge donation from the nitrogen and oxygen atoms into the

ring. The magnitude of the π -donation is large for the molecules, presumably because of their planarity and better overlap of the lone pairs with the naphthalene π -orbitals. The π -charge distribution show large negative charges at the ortho- and para-positions supporting the usual ideas of contributing valence structures (Figure 35).

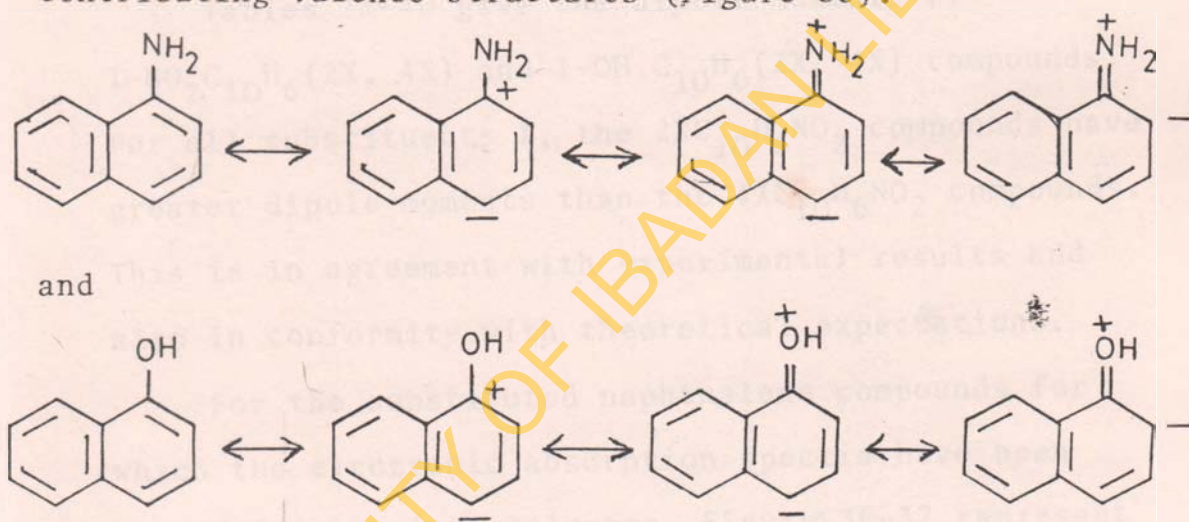


Figure 35: Valence structures of charge distribution in 1-naphthylamine and 1-naphthol

For $1\text{-C}_{10}\text{H}_7\text{NO}_2$ and $1\text{-C}_{10}\text{H}_7\text{CO}_2\text{H}$, the charge distributions show withdrawals of π -electrons from the ring.

In $\text{C}_{10}\text{H}_7\text{NO}_2$, the calculated dipole moment of 3.35D is close to the experimental value of 3.87D. The agreement between the calculated and observed dipole

moments for the 2-C₁₀H₇X compounds is poorer than for the 1-C₁₀H₇X compounds. Also, a comparison of the dipole moments, $\mu_{\text{calc.}}$ of 1-C₁₀H₇X with those of 2-C₁₀H₇X indicate that $\mu_{\text{calc.}}$ was somewhat higher for the 2-C₁₀H₇X compounds.


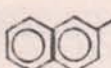
Tables 38-40 give the dipole moments of 1-NO₂C₁₀H₆ (2X, 4X) and 1-OH C₁₀H₆ (2X, 4X) compounds. For all substituents X, the 2XC₁₀H₆NO₂ compounds have greater dipole moments than the 4XC₁₀H₆NO₂ compounds. This is in agreement with experimental results and also in conformity with theoretical expectations.

For the substituted naphthalene compounds for which the electronic absorption spectra have been recorded in various solvents, Figures 36-37 represent plots of transition energies against $f(D)$ as given by McRae [111] in the form of

$$\Delta E = \Delta\mu_{g-e} \frac{\mu_g}{a^3} \Delta f(D) \quad \dots \quad (57)$$

where,

- ΔE = transition frequency in wave numbers
- μ_g = ground state dipole moment of molecules
- μ_e = excited state dipole moment of molecules

Table 38: Calculated ground state dipole moments compared with experimental values for  and  in Debyes

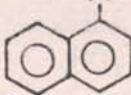
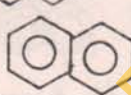
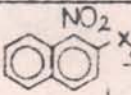
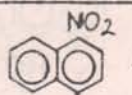
Substituent X				
	$\mu_{\text{calc.}}$	$\mu_{\text{exp.}}$	$\mu_{\text{calc.}}$	$\mu_{\text{exp.}}$
H	0.00	0.00	0.00	0.00
CH ₃	0.74	0.28	1.04	0.44
CO ₂ H	1.54	1.87	1.72	1.95
NO ₂	3.35	3.87	3.46	4.40
CHO	3.58	-	2.04	-
OCH ₃	2.00	1.76	2.18	1.25
Br	1.05	1.29	3.00	1.70
NH ₂	1.50	1.50	2.13	1.79
OH	1.85	1.46	2.41	1.54

Table 39: Calculated ground state dipole moments compared with experimental values for  and  in Debyes

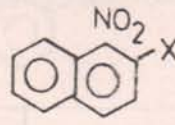
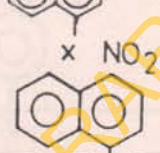
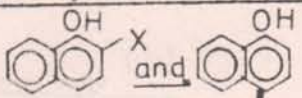
Substituent X				
	μ calc.	μ exp.	μ calc.	μ exp.
NO ₂	7.28	6.48	0.25	1.42
Br	6.53	-	2.34	-
CH ₃	2.44	-	2.43	-
CN	6.19	-	0.55	-
NH ₂	4.13	4.45	5.64	6.43
OH	4.02	3.89	5.36	5.27
CO ₂ H	4.38	-	1.66	-

Table 40: Calculated ground states dipole moments compared with experimental values for  in Debyes

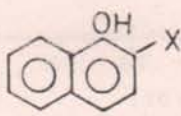
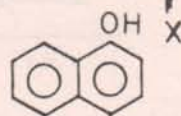
Substituent X				
	$\mu_{\text{calc.}}$	$\mu_{\text{exp.}}$	$\mu_{\text{calc.}}$	$\mu_{\text{exp.}}$
NO ₂	4.13	4.11	5.36	5.27
Br	3.39	-	2.80	-
CH ₃	0.71	-	2.45	-
CN	4.45	-	5.70	-
NH ₂	1.58	1.67	1.25	-
OH	1.00	-	0.00	-
CO ₂ H	2.35	2.83	3.50	3.57

Fig. 36: Plots of ν_{\max} ($^{\circ}\text{L}_b$) vs $2(D-1)/(2D+1)$ for (a) 1-naphthol (b) 4-nitro-1-naphthylamine (c) naphthalene (d) 1-naphthylamine (e) 1-nitronaphthalene (f) 4-bromo-1-naphthylamine from different solvents: (1) methylcyclohexane (2) cyclohexane (3) ethanol (4) methanol (5) chloroform (6) acetonitrile

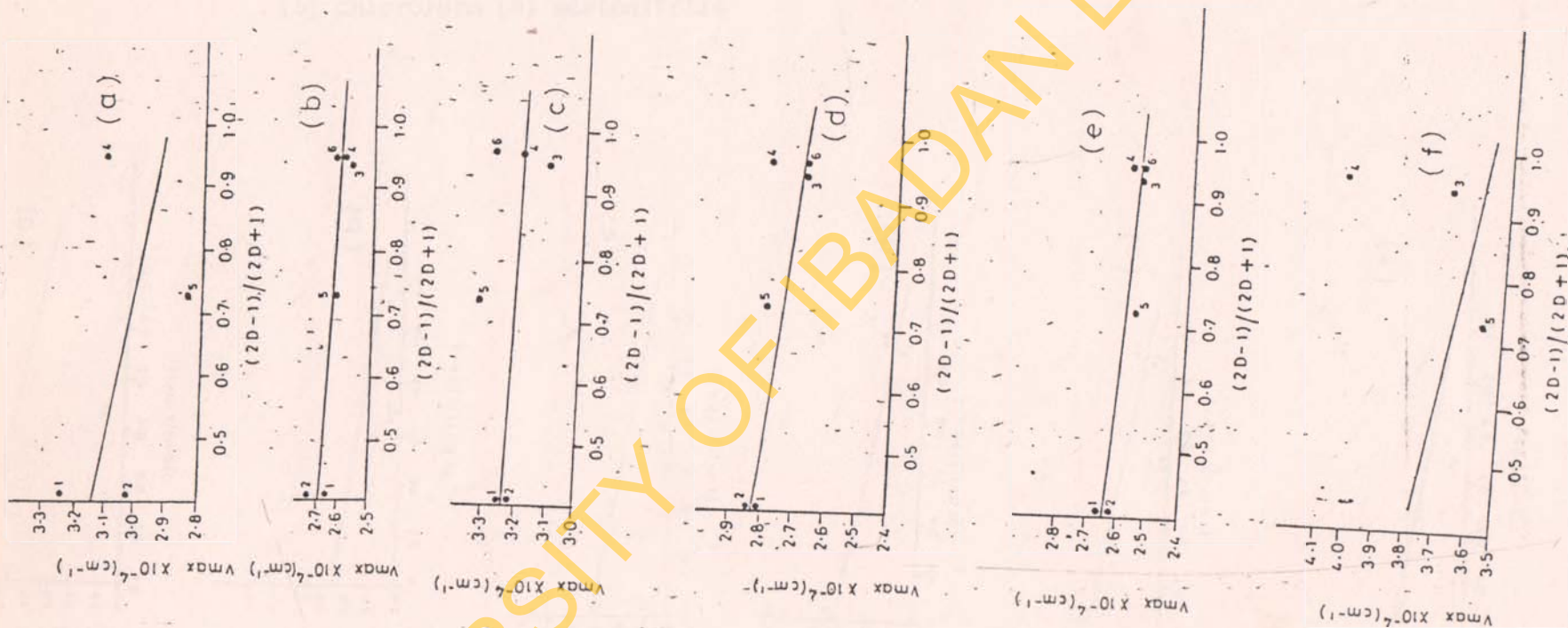
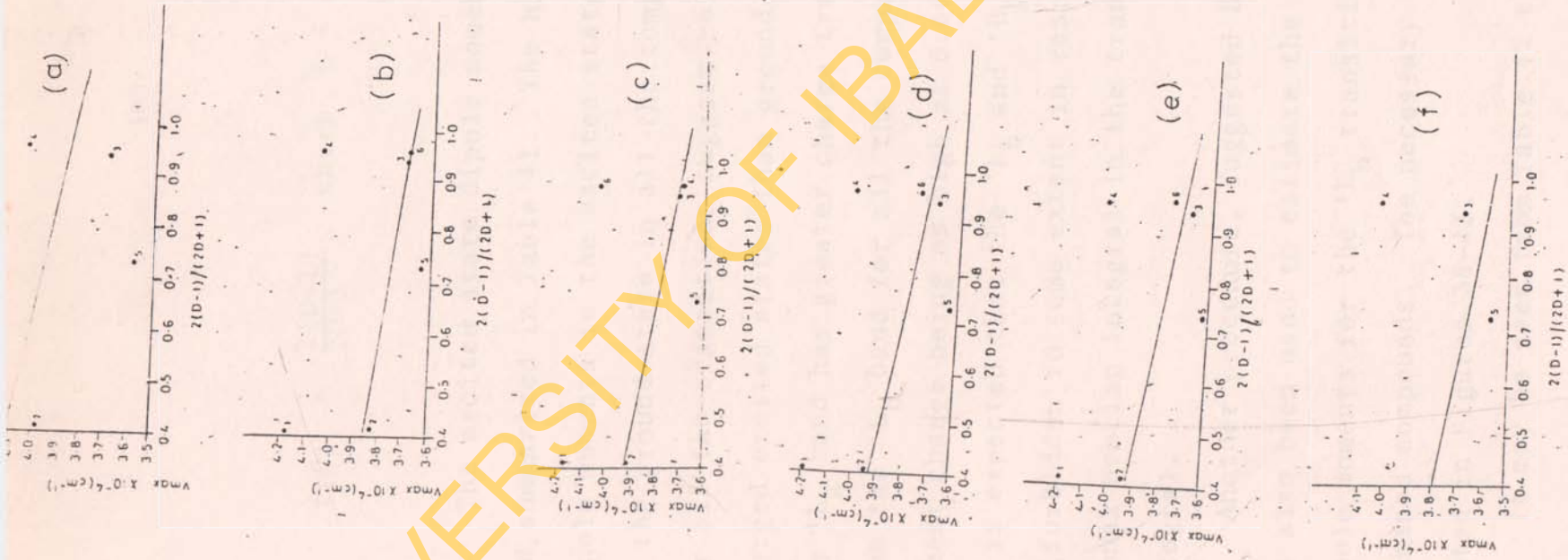


Fig. 37: Plots of $\nu_{\max} ('L_a)$ vs $2(D-1)/(2D+1)$ for (a) 1-naphthol (b) 4-nitro-1-naphthylamine (c) naphthalene (d) 1-naphthylamine (e) 1-nitronaphthalene (f) 4-bromo-1-naphthylamine for different solvents: (1) methylcyclohexane (2) cyclohexane (3) ethanol (4) methanol (5) chloroform (6) acetonitrile



$$f(D) = \frac{2(D-1)}{2D+1}, \text{ where } D = \text{dielectric constant of solvent medium.}$$

The excited state dipole moments were computed and summarized in Table 41. The higher values of the dipole moments in the excited state relative to that of the ground state in all the compounds studied and for all the transitions suggest relatively more charged excited states than ground states. However, the $'L_a$ band has greater charge transfer character than the $'L_b$ band for all the compounds, the dipole moment change being as high as $6.66D$ in 1-naphthol. It is expected that the $'L_b$ and $'B_b$ transition should be forbidden to some extent in respect of the vibrational overlap integral in the transition moment integral.

Another procedure, suggested by Rao et al [142] has also been used to estimate the excited state dipole moments for the $'L_b$ transitions of the examined compounds. The necessary plots are represented in Figures 38-43.

It may be seen from Table 42 that the μ_e estimated

Table 41: Molecular Volumes (a^3): dipole moments in the ground (μ_g) and excited (μ_e) states estimated by McRae's method for 1L_a and 1L_b bands

Compound	$10^{23} a^3 (\text{cm}^3)$	μ_g	1L_b			1L_a		
			$\Delta\mu\mu^*$	μ_e	θ	$\Delta\mu\mu^*$	μ_e	θ
Naphthalene	7.48	0.00	-	-	-	-	-	-
1-naphthylamine	8.25	1.50	3.74	5.24	73	5.65	7.15	78
1-naphthol	7.73	1.46	5.94	7.40	79	6.66	8.12	80
1-nitronaphthalene	8.62	3.87	0.58	4.45	30	2.36	6.23	52
4-bromo naphthylamine	9.74	3.72	2.41	6.13	54	2.90	6.62	56
4-nitro-1-naphthylamine	9.58	6.43	1.75	8.18	38	1.32	7.75	34

Table 42: Molecular Volumes(a^3); dipole moments in the ground (μ_g) and excited (μ_e) states estimated by Rao's method for 1L_b band

Compound	$10^{23} a^3 (\text{cm}^3)$	μ_g	1L_b		
			$\Delta\mu\mu^*$	μ_e	θ
Naphthalene	7.48	0.00	6.81	6.81	90
1-naphthylamine	8.25	1.50	11.67	13.17	83
1-naphthol	7.73	1.46	13.05	14.51	84
1-nitronaphthalene	8.62	3.87	7.09	10.96	69
4-bromo-1-naphthylamine	9.74	3.72	4.84	8.56	64
4-nitro-1-naphthylamine	9.58	6.43	16.33	22.76	74

Fig. 38: A plot of X vs Y in Rao's method of estimating excited state dipole moment of the L_b band in Naphthalene.

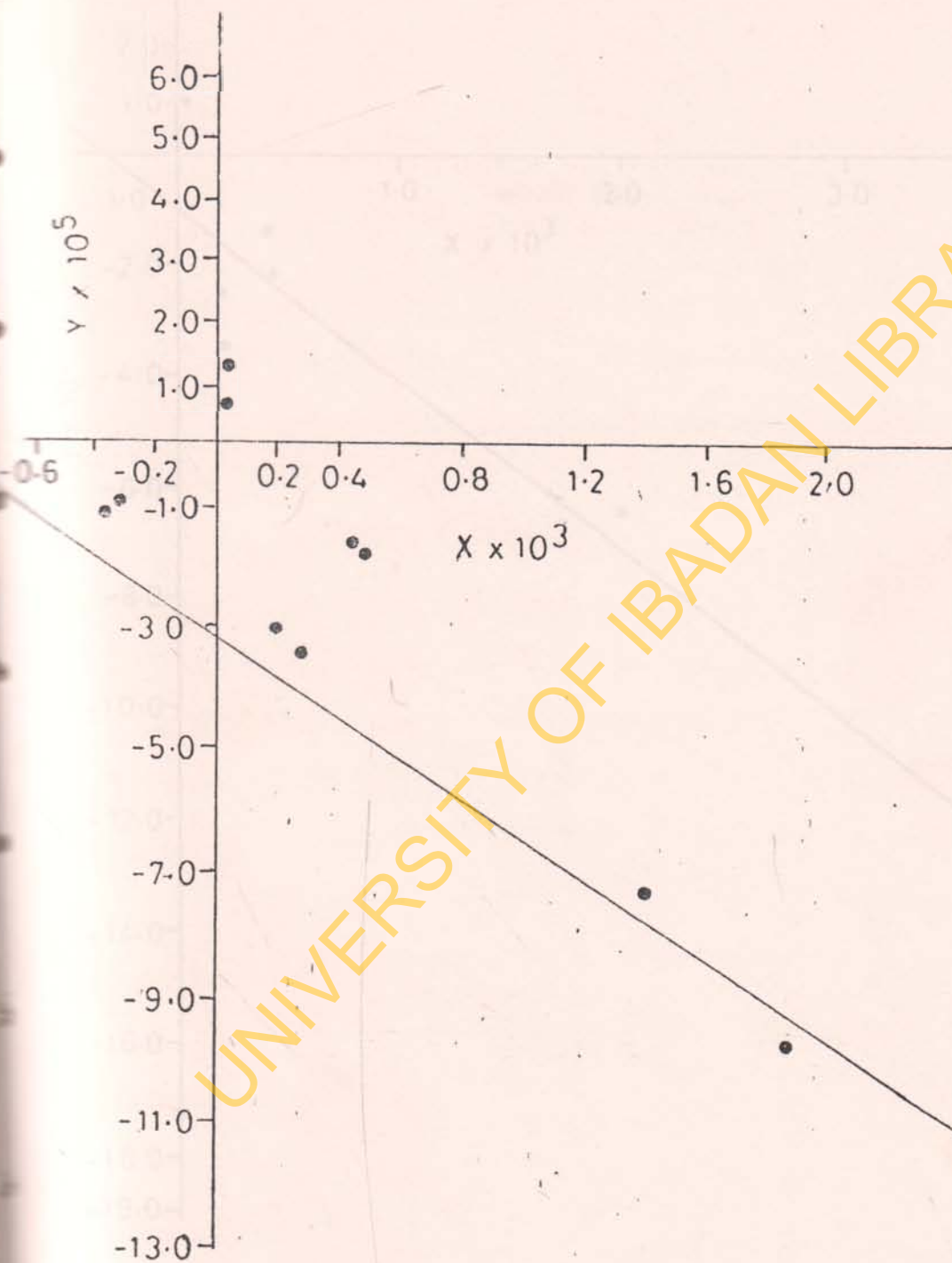
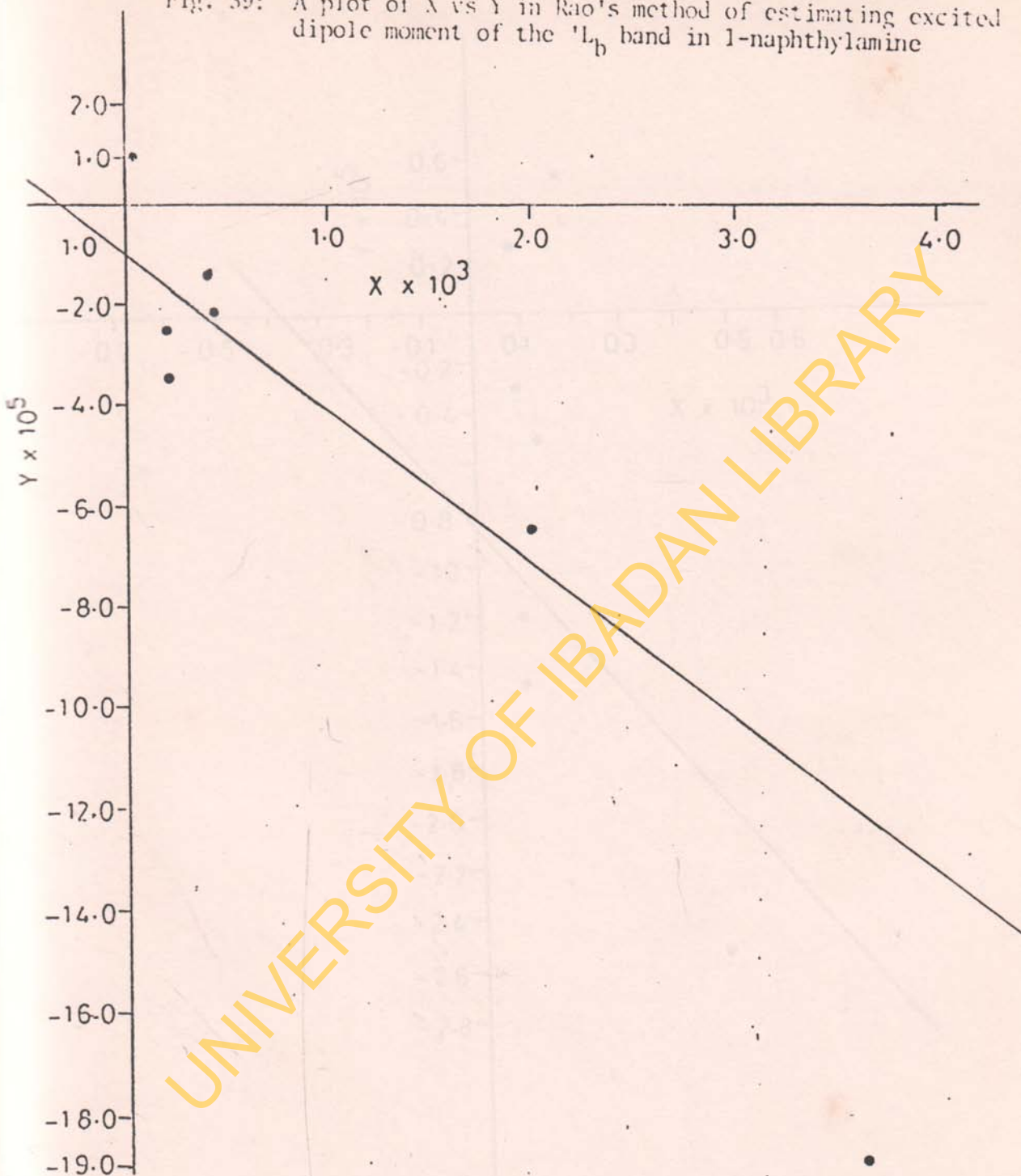


Fig. 59: A plot of X vs Y in Rao's method of estimating excited dipole moment of the 1L_b band in 1-naphthylamine



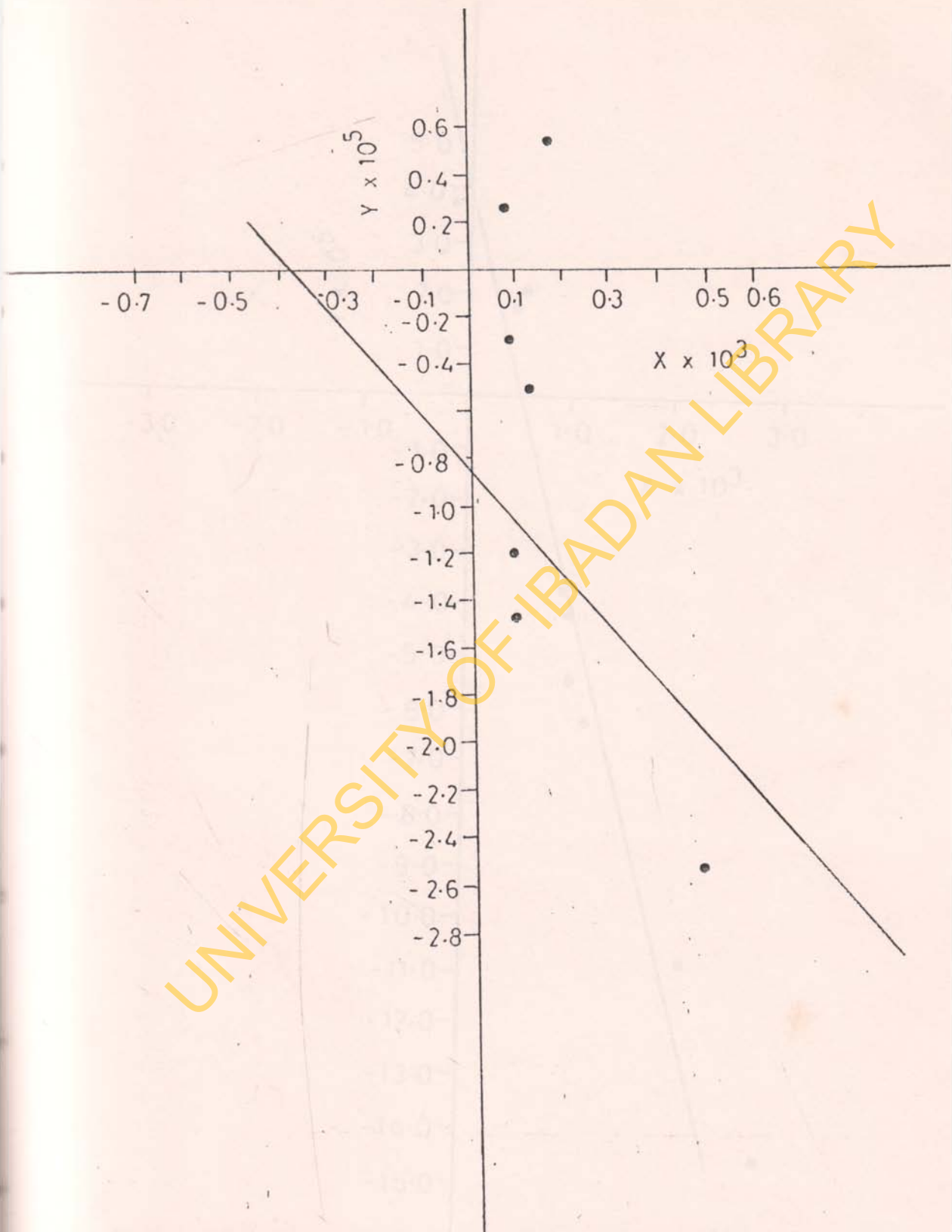


Fig. 40: A plot of X vs Y in Rao's method of estimating excited state dipole moment of the 1L_b band in 1-naphthol.

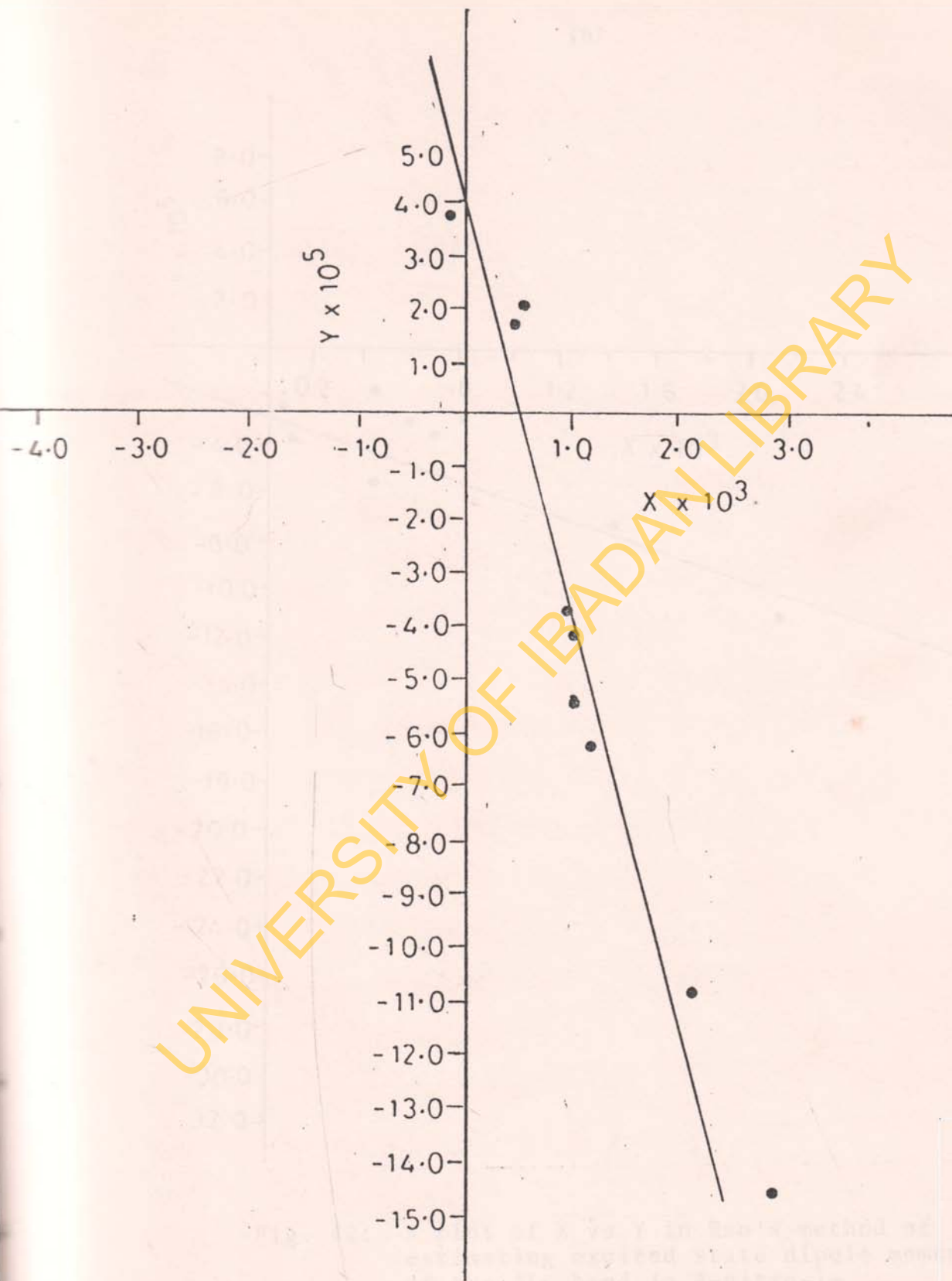


Fig. 41: A plot of X vs Y in Rao's method of estimating excited state dipole moment of the 1L_b band in 1-nitronaphthalene

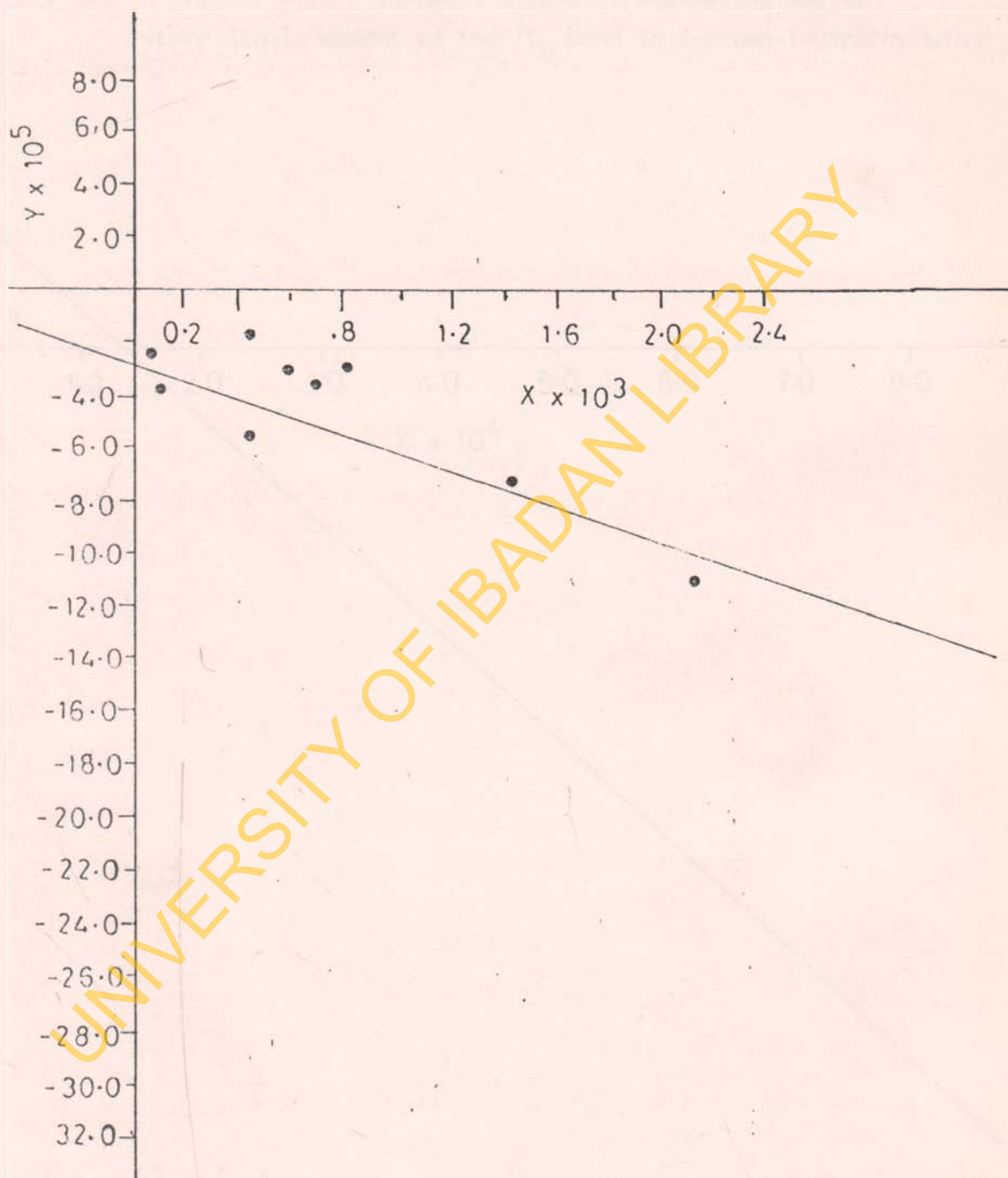
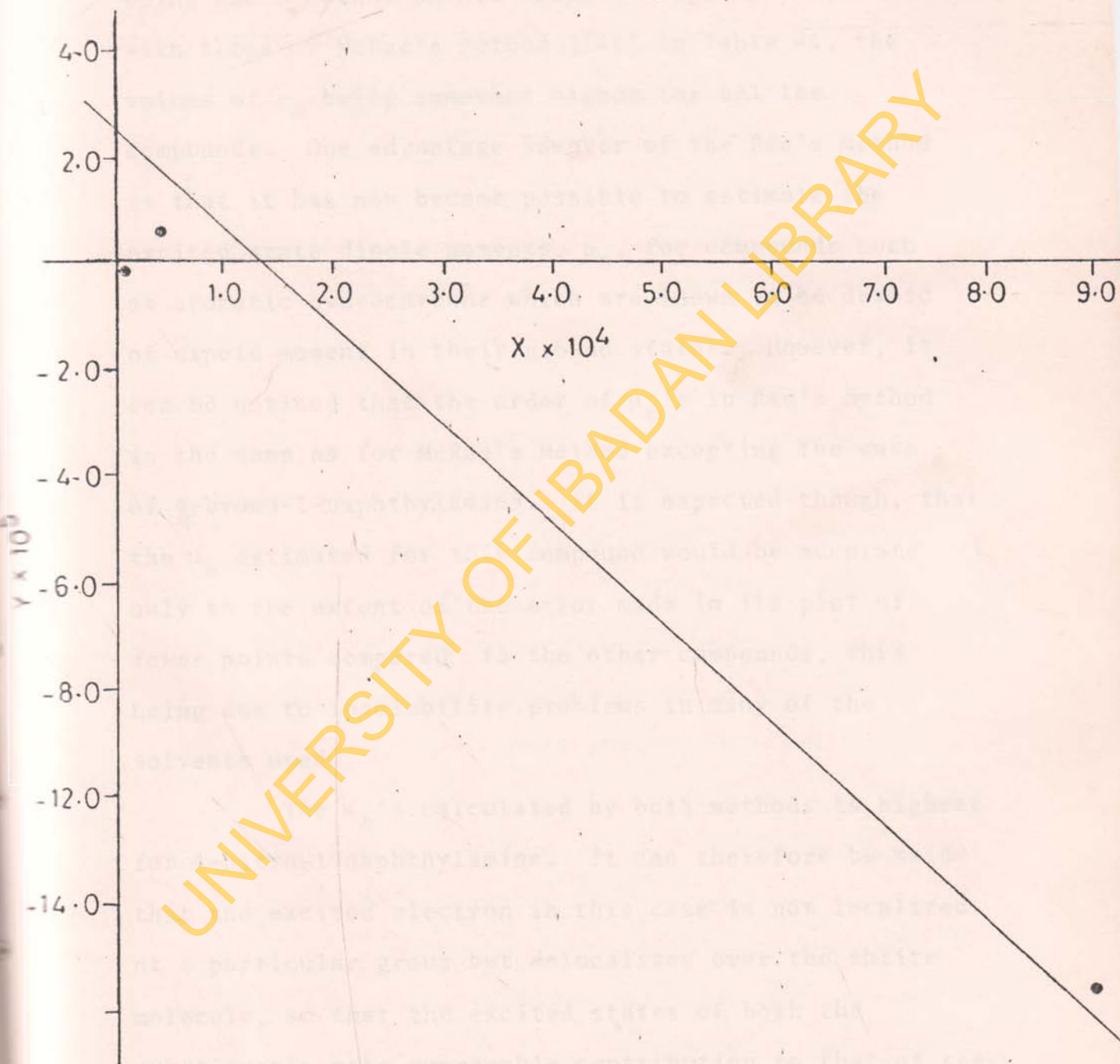


Fig. 42: A plot of X vs Y in Rao's method of estimating excited state dipole moment of the $'L_b$ band in 4-nitro-1-naphthylamine.

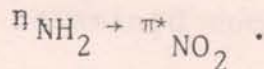
Fig. 43: A plot of X vs Y in Rao's method of estimating excited state dipole moment of the 1L_b band in 4-bromo-1-naphthylamine



using Rao's method do not compare reasonably well with those of McRae's method [141] in Table 41, the values of μ_e being somewhat higher for all the compounds. One advantage however of the Rao's method is that it has now become possible to estimate the excited state dipole moments, μ_e , for compounds such as aromatic hydrocarbons which are known to be devoid of dipole moment in their ground states. However, it can be noticed that the order of μ_e 's in Rao's method is the same as for McRae's method excepting the case of 4-bromo-1-naphthylamine. It is expected though, that the μ_e estimated for this compound would be accurate only to the extent of the error made in its plot of fewer points compared to the other compounds, this being due to insolubility problems in many of the solvents used.

The μ_e 's calculated by both methods is highest for 4-nitro-1-naphthylamine. It can therefore be said that the excited electron in this case is not localized at a particular group but delocalizes over the entire molecule, so that the excited states of both the substituents make comparable contribution to that of the

disubstituted molecule. The estimation by Rao's method clearly indicates that the L_b band is associated with intermolecular charge transfer of the type




The μ_e 's obtained from Rao's method seem too high for all the compounds. This can probably be explained in terms of considerable uncertainties that have been generally associated with the solute parameters used in the theoretical treatments of solvent effects on electronic spectra, particularly the assumption that the solute molecule is spherical and isotropic in polarizability and that it contains a point dipole. It is now known, for example, that the energy of a spherical point dipole can change substantially when the dipole is moved from the center of the molecule [143].

4.5 OSCILLATOR STRENGTHS AND RADIATIVE LIFETIMES OF EXCITED STATES

The oscillator strengths calculated by the HMO method, of the three absorption wavelengths, for most of the compounds have values above unity. However, it

is known that oscillator strengths calculated with LCAO functions are generally larger than observed values [107]. From Tables 31-36, it is seen that the observed f -values are generally low for all the examined compounds in most of the solvents. The differences in f -values from solvent to solvent is minimal but this is not unexpected since differences in bulk properties of the solvents from solvent to solvent are minimal. Notwithstanding the fact that the f -values are very low for the 1L_a (I) and 1L_b (II) bands to be assigned as single electronic transitions, the electronic relaxation times (Tables 43-48) calculated for each of the compounds in several solvents indicate that in most of the cases, the bands are due to transitions from mixed states and therefore cannot be truly described as homogenous.

Figures 44-48 give the relationships between the relaxation times τ , and the viscosities for the solvents η , for the 1L_a (I) and 1L_b (II) bands. From the calculated slopes of the plots for the 1L_a bands, it is expected that deviation from spherical symmetry of the solute molecules on excitation in the solvent would be

Table 43: Relaxation times, τ (s) of  in various solvents

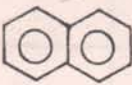
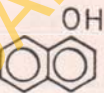
Compound	Solvents	$10^9 \tau_I$	$10^9 \tau_{II}$
	Acetonitrile	12.0	19.8
	Chloroform	2.6	-
	Methanol	5.1	14.6
	n-heptane	11.7	-
	cyclohexane	1.6	-
	Ethanol	101.2	32.3
	Methylcyclohexane	5.0	5.5

Table 44: Relaxation times τ (s) of  in various solvents

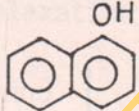
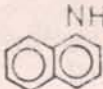
Compound	Solvents	$10^9 \tau_I$	$10^9 \tau_{II}$
	Acetonitrile	-	-
	Chloroform	2.5	0.8
	Methanol	1.7	6.5
	n-heptane	7.5	-
	cyclohexane	0.7	4.6
	Ethanol	27.0	13.4
	Methylcyclohexane	1.3	1.2

Table 45: Relaxation times, τ (s) of  in various solvents

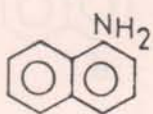
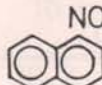
Compound	Solvents	$10^3 \tau_I$	$10^3 \tau_{II}$
	Acetonitrile	10.4	2.2
	Chloroform	4.0	2.3
	Methanol	0.7	2.0
	n-heptane	3.7	3.9
	cyclohexane	1.0	5.3
	Ethanol	37.3	4.3
	Methylcyclohexane	2.8	3.0

Table 46: Relaxation times τ (s) of  in various solvents

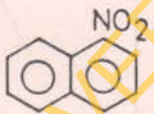
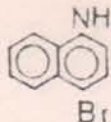
Compound	Solvents	$10^3 \tau_I$	$10^3 \tau_{II}$
	Acetonitrile	271.6	1.7
	chloroform	2.6	2.0
	methanol	0.8	3.2
	n-heptane	1.8	3.4
	cyclohexane	2.6	1.2
	Ethanol	5.4	2.9
	methylcyclohexane	1.6	2.4

Table 47: Relaxation times τ (s) of  in various solvents


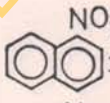
Compound	Solvents	$10^3 \tau_I$	$10^3 \tau_{II}$
	Acetonitrile	-	-
	Chloroform	1.1	0.3
	Methanol	12.5	3.0
	n-heptane	-	-
	Cyclohexane	-	-
	Ethanol	9.4	8.8
	Methylcyclohexane	-	-

 Table 48: Relaxation times τ (s) of  in various solvents

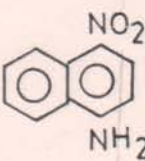
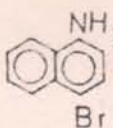
Compound	Solvents	$10^3 \tau_I$	$10^3 \tau_{II}$
	Acetonitrile	28.8	1.8
	Chloroform	0.8	1.1
	Methanol	1.4	3.7
	n-heptane	3.0	2.3
	cyclohexane	0.3	0.7
	Ethanol	31.9	3.4
	Methylcyclohexane	1.6	2.6

Table 47: Relaxation times $\tau_{(s)}$ of  in various solvents

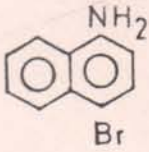
Compound	Solvents	$10^3 \tau_I$	$10^3 \tau_{II}$
	Acetonitrile	-	-
	Chloroform	1.1	0.3
	Methanol	12.5	3.0
	n-heptane	-	-
	Cyclohexane	-	-
	Ethanol	9.4	8.8
	Methylcyclohexane	-	-

 Table 48: Relaxation times $\tau_{(s)}$ of  in various solvents

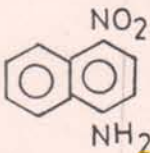
Compound	Solvents	$10^3 \tau_I$	$10^3 \tau_{II}$
	Acetonitrile	28.8	1.8
	Chloroform	0.8	1.1
	Methanol	1.4	3.7
	n-heptane	3.0	2.3
	cyclohexane	0.3	0.7
	Ethanol	31.9	3.4
	Methylcyclohexane	1.6	2.6

Fig. 41: A plot of log of relaxation times, τ , vs log of solvent viscosity, η , for the absorption band systems of naphthalene.

log η

0.5

1.0

1.5

2.0

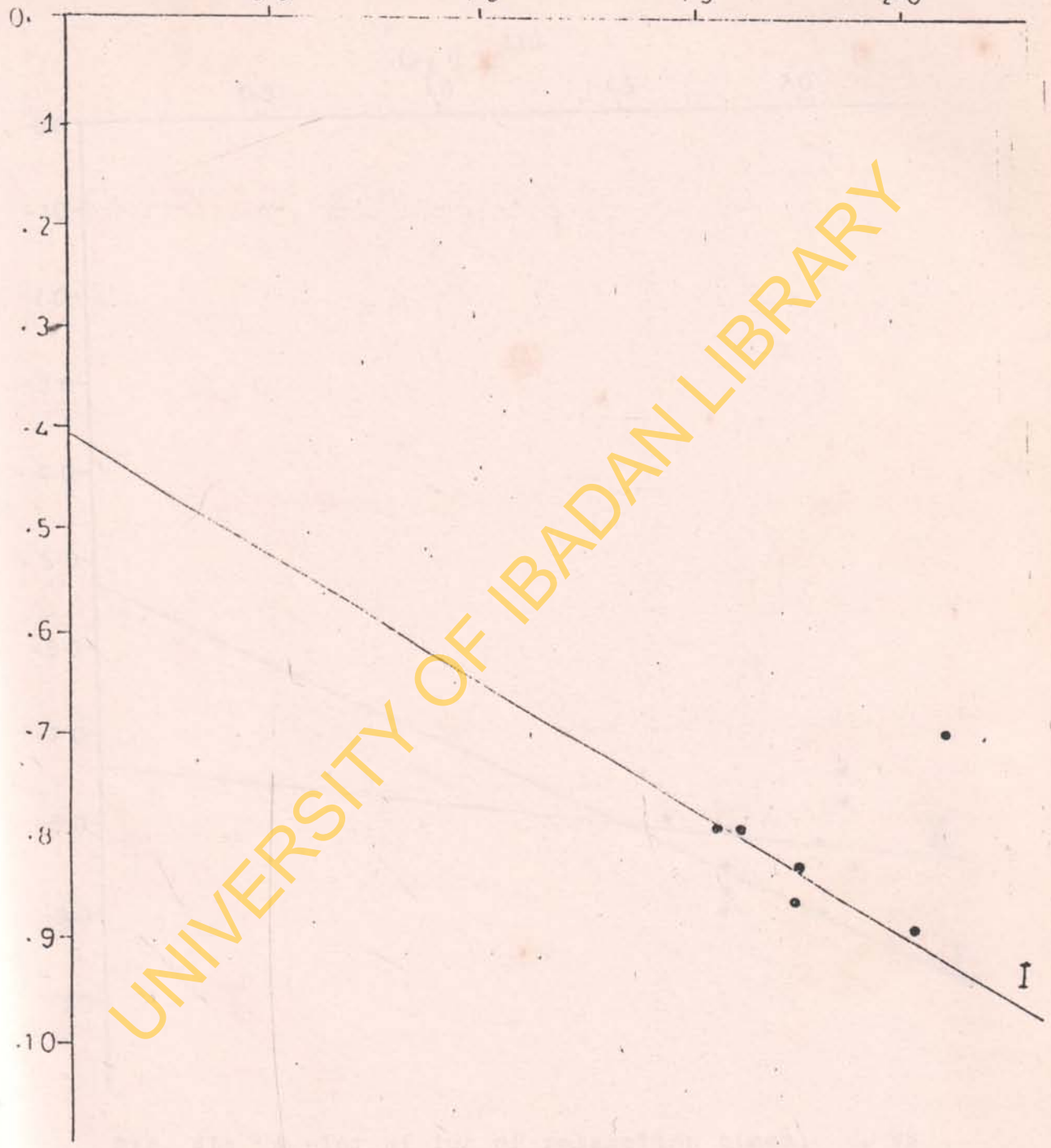


Fig. 44: A plot of log of relaxation times, τ , vs log of solvent viscosities η , for the absorption band systems of naphthalene.

log η

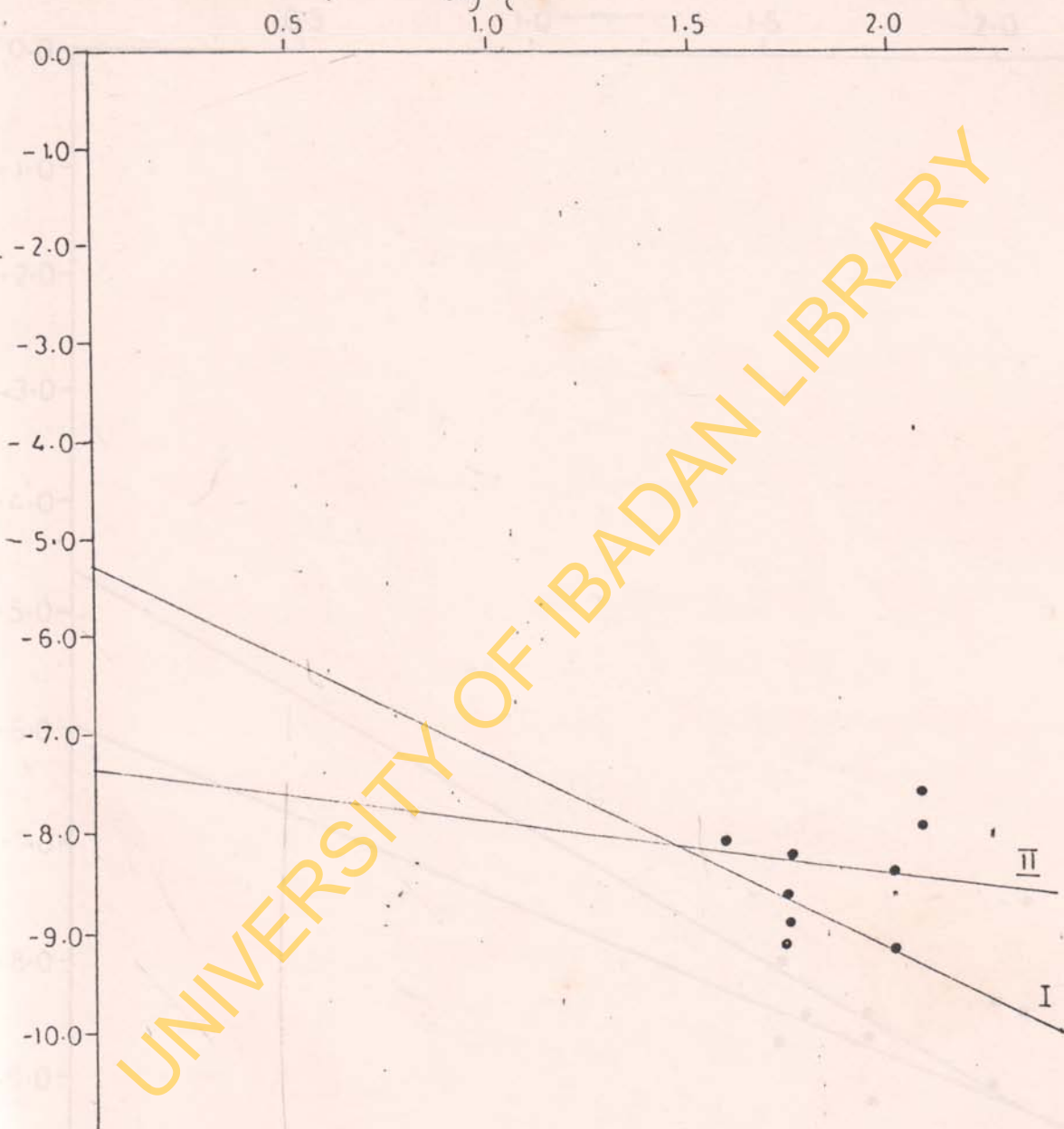


Fig. 45: A plot of log of relaxation times, τ , vs log of solvent viscosities, η , for the absorption band systems of 1-naphthol.

$\log \tau$

0.5

1.0

1.5

2.0

0.0

-1.0

-2.0

-3.0

-4.0

-5.0

-6.0

-7.0

-8.0

-9.0

UNIVERSITY OF IBADAN LIBRARY

II
I

Fig. 46: A plot of log of relaxation times, τ , vs log of solvent viscosities η , for the absorption band systems of 1-naphthylamine.

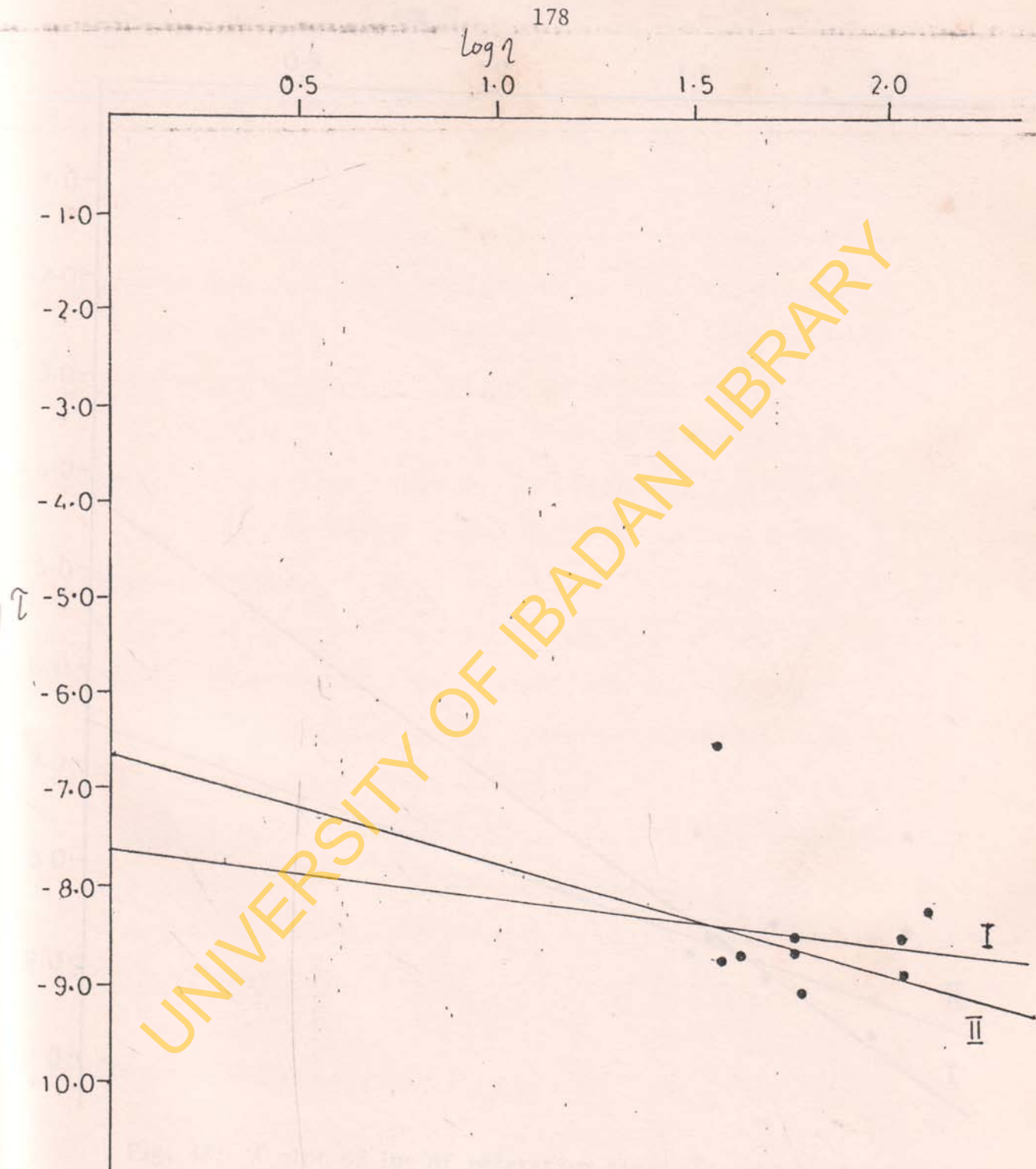


Fig. 47: A plot of log of relaxation times, $\hat{\tau}$, vs log of solvent viscosities η , for the absorption band systems of 1-nitronaphthalene.

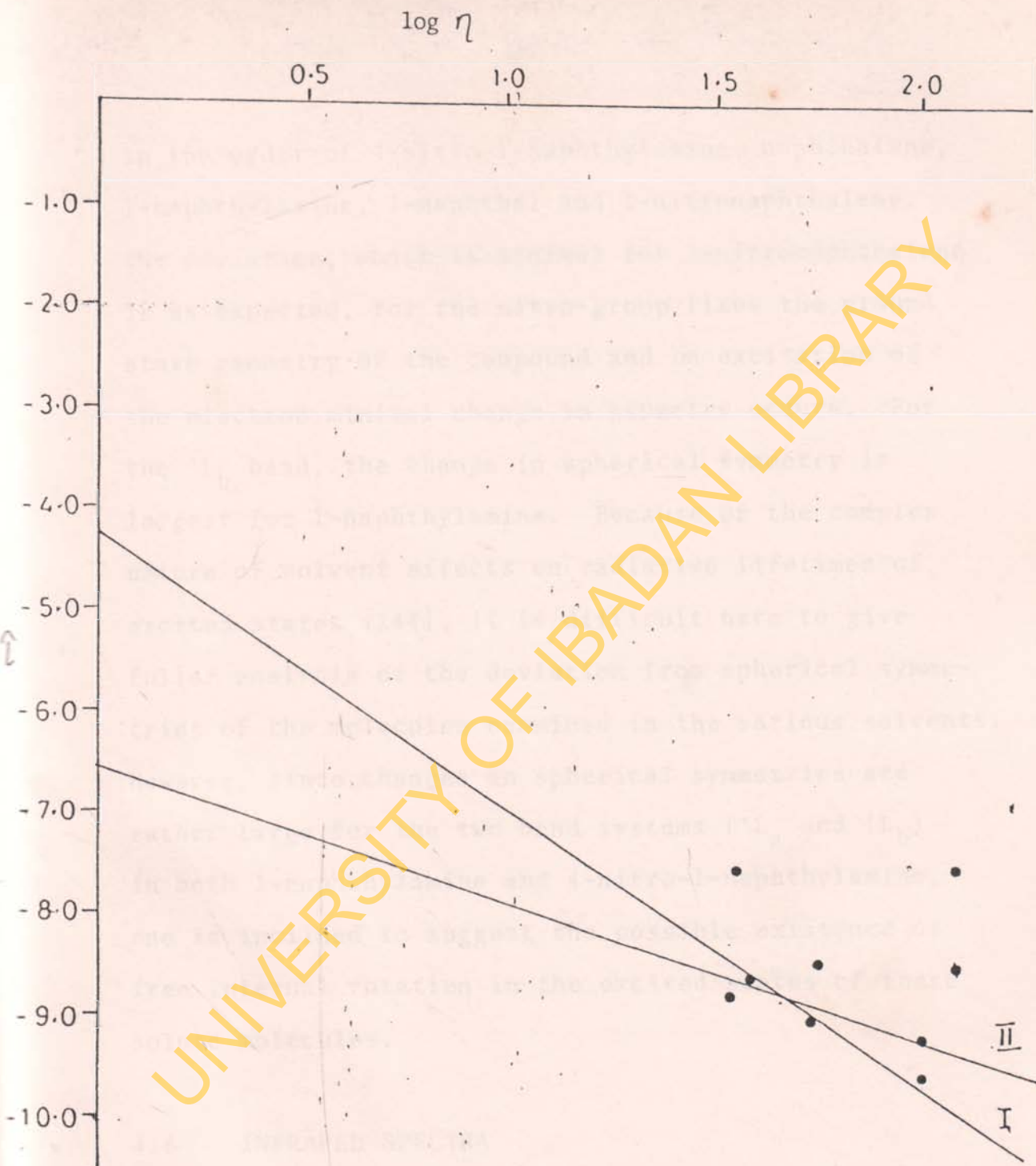


Fig. 48: A plot of log of relaxation times, τ ; vs log of solvent viscosities η , for the absorption band systems of 4-nitro-1-naphthylamine

in the order of 4-nitro-1-naphthylamine, naphthalene, 1-naphthylamine, 1-naphthol and 1-nitronaphthalene. The deviation, which is minimal for 1-nitronaphthalene is as expected, for the nitro-group fixes the ground state geometry of the compound and on excitation of the electron minimal change in geometry occurs. For the 1L_b band, the change in spherical symmetry is largest for 1-naphthylamine. Because of the complex nature of solvent effects on radiative lifetimes of excited states [144], it is difficult here to give fuller analysis of the deviation from spherical symmetries of the molecules examined in the various solvents. However, since changes in spherical symmetries are rather large for the two band systems (1L_a and 1L_b) in both 1-naphthylamine and 4-nitro-1-naphthylamine, one is inclined to suggest the possible existence of free internal rotation in the excited states of these solute molecules.

4.6 INFRARED SPECTRA

The infrared spectra of $1-C_{10}H_7X$ ($X = H, OH, NH_2, NO_2$), $4NH_2C_{10}H_6NO_2$, $2-NO_2C_{10}H_6-1OH$ and $4-Br C_{10}H_6-1NH_2$

as KBr pellets and in solution of CCl_4 are reproduced in Figures 49-55 while the data of assigned vibrational frequencies are tabulated in Tables 49-55. These assignments of vibrational modes, in the tables, have been aided by making comparisons with assignments already made for several monosubstituted benzenes

145-

Generally, the infrared spectra of the substituted naphthalene compounds can be conveniently considered in three parts

- (i) naphthyl-ring modes insensitive to the nature of the substituent,
- (ii) naphthyl-ring modes sensitive to the substituent, and
- (iii) the modes of the substituent X or X-Y group.

For each of the compounds, the planar model has been accepted as basis for the infrared studies and the naphthyl ring assumed to have dimensions of the naphthalene ring. The molecular symmetry for each of the compounds is taken as C_s , for which all the normal modes are expected to be infrared and Raman active. The species designations A_g , B_{1g} , B_{2g} and B_{3g} used for

Fig. 49a: Infrared spectrum of naphthalene: as solid in KBr

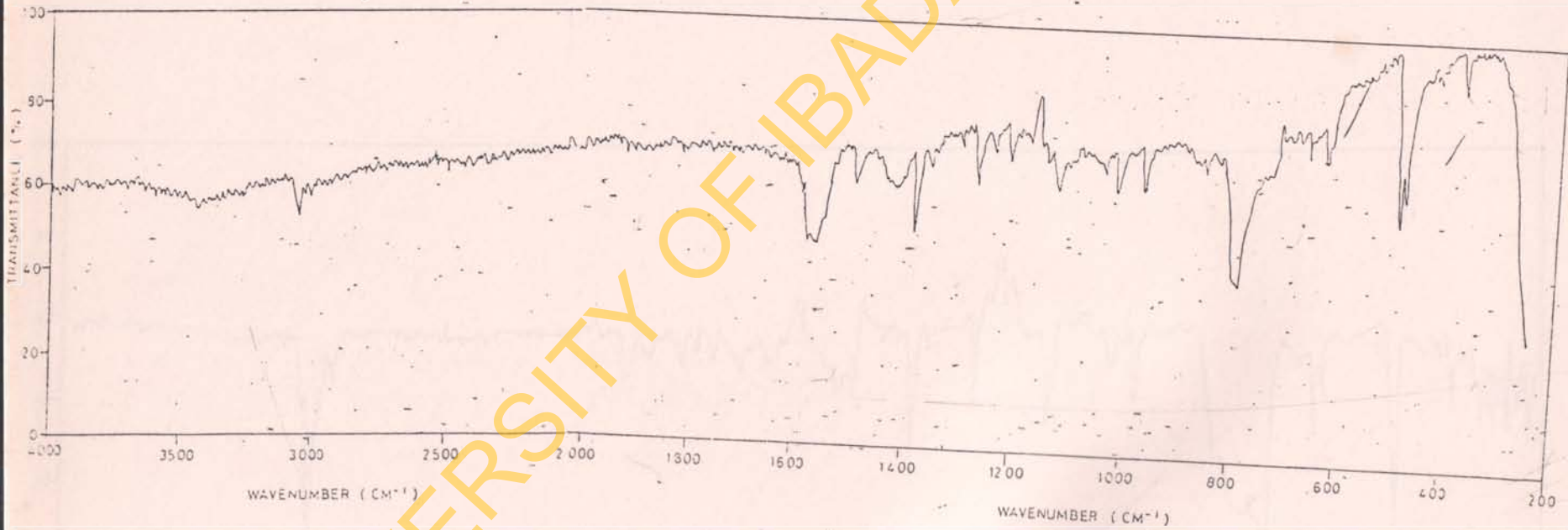


Fig. 49b: Infrared spectrum of naphthalene: as solution in CCl_4 .

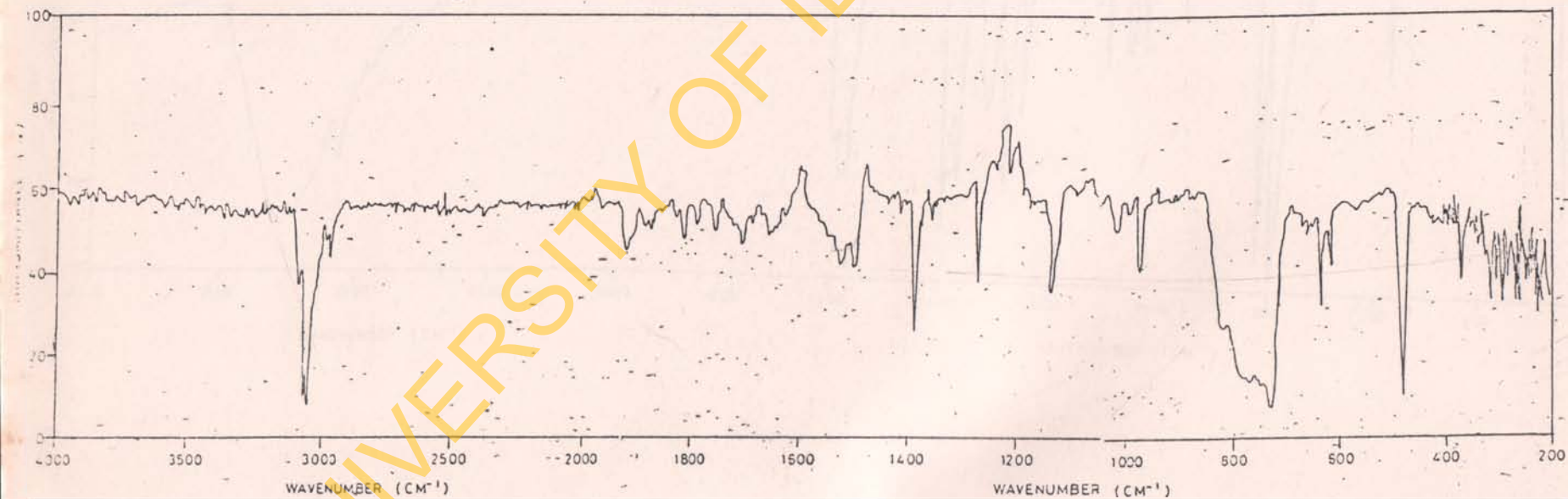


Fig. 50a: Infrared spectrum of 1-naphthol: as solid in KBr.

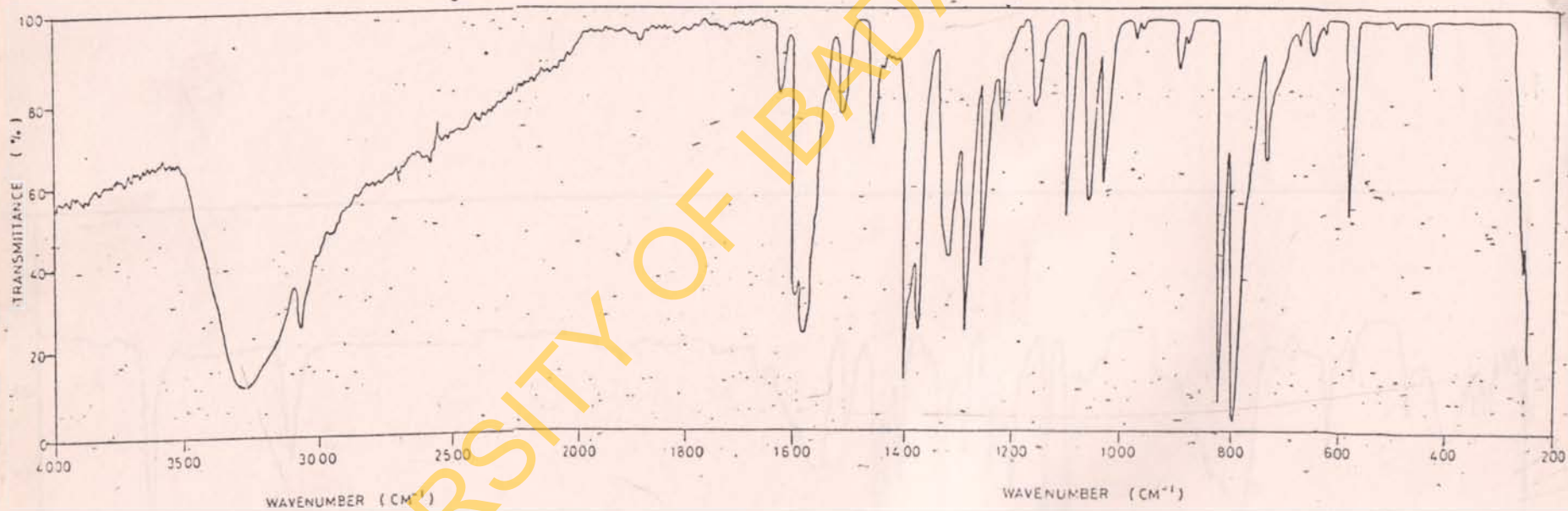


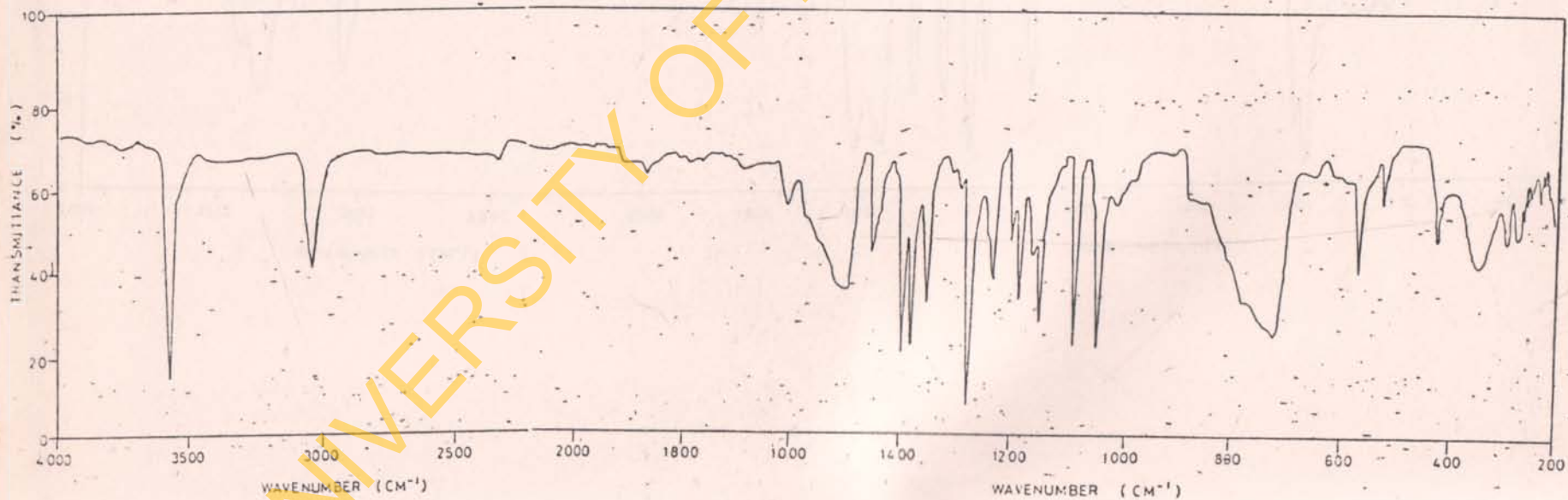
Fig. 50b: Infrared spectrum of 1-naphthol: as solution in CCl_4 .

Fig. 51a: Infrared spectrum of 1-naphthylamine: as solid in KBr.

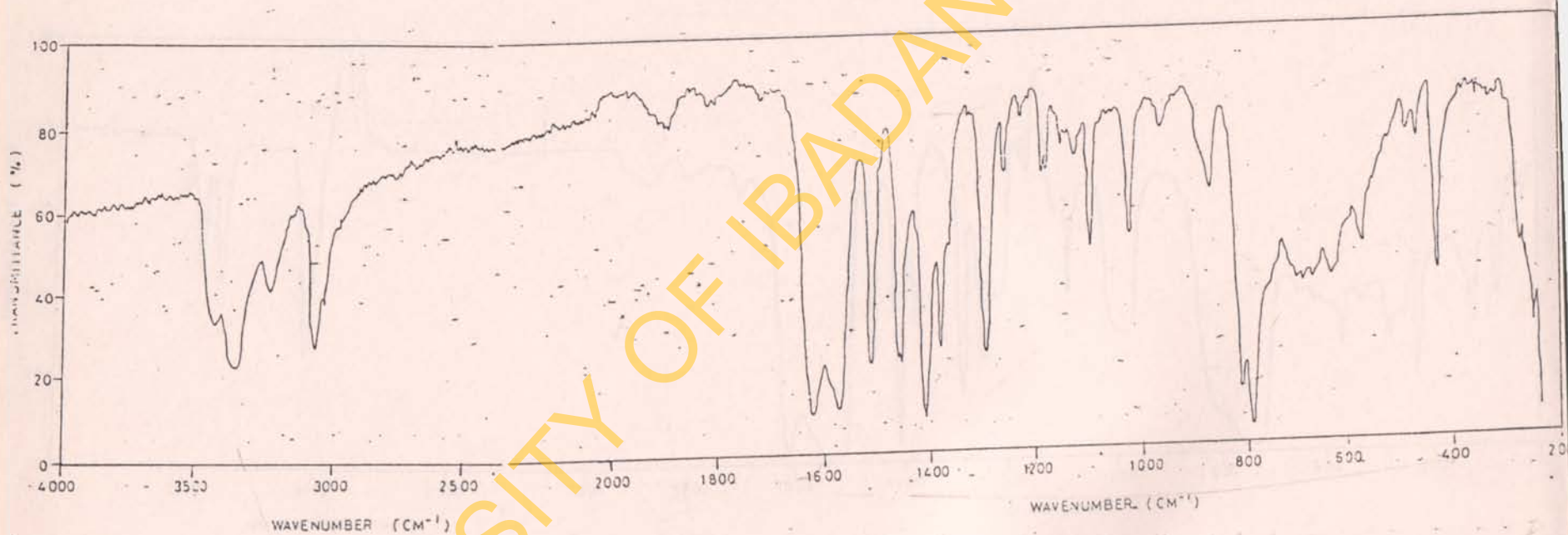


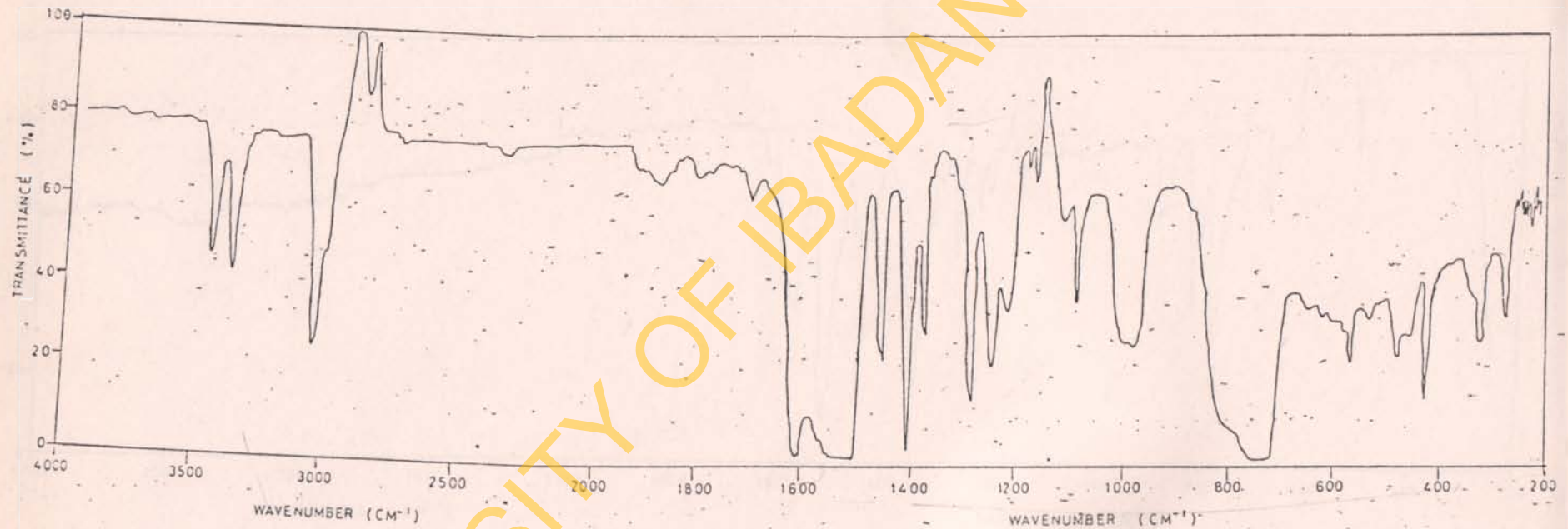
Fig. 51b: Infrared spectrum of 1-naphthylamine: as solution in CCl_4 

Fig. 52a: Infrared spectrum of 1-nitronaphthalene: as solid
in KBr.

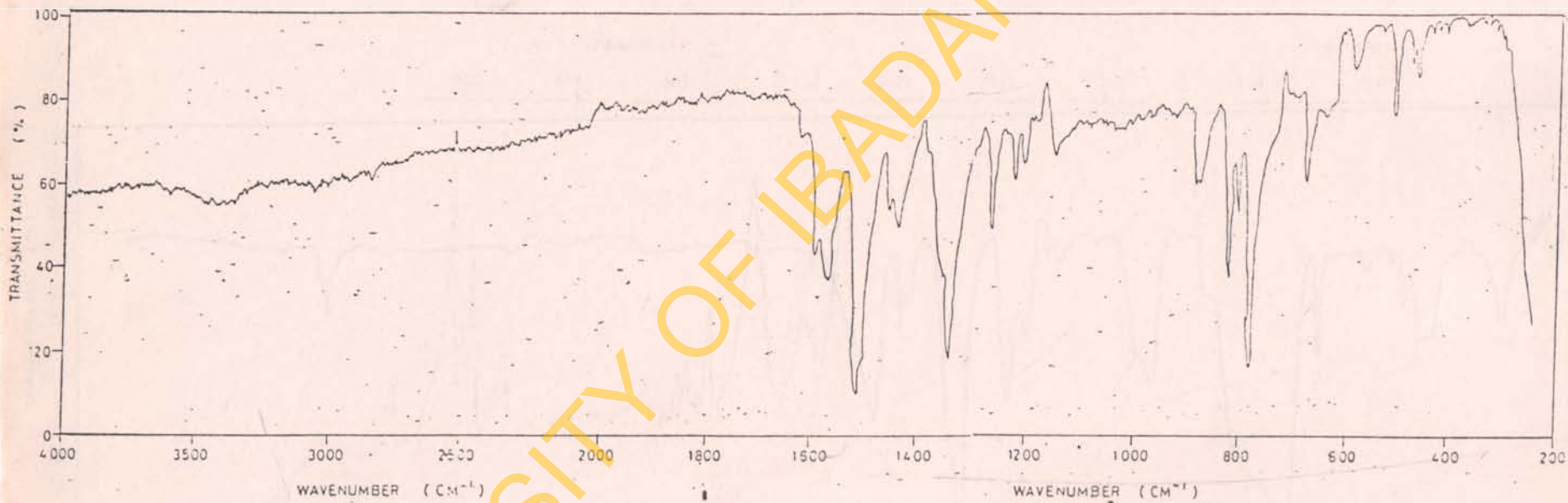


Fig. 52b: Infrared spectrum of 1-nitro naphthalene: as solution in CCl_4

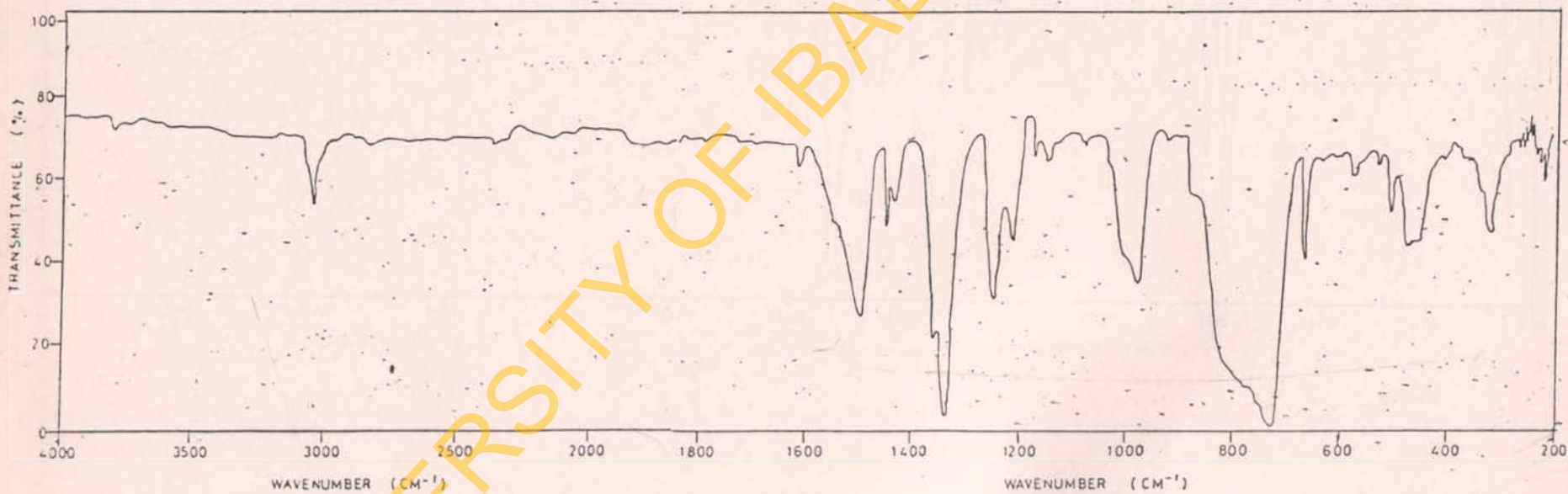


Fig. 53a: Infrared spectrum of 4-nitro-1-naphthylamine: as solid in KBr.

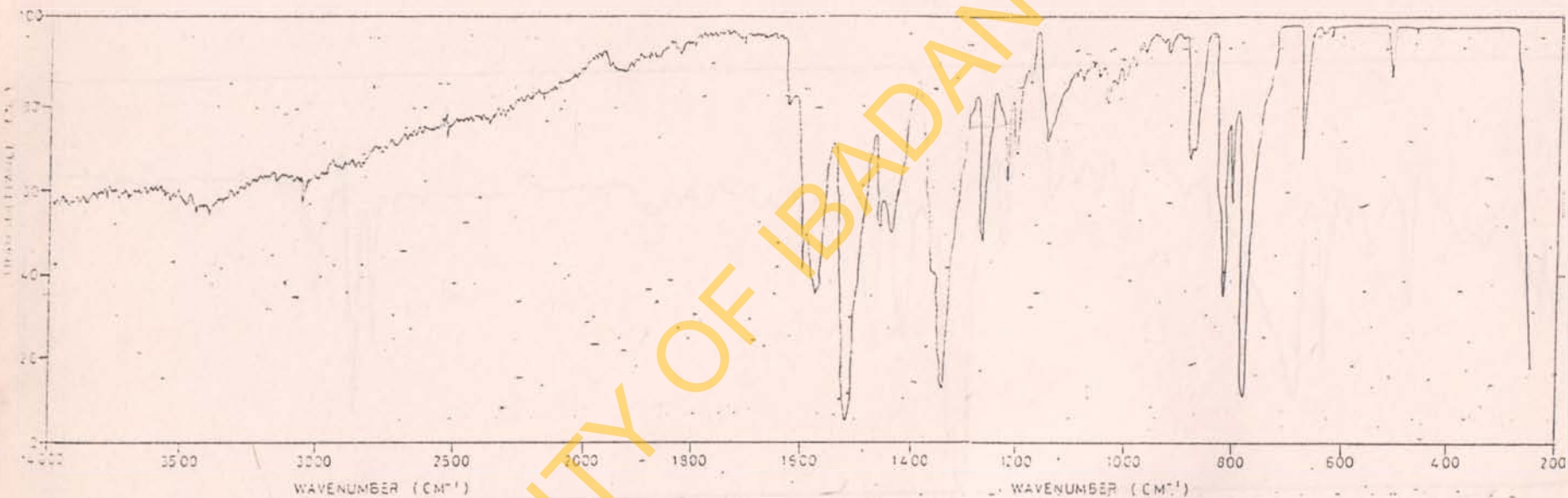


Fig. 53b: Infrared spectrum of 4-nitro-1-naphthylamine: as solution in CCl_4 .

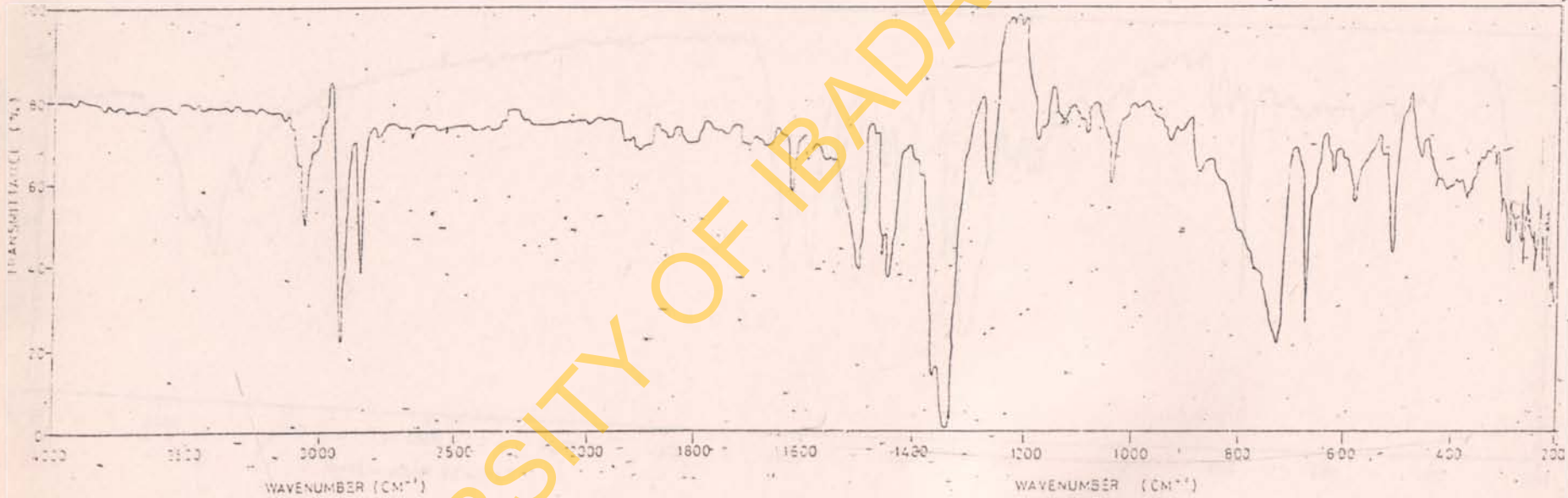


Fig. 54: Infrared spectrum of 2-nitro-1-naphthol: as solid in KBr.

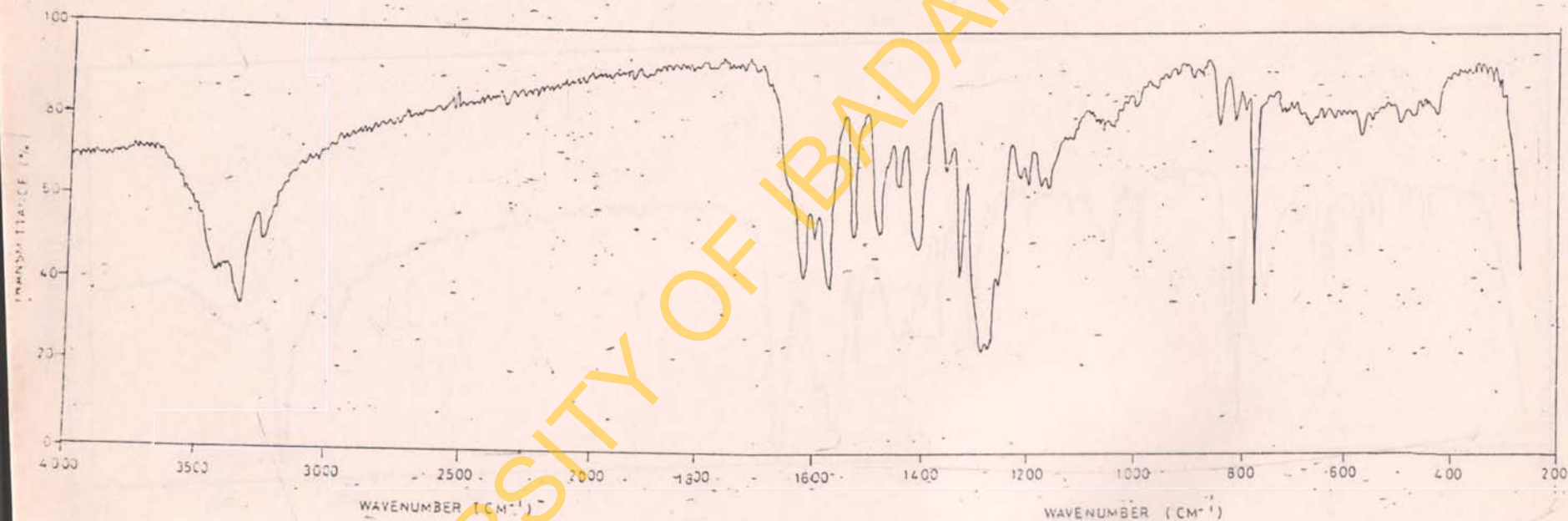


Fig. 55: Infrared spectrum of 4-bromo-1-naphthylamine as solid in KBr.

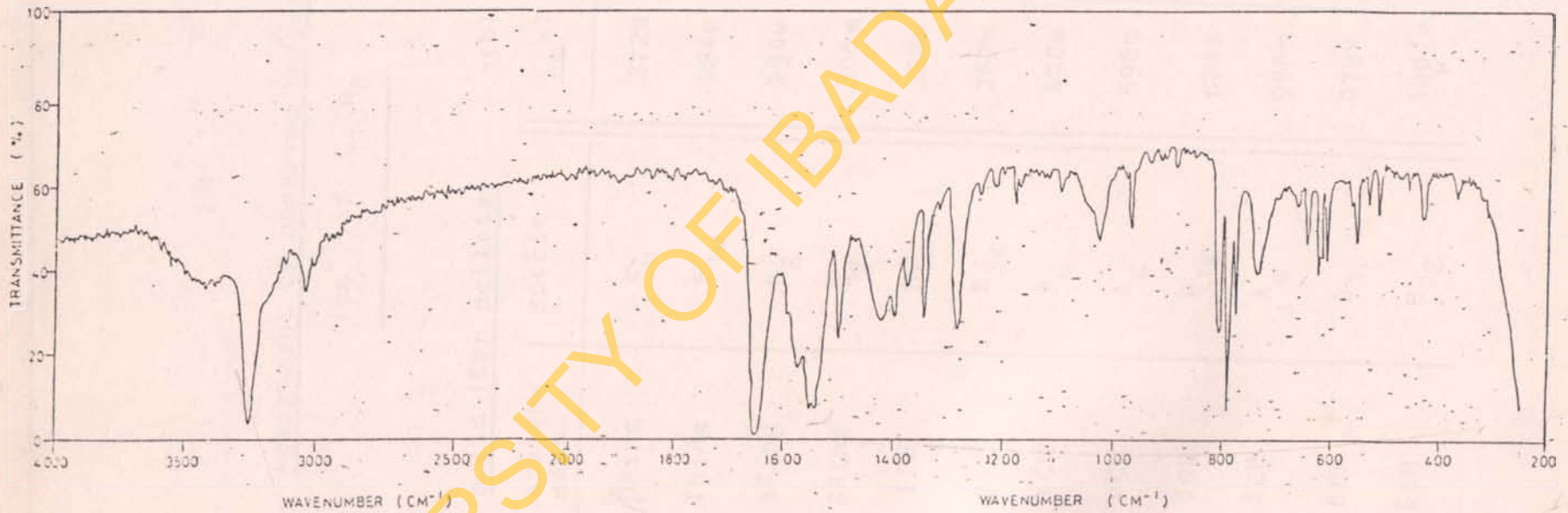


Table 49: Assignment of observed infrared frequencies(cm⁻¹) of C₁₀H₈

(a) <u>solid (KBr pellets)</u>			(b) <u>solution (CCl₄)</u>		
cm ⁻¹	assignment	specie	cm ⁻¹	assignment	specie
366m	βRing	A _u	272w	γRing	B _{3g}
474s	γRing	B _{1u}	284w	γRing	B _{3g}
486s	βRing	A _g	294w	γRing	B _{3g}
626m	βRing	B _{2u}	306m	νRing	B _{3g}
794s	γCH	B _{1u}	338w	βRing	B _{2u}
851w	γCH	B _{3g}	362m	βRing	A _u
961w	γCH	B _u	470s	γRing	B _{1u}
1015m	νCC	A _g	598m	βRing	B _{2u}
1126m	βCH	B _{1g}	624s	βRing	B _{2u}
1146w	βCH	A _g	956m	γCH	B _u
1230m	βCH	B _{3u}	979w	γCH	B _{3u}
1260m	βCH	B _{2g}	1007w	νCC	A _g

Table 49 (contd.)

(a) solid (KBr pellets)			(b) solution (CCl ₄)		
cm ⁻¹	assignment	specie	cm ⁻¹	assignment	specie
1285m	βCH	B _{2u}	1129s	βCH	B _{1g}
1375w	νCC	B _{2u}	1137w	βCH	A _g
1404s	νCC	A _g	1221w	βCH	B _{2u}
1515m	νCC	B _{3u}	1277s	βCH	B _{2u}
1580s	νCC	A _g	1374w	νCC	B _{2u}
1600s	νCC	B _{2u}	1397s	νCC	A _g
3037m	νCH	A _g	1428w	βCH	A _g
3057m	νCH	A _g	1505m	νCC	B _{3u}
			1717m	νCC	B _{3u}
			2965w	νCH	B _{1g}
			2980w	νCH	B _{3u}
			3037w	νCH	A _g
			3057s	νCH	B _{2u}
			3071s	νCH	A _g
			3087w	νCH	B _{3u}

Table 50: Assignment of observed infrared frequencies
 (cm^{-1}) of $\text{C}_{10}\text{H}_7\text{OH}$

(a) <u>solid (KBr pellets)</u>			(b) <u>solution(CCl_4)</u>		
cm^{-1}	assignment	species	cm^{-1}	assignment	species
421m	β Ring	A''	264w	X-sensitive	A'
566m	β Ring	A'	284w	γ Ring	A'
636w	$\gamma(\text{OH})$	A''	340m	β Ring	A''
716m	γ CH	A''	414m	β Ring	A''
771s	γ CH	A''	518w	β Ring	A''
796s	γ CH	A''	561m	β Ring	A''
			561m	β Ring	A''
866w	γ CH	A'	872m	γ CH	A'
881m	γ CH	A'	956w	γ CH	A''
951w	γ CH	A''	1008w	β CH	A''
961w	β CH	A''	1038s	β CC	A'
1020m	β CH	A''	1080s	β CH	A'
1050m	ν CC	A'	1142s	β CH	A''
1085s	β CH	A'	1177s	β CH	A'

Table 50 (contd.)

(a) Solid (KBr pellets)			(b) solution (CCl ₄)		
cm ⁻¹	assignment	species	cm ⁻¹	assignment	species
1146m	βCH	A'	1209w	νCO	-
1225m	νCO	-	1241m	βCH	A'
1255s	βCH	A'	1283s	βCH	A'
1285s	βCH	A''	1363s	νCC	A''
1320s	βCH	-	1391s	νCC	A'
1375s	νCC	A''	1401s	νCC	A'
1395s	νCC	A'	1468m	νCC	A'
1465m	νCC	A'	1631w	νCC	A'
1523m	νCC	A''	1715w	νCC	A''
1580s	νCC	A'	3057m	νCH	A'
1600s	νCC	A''	3067w	νCH	A'
1637m	νCC/β-OH	A'	3576s	νOH	-
3037w	νCH	A'			
3057w	νCH	A'			
3157w	νOH	-			
3227s	νOH	-			
3287s	νOH	-			

Table 51: Assignment of observed infrared frequencies (cm^{-1}) of $\text{C}_{10}\text{H}_7\text{NH}_2$

(a) <u>solid (KBr pellets)</u>			(b) <u>solution (CCl_4)</u>		
cm^{-1}	assignment	species	cm^{-1}	assignment	species
416s	β Ring	A''	258m	X-sensitive	A'
456w	γ Ring	A''	281w	γ Ring	A'
481w	β Ring	A'	309m	γ Ring	A'
511w	β Ring	A'	414s	β Ring	A''
561w	NH_2 wag	A''	446w	X-sensitive	A''
621w	β Ring	A''	469m	γ Ring	A''
771s	γ CH	A''	521w	β Ring	A'
791s	γ CH	A''	558m	NH_2 wag	A''
856m	γ CH	A'	611w	β Ring	A''
951w	γ CH	A''	636w	β Ring	A'
1020s	γ CC	A'	1086s	β CH	A'
1070w	β CH	A'	1111w	β CH	A''
1091s	β CH	A'	1164w	β CH	A''
1116w	β CH	A''	1173w	β CH	A''

Table 51 contd.

(a) solid (KBr pellets)			(b) solution (CCl ₄)		
cm ⁻¹	assignment	species	cm ⁻¹	assignment	species
1146w	βCH	A'	1223s	βCH	A'
1171m	βCH	A'	1255s	βCH	A''
1181m	βCH	A''	1295s	νCN	-
1235w	βCH	A'	1384s	νCC	A''
1265m	βCH	A''	1409s	νCC	A'
1300s	νCN	-	1457s	βCH	A'
1390s	νCC	A''	1465w	NH bending	A'
1415s	νCC	A'	1610s	νCC	A'
1465s	NH bending	A'	1707w	νCC	A''
1470w	νCC	A'			
1502s	νCC	A''	3017w	νCH	A'
1580s	νCC	A''	3047w	νCH	A''
1632s	νCC/NH bending	A'			
3027w	νCH	A'	3057w	νCH	A'
3057s	νCH	A'	3377s	νNH	-
3227m	νNH	-	3457s	νNH	-
3247w	νNH	-			
3357s	νNH	-			
3472m	νNH	-			

Table 52: Assignment of observed infrared frequencies(cm⁻¹) of C₁₀H₇NO₂

(a) <u>solid (KBr pellets)</u>			(b) <u>solution (CCl₄)</u>		
cm ⁻¹	assignment	species	cm ⁻¹	assignment	species
361w	βRing	A''	306m	βRing	A''
461m	γRing	A''	440w	X-sensitive	A'
466m	γRing	A''	498w	βRing	A'
501s	βRing	A'	520w	r(NO ₂)	A''
526w	r(NO ₂)	A''	571m	βRing	A''
581m	βRing	A''	661s	βRing	A''
631w	βRing	A''	718s	χ(NO ₂)	A''
666s	βRing	A''	916w	χCH	A''
771s	χCH	A''	971s	χCH	A''
796s	χCH	A''	1074w	βCH	A'
811s	δ(NO ₂)	A''	1143w	βCH	A'
866m	χCH	A'	1167w	βCH	A'
876m	χCH	A''	1224m	βCH	A''
918w	χCH	A''	1255s	βCH	A'
1035m	νCC	A'	1345s	νNO ₂	-

Table 52 (contd.)

(a) solid (KBr pellets)			(b) solution (CCl ₄)		
cm ⁻¹	assignment	species	cm ⁻¹	assignment	species
1146w	βCH	A'	1367s	νCC	A''
1215m	βCH	A''	1447m	βCH	A'
1277s	βCH	A''	1463m	νCC	A'
1353s	νNO ₂	-	1507s	νCC	A''
1450m	βCH	A'	1629w	νCC	A'
1470w	νCC	A'	3057m	νCH	A'
1575m	νCC	A'			
1585m	νNO ₂				
1609m	νCC	A''			
1632w	νCC	A'			
3067m	νCH	A'			
3107w	νCH	A'			

Table 53: Assignment of observed Infrared Frequencies (cm^{-1}) of $\text{NH}_2\text{C}_{10}\text{H}_6\text{NO}_2$

(a) solid (KBr pellets)			(b) solution (CCl_4)		
cm^{-1}	assignment	species	cm^{-1}	assignment	species
561m	NH_2 wag	A''	271w	X-sensitive	A'
666m	β Ring	A''	281w	γ Ring	A'
771s	δ CH	A''	294w	γ Ring	A'
796m	γ CH	A''	306w	γ Ring	A'
811s	$\gamma(\text{NO}_2)$	A''	361w	β Ring	A''
866m	γ CH	A'	399w	β Ring	A''
876m	γ CH	A''	454m	X-sensitive	A''
918w	γ CH	A'	500s	$\nu(\text{NO}_2)$	A'
1035w	νCC	A'	572m	NH_2 wag	A''
1146m	β CH	A'	661s	β Ring	A'
1176w	β CH	A'	866m	γ CH	A'
1215m	β CH	A''	918w	γ CH	A'
1235m	β CH	A'	1028m	νCC	A'
1275s	β CH	A''	1075m	β CH	A'

Table 53 (contd.)

(a) solid (KBr pellets)			(b) solution (CCl ₄)		
cm ⁻¹	assignment	species	cm ⁻¹	assignment	species
1350s	νNO ₂		1149m	βCH	A'
1450m	βCH	A'	1169s	βCH	A''
1470m	νCC	A'	1210w	βCH	A'
1525s	νCC	A''			
1580s	νCC	A'	1225w	βCH	A''
1607s	νCC	A''	1270s	βCH	A'
1637w	νCC/NH bending	A'	1445s	βCH	A'
2850w	νNH	-	1463s	νCC	A''
3072w	νCH	A'	1505s	νCC	A''
			1595w	νCC	A'
			1632m	νCC/NH bending	A''
			1715s	νCC	A''
			2850s	νNH	-
			2925s	νNH	-
			3063m	νCH	A'
			3087w	νCH	A''

Table 54: Assignment of observed infrared frequencies(cm^{-1} of $2\text{-NO}_2\text{C}_{10}\text{H}_6\text{-OH}$)Solid (KBr pellets)

cm^{-1}	assignment	Species
311w	γ Ring	A'
481w	X-sensitive	A''
491w	β Ring	A'
541w	$\gamma(\text{NO}_2)$	A''
566w	β Ring	A'
661w	β Ring	A''
761s	γ CH	A''
806m	$\delta(\text{NO}_2)$	A''
831m	γ CH	A'
995w	β CH	A''
1156w	β CH	A'
1171w	β CH	A'
1210w	β CH	A''
1225w	β CH	A''
1265w	β CH	A'

Table 54 (contd.)

solid (KBr pellets)

cm^{-1}	assignment	Species
1280s	βCH	A''
1295s	βCH	A'
1330s	$\nu(\text{NO}_2)$	A''
1360m	νCC	A'
1415s	νCC	A'
1450m	βCH	A'
1485s	νCC	A'
1535s	νCC	A''
1575s	νCC	A''
1615w	νCC	A''
1627s	νCC	A'
3257m	νOH	-
3337m	νOH	-

Table 55: Assignment of observed infrared
frequencies (cm^{-1}) of 4-BrC₁₀H₆¹-NH₂

solid (KBr pellets)

cm^{-1}	assignment	species
361w	β Ring	A''
426m	β Ring	A''
451w	X-sensitive	A''
506m	β Ring	A'
526w	β Ring	A''
546m	β Ring	A''
561w	NH ₂ wag	A'
606m	β Ring	A''
616m	β Ring	A''
636m	β Ring	A''
656w	β Ring	A''
731m	γ CH	A''
766s	γ CH	A''
781s	γ CH	A''
796s	γ CH	A''
881w	γ CH	A'

Table 55 (contd.)

solid (KBr pellets)

cm ⁻¹	assignment	species
926w	γCH	A'
961m	γCH	A''
1025m	νCC	A'
1096w	βCH	A'
1176w	βCH	A''
1230w	βCH	A''
1255w	βCH	A'
1295s	νCN	-
1360s	νCC	A'
1385m	νCC	A''
1410w	νCC	A'
1440m	βCH	A'
1515s	νCC	A'
1550s	νCC	A'
1560s	νCC	A'
1580w	νCC	A''
1662s	νCC/NH bending	A'
3037w	νCH	A'
3067s	νCH	A'
3257s	νNH	-
3277s	νNH	-

naphthalene for D_{2h} symmetry have been strictly replaced by A' while A_u , B_{1u} , B_{2u} and B_{3u} are replaced by A'' in the substituted naphthalene compounds.

Most of the skeletal modes which are insensitive to substituent X (X-insensitive modes) for each of the compounds require no additional discussion and may be found in Tables 49-55.

It is not possible here to give a fairly complete assignment for the X-sensitive modes of the compounds studied due to the fact that some of the expected X-sensitive modes occur at frequencies beyond the limits of the available infrared instrumentation. However, the modes at $258\text{ cm}^{-1}(\omega)$ and $446\text{ cm}^{-1}(\dot{\omega})$ in 1-naphthylamine, $264\text{ cm}^{-1}(\omega)$ in 1-naphthol, $440\text{ cm}^{-1}(\omega)$ in 1-nitronaphthalene, $271\text{ cm}^{-1}(\omega)$ and $454\text{ cm}^{-1}(\text{m})$ in 4 nitro-1-naphthylamine, $481\text{ cm}^{-1}(\omega)$ in 2 nitro-1-naphthol and $451\text{ cm}^{-1}(\omega)$ in 4 bromo-1-naphthylamine have been assigned as X-sensitive.

The remaining modes to discuss are those of the substituent X for each of the compounds. In 1-naphthylamine ($X=\text{NH}_2$), there are two band-stretching

modes at ca 3360 cm^{-1} and ca 3470 cm^{-1} while there is a third band at 3230 cm^{-1} in the solid but missing in the solution spectra. The NH_2 bending or scissors mode may be expected where ν_{CC} stretching mode is observed at ca 1620 cm^{-1} . There are two more NH_2 modes to be assigned, the wagging mode, which is analogous to the inversion mode of ammonia and the NH_2 torsional mode. The solid and solution spectra of 1-naphthylamine show a weak band at ca 560 cm^{-1} and this has been assigned to the wagging mode. The NH_2 torsional mode of 1-naphthylamine is expected to be low-lying.

The remaining three modes for 1-naphthol ($x=\text{OH}$) are OH stretching, OH in-plane bending and out-of-plane OH bending or torsional mode.

The OH stretching mode, $\nu(\text{OH})$ has been the subject of numerous investigations related to hydrogen bonding [137]. In this study, the broad band at ca 3280 cm^{-1} in the solid spectra, which is shifted to higher wavelength at ca 3570 cm^{-1} in the solution spectra have been assigned to $\nu(\text{OH})$ mode. Also, Mecke and Rossmly [147] in a study of phenols have described the coupling of the OH in-plane bending mode with one of the ring

stretching modes derived from the R_{2u} mode of benzene. In the absence of any conflicting evidence, the band at 1633 cm^{-1} already assigned to ν_{OH} mode is also the OH in-plane bending mode. A broad band at 636 cm^{-1} in the solid spectra of 1-naphthol has been assigned to the out-of-plane OH bending mode, $\gamma(OH)$. This mode is absent in the solution spectra. Davies [148], is studying associated molecules has made similar assignment for the broad band in the $600\text{-}700\text{ cm}^{-1}$ region of phenols to the out-of-plane bending mode, $\gamma(OH)$. The position of this mode in the free molecule has not yet been reported.

Cencelj and Hadzi [149], have concluded that interactions between the hydrogens and substituents on different rings in naphthalene are minimal and characteristic frequencies may therefore be sought for each ring separately. Thus, for meaningful discussion of the bending vibrations of the NO_2 group in 1-nitronaphthalene, previous discussions [150] of the vibrational spectra of nitrobenzene should be very useful. The bending vibrations of the NO_2 group comprise the asymmetric deformation $\delta(\text{NO}_2)$, wagging $\gamma(\text{NO}_2)$,

rocking $r(\text{NO}_2)$ and torsional NO_2 modes. The fundamental at 718 cm^{-1} in the solution spectra of 1-nitronaphthalene is probably predominant the (NO_2) mode. This assignment has been based on that made for the fundamental at 704 cm^{-1} in gas phase studies of nitrobenzene [151-152]. A band at 811 cm^{-1} in the solid spectra has been assigned largely to the $\delta(\text{NO}_2)$ mode, while the absorption at 526 cm^{-1} in the solid and 520 cm^{-1} in the solution spectra is assigned to the $r(\text{NO}_2)$ mode. ¹⁸O shift studies [151] have been used to establish similar bands for nitrobenzene. Again, no assignment of the NO_2 torsional frequency of 1-nitronaphthalene has been made here, for it is also expected to be low-lying.

The two band systems at 2850 cm^{-1} and 2925 cm^{-1} in 4-nitro-1-naphthylamine have been assigned to the νNH modes while the medium intensity bands at 561 cm^{-1} in solid spectra and 572 cm^{-1} in solution spectra have been assigned to the NH_2 wagging mode. The already assigned νCC at 1637 cm^{-1} in solid spectra and 1632 cm^{-1} in solution is further reassigned to the NH_2 bending or scissors mode which is reasonably expected in this region. The strong bands at 811 cm^{-1} in the

solid spectra and 500 cm^{-1} in the solution spectra are respectively assigned to the $\delta(\text{NO}_2)$ and $r(\text{NO}_2)$ modes.

The $\nu(\text{OH})$ band at 3337 cm^{-1} in 2-nitro-1-naphthol occurs at higher wavelength than the corresponding band in 1-naphthol ($\nu(\text{OH})$ at 3287 cm^{-1}) and is also of weaker intensity. In the same compound, the 541 cm^{-1} band has been assigned to $r(\text{NO}_2)$ mode while the 806 cm^{-1} band is assigned to $\delta(\text{NO}_2)$.

In 4-bromo-1-naphthylamine, the two-band systems at 3257 cm^{-1} and 3277 cm^{-1} have been assigned to the νNH modes while the NH_2 wagging mode is assigned to the frequency at 561 cm^{-1} . The νCC mode at 1662 cm^{-1} is again reassigned to the NH bending mode which is also expected in this region.

CHAPTER 5

CONCLUSION

Huckel molecular orbital calculations have indicated that substitution in 1-position of naphthalene cause increases in the mobilities of π -electrons in the direction of the short molecular axis whereas those in 2-position lead to decreased π -electron mobilities in this direction. Also, the magnitude of π -donation into the ring is large for 1-naphthylamine, 1-naphthol and 1-methoxynaphthalene.

The electronic transitions in each of the substituted naphthalene compounds studied are $\pi \rightarrow \pi^*$. The electronic excited states of the compounds investigated correspond to configurations which are more charged than in the ground states. Hydrogen bonding effects are more pronounced for 1-naphthol and 1-naphthylamine.

The fundamental ν_{CH} modes for substituted naphthalenes occur in the same region as for naphthalene. The frequencies of the infra-red bonds in the $1620\text{-}1350\text{ cm}^{-1}$ region are independent of the

nature of the substituent.

5.1 RECOMMENDATION FOR FURTHER WORK

For a more detailed understanding of the ground and excited state properties of naphthalene and some of its derivatives, MINDO/3 calculations are desirable. Also, the Raman, the magnetic resonance (e.s.r., endor) and the photoelectron spectra of these systems would be useful for the purposes of obtaining more detailed physico-chemical information about them.

The studies recommended for substituted naphthalene compounds can later on be made for systems which are of real significance in life (e.g. pharmacologically) and for which little physico-chemical information is available for now.

LIST OF REFERENCES

1. Morrisson R.T. and Boyd R.N. 1973. Organic Chemistry 3rd Edition. Allyn and Bacon, Inc. Boston.
2. Thomson J.B. (Editor). 1965. Dictionary of Organic Compounds. 4th edition. London, Eyre and Spottiswoode Publishers Ltd.
3. Thomson R.H. 1971. Naturally occurring quinones. 2nd edition. Academic Press, London and New York.
4. Bendz C., Wallmark C. and Oblom K. 1947. Antibiotic agent from Marasmius ramealis. Nature 159, 840.
5. Latif A. 1959. Isolation of a vitamin K activity compound from the leaves of Lawsonia spp: Composition of the air-dried leaves. Indian Journal of Agricultural Science, 29, 147. CA 55: 1482f.
6. Daglish C. 1950. Isolation and identification of a hydrojuglone glycoside occurring in the walnut. Biochemical Journal, 47, 458. CA 45: 3125d.

7. Hurbin J.B. 1964. Biochemistry of phenolic compounds. Academic Press, London and New York.
8. Walker N. and Wiltshire G.H. 1953. Breakdown of naphthalene by a soil bacterium. *Journal of General Microbiology* 8, 273. CA 47: 6499b.
9. Treccani V., Walker N. and Wiltshire G.H. 1954. Salicyclic acid production from naphthalene by a schizomycetes isolated from petroleum soils. *Journal of General Microbiology* 11, 341. CA 48: 7700e.
10. Fernley H.N. and Evans W.C. 1958. Oxidative metabolism of polycyclic hydrocarbons by soil pseudomonads. *Nature* 182, 373. CA 53: 4610e.
11. Rogoff M.H. and Wender I. 1959. Methyl-naphthalene oxidation by pseudomonads. *Journal of Bacteriology* 77, 783. CA 53: 1816a.
12. Walker N. and Wiltshire G.H. 1955. Decomposition of 1-chloro- and 1-bromonaphthalene by soil bacteria. *Journal of General Microbiology* 12, 478. CA 49: 11223g.
13. Byrde R.J.W., Harris J.F. and Woodcock D. 1956. Fungal detoxication - metabolism of

- ω -(naphthyl)-n-alkyl carboxylic acids by Aspergillus niger. Biochemical Journal 64, 154. CA 50: 16955g.
14. Byrde R.J.W. and Woodcock D. 1958. Fungal detoxication-metabolism of ω -(naphthyl)-n-alkyl carboxylic acids by Sclerotinia laxa. Biochemical Journal 69, 19. CA 52: 13852i.
15. Deichmann W.B. and Gerarde H.W. 1969. Toxicology of Drugs and Chemicals. Academic Press, New York.
16. Sakhawra L.N., Pavlovskaya G.S. and Tolgskaya M.S. 1980. Toxicological hygienic evaluation of dinitronaphthalene production. Gig. Tr. Rof. Zabol 139-142 (Russian). CA 92: 185093y.
17. Knowles C.O. and Kadir H.A. 1981. Inhibition of rat brain monoamine oxidase by insecticides, acaricides and related compounds. General Pharmacology 12(4) 239-47. CA 95: 181946t.
18. Dougherty R.C., Whitaker M.J., Tang S., Bottcher R., Killer M. and Knehl D.W. 1981. Sperm density and toxic substances; a potential key to environmental health hazards. Environm.

- Health Chem: Chem. Environ. Agents, Potential Human Hazards, [Symp] 1979, 263-78. CA 94: 115435d.
19. Bolton J.R. and Fraenkel J.R. 1964. Electron spin resonance study of the pairing theorem for alternant hydrocarbons; ^{13}C splittings in the anthracene positive and negative ions. Journal of Chemical Physics 40, 3307.
20. Borggard O., Christensen H.E.M., Nielsen T.K. and Willems M. 1982. Comparison of four ligands for the determination of cobalt in trace amounts by solvent extraction and graphite furnace atomic absorption spectrophotometry. Analyst (London) 107 (1281), 1479-83. CA 98: 46136a.
21. Streitweisser A. (Jnr) 1961. Molecular Orbital Theory for Organic Chemists. Wiley, New York.
22. Yates K. 1978. Huckel Molecular Orbital Theory. Academic Press, New York.
23. Dewar M.J.S. and Weiner P. 1972. Ground states of molecules XXIII. MINDO/2 calculations for Naphthalene. Theor. Chim. Acta 27(4) 373-5. CA 78: 34114r.

24. Rashiwagi H., Iwata S. and Nagakura S. 1973. π -electron structures of aromatic hydrocarbons in their low-lying triplet states. Bulletin of the Chemical Society of Japan 46: 3289-90.
25. Buss V. and Forsterling H.D. 1973. Self-consistent wavefunctions of conjugated molecules by the one-dimensional electron gas model. Application to geometries and absorption spectra. Tetrahedron 29(19) 3001-3009.
26. Ohno K., Hirooka T., Harada Y. and Inokuchi H. 1973. Modified CNDO/2 calculations of ionization potentials for some unsaturated hydrocarbons. Bulletin of the Chemical Society of Japan 46: 2353-2355.
27. Tinland B. 1969. Molecular Physics 16, 413; Bene J.D. and Jaffe H.H. 1968. Use of the CNDO method in spectroscopy. I. Benzene, Pyridine and the Diazines. Journal of Chemical Physics 48, 1807.
28. Caldow G.L. 1970. Self-consistent Huckel Theory. Molecular Physics 18(3), 383-92.

29. Billingsley F.P. and Bloor J.E. 1968. Theoretical studies on the electronic spectra of substituted aromatic molecules IV. Pariser-Parr-Pople Self-consistent field (S.C.F) parameters for polysubstituted benzenes and five-membered ring heterocyclics containing nitrogen, oxygen and sulfur. *Theor. Chim. Acta* 11(4), 325-43. CA 70; 31783g.
30. Nishimoto K, and Fujishiro R. 1962. Electronic spectra of naphthols. *Journal of Chemical Physics* 36, 3494-5.
31. Forster L.S, and Nishimoto K. 1965. Self-consistent field calculations of α - and β -naphthol. *Journal of American Chemical Society* 87(7) 1459-63.
32. Nishimoto K. 1963. Electronic spectra and structure of α - and β -naphthols. *Journal of Physical Chemistry* 67, 1443-6.
33. Bloor J.E. 1961. Theoretical studies on the electronic spectra of substituted aromatic molecules. Part I. The intramolecular electron transfer model. *Canadian Journal of Chemistry* 39, 2256-61.

34. Burawoy A. 1958. Theory of electronic spectra of organic molecules. *Tetrahedron* 2, 122-139.
35. Baba H. and Suzuki S. 1961. Electronic spectra of substituted aromatic hydrocarbons. II. Naphthols and Naphthylamines. *Bulletin of the Chemical Society of Japan* 34, 82.
36. Ridley J.E. and Zeiner M.C. 1974. The calculated spectra of the azanaphthalenes. *Journal of Molecular Spectroscopy* 50, 457-473.
37. Nishimoto K. and Fujishiro R. 1962. Electronic structures of naphthalenediols. II. β . β' -Naphthalenediols. *Bulletin of the Chemical Society of Japan* 35, 390-4.
38. McClure D.S. 1954. Excited states of the Naphthalene molecule I. Symmetry properties of the first two excited singlet states. *Journal of Chemical Physics* 22, 1668.
39. McClure D.S. 1956. Excited states of the Naphthalene molecule II. Further studies on the first singlet-singlet transition. *Journal of Chemical Physics* 24, 1.

40. Pariser R. 1956. Theory of the electronic spectra and structure of the polyacenes and of alternant hydrocarbons. *Journal of Chemical Physics* 24, 250.
41. El-Sayed M.A. 1962. Perturbational enhancement of the coupling between the lowest two electronic $\pi-\pi^*$ states in Naphthalene. *Journal of Chemical Physics* 36, 1943-4.
42. Nagakura S. and Gouterman M. 1957. Effect of hydrogen bonding on the near ultraviolet absorption of naphthol. *Journal of Chemical Physics* 26, 881-6.
43. Mataga N. 1963. Solvent effects on the absorption and fluorescence spectra of naphthylamines and isomeric aminobenzoic acids. *Bulletin of the Chemical Society of Japan* 36, 654-62.
44. Tichy M. and Zahradnik R. 1969. Physical properties and chemical reactivity of alternant hydrocarbons and related compounds. XVII. Electronic spectra of amino- and hydroxy-derivatives of benzenoid hydrocarbons. *Journal of Physical Chemistry* 73(3) 534-44.

45. Lutskaa A.E. and Antropova L.A. 1965. Some regularities in the electronic-vibrational spectra of substituted aromatic hydrocarbons II. Monosubstituted naphthalenes. Zhur. Fiz. Khim 39(9) 2120-30.
46. Hirshberg Y.H. and Norman-Jones R. 1949. The ultraviolet absorption spectra of some carboxy derivatives of naphthalene. Canadian Journal of Research 27B, 437.
47. Daghish C. 1950. The ultraviolet absorption spectra of some hydroxynaphthalenes. Journal of American Chemical Society 72, 4859-64.
48. Popov K.R. and Platonova N.V. 1980. Excited electronic states and polarization of electron transitions in molecules of 1,2 disubstituted naphthalenes containing donor and acceptor groups. Zh. Prikl. Spectrosk. 33(5) 876-82.
CA 94; 73874p.
49. Milea I. 1979. Solvent effects on the electronic spectra of monosubstituted naphthalenes I. Stud. Univ. Babes Bolyai [Ser] Phys. 24(2) 75-6 (Rom). CA 93; 57152a.

50. Miller J.C., Meek J.S. and Strickler S.J. 1977. Heavy atom effects on the triplet lifetimes of naphthalene and phenanthrene. *Journal of American Chemical Society* 99(25) 8175-9.
51. Singh S.N. and Singh R.D. 1977. Forbidden character in allowed electronic spectra of monohalonaphthalenes. *Indian Journal of Physics* 51(B) 2152-6. CA 88: 81361k.
52. Daryl F.E. and Ross I.G. 1960. Planar vibrations of naphthalene. *Spectrochimica Acta* 16, 1393-408.
53. Claverie N. and Gunigon-Lagrange C. 1964. Infrared spectroscopy of naphthalenic derivatives in the $350-1750\text{ cm}^{-1}$ region. *J. Chim. Phys.* 61(6) 889-908. CA 61: 11480g.
54. Soda R. 1961. Structures of p-tertbutyl phenol resin and α -naphthol resin II. Infrared absorption spectra of p-tertbutyl phenol and α -naphthol. *Bulletin of Chemical Society of Japan* 34, 1482-91.
55. Keussler V.r. and Rossmly G. 1956. Infrared and ultraviolet spectroscopic investigations of

- hydrogen bonds. Z. Elektrochem. 60, 136-41.
CA 50: 8328a.
56. Orville-Thomas W.J., Parsons A.E. and Ogden C.P. 1958. NH_2 -stretching frequencies in primary amines. Journal of Chemical Society 1958, 1047-9.
57. Kamada H. and Nishiro Y. 1953. Infrared spectra of monosubstituted naphthalenes. Analyst 2, 338-42. CA 47: 11988i.
58. Weiner R.C., Kennaw W. and Rayson D. 1955. An infrared spectroscopic study of naphthalene substitution. Australian Journal of Chemistry 8, 346-54.
59. Oi N. 1957. The infrared characteristic absorption bands of monosubstituted naphthalenes in the regions of $1650\text{-}2000\text{ cm}^{-1}$. Pharm. Bull (Tokyo) 5, 155-7. CA 51: 13574f.
60. Cox B.X., Keena M.A., Topson R.D. and Wright G.J. 1965. The infrared spectra of naphthalene derivatives in the regions of $1650\text{-}2000\text{ cm}^{-1}$. Spectrochimica Acta 21(9) 1663-7.

61. Luther H. and Gunzler H. 1955. Molecular vibration spectra of naphthalene and its derivatives, III. Infrared measurements of nitronaphthols. *Z. Naturforsch* 106, 445-57. CA 50; 13610i.
62. Bayer R.W. and O'Reill E:J. (Jnr) 1958. 1,5, dibromo 4,8 diidonaphthalene. *Journal of Organic Chemistry* 23, 746-7.
63. Cesare P, and Brund L. 1967. The vibrational spectrum of quinones. Part II. Infrared spectrum of 1, 4 Naphthoquinone and 1,4[²H₆] Naphthoquinone. *Journal of Chemical Physics* 46, 2109.
64. Michaelian K.H. and Zeigler S.M. 1973. Vibrational spectra and assignments for a series of mono- and dihalonaphthalenes. *Appl. Spectros.* 27(1) 13-21. CA 78; 906432.
65. Luther H. 1948. Complete analysis of absorption spectra VI. Physical-chemical properties of the chromophoric naphthalene nucleus. *Z. Elektrochem.* 52, 210-18. CA 36; 4415i,

66. Segal B.G., Raymond A. and Fraenkel G.K. 1969. Study of the linewidths of the electron spin resonance spectra of some aromatic hydrocarbon radical ions. *Journal of Chemical Physics* 51(4) 1336-52.
67. Owen G.S. and Vincow G. 1970. Computer simulation of the ESR spectra of the Naphthalene, Anthracene and Perylene radical cations in a polycrystalline medium. *Journal of Chemical Physics* 54(1) 368-75.
68. Hutchinson C.A. (Jnr), Nicholas J.V. and Scott G.W. 1970. Magnetic resonance spectroscopy of triplet-state organic molecules in zero external magnetic field. *Journal of Chemical Physics* 53(5) 1906-7.
69. Chong T. and Itoh N. 1973. Electron paramagnetic resonance and optical absorption studies of radiation-induced radicals in naphthalene single crystals. *Journal of Physical Society of Japan* 35(2) 518-24.
70. Smaller B., Avery E.C. and Remko J.R. 1967. Triplet-state zero-field-splitting correlation in

- substituted molecules. *Journal of Chemical Physics* 46(10) 3976-83.
71. Adams M.A., Blois M.S. (Jnr) and Sands R.H. 1958. Paramagnetic resonance spectra of some semiquinone free radicals. *Journal of Chemical Physics*, 28, 774-6.
72. Kommandeur J. 1961, E.S.R. of aromatic ions in iodine. *Molecular Physics* 4, 509-11.
73. Mispelter J., Grivet J.P. and Lhoste J.M. 1971. Electron spin resonance of phosphorescent fluorine-substituted aromatics I. 1-Fluoronaphthalene and 2-fluoronaphthalene in durene single crystals. *Molecular Physics* 21(6) 999-1013. CA 75: 145959c.
74. Ashford N.A. 1971, Paramagnetic resonance absorption and triplet state energy transfer of photoexcited β -methylnaphthalene molecules in naphthalene single crystals. *Journal of Chemical Physics* 54(3) 1165-77.
75. Fischer P.H.H. and McDowell C.A. 1965. The electron spin resonance spectra of dinitro-naphthalene anion radicals. *Canadian Journal of*

- Chemistry 43(12) 3400-6.
76. Gutch G.J.W., Waters W.A. and Symons M.C.R. 1970. Solvation-induced linewidth alternation in the electron spin resonance spectra of the meta-Dinitro benzene anion and of various symmetrically substituted dinitro-compounds in the benzene and naphthalene series. *Journal of Chemical Society* 7, 1261-71.
77. Smith W.B. and Chiranjeev S. 1966. The nuclear magnetic resonance spectra of some 1,4 disubstituted naphthalenes. *Journal of Physical Chemistry* 70(11), 3505-8.
78. Gupta R.C. 1967. Nuclear magnetic resonance study of α - and β -naphthols. *Journal of Physical Society of Japan* 23(1) 140. CA 68: 64375n.
79. Gupta R.C. 1968. Proton magnetic resonance spectra of polycrystalline α - and β -naphthols. *Indian Journal of Physics* 42(6) 344-53. CA 70: 82820z.

80. Seita J., Sandstrom J. and Drakenberg, T. Assignment of ^{13}C -H coupling patterns for some mono-, di- and trisubstituted naphthalene and substituted nitronaphthalenes. *Organic Magnetic Resonance* 11(5) 239-45. CA 89: 196452d.
81. Ludger E. 1976. Carbon-13 NMR study of substituted nitronaphthalenes, *Journal of Magnetic Resonance* 22(2). 279-87. CA 94: 120362g.
82. Mechin B., Richer J.C. and Odier S. 1980. Carbon-13 NMR spectroscopy of polycyclic aromatics. VII. Naphthalenes carrying electron-withdrawing substituents. Correlations between substituent-induced shifts and INDO-MO charge densities. *Organic Magnetic Resonance* 14(2) 79-85. CA 85: 142154g.
83. Boschi R., Clar E, and Schmidt W, 1974. Photoelectron spectra of polynuclear aromatics III. The effect of nonplanarity in sterically overcrowded hydrocarbons. *Journal of Chemical Physics* 60, 4406.

84. Klopman G. 1964. A semi-empirical treatment of molecular structures. II. Molecular terms and application to diatomic molecules. *Journal of American Chemical Society* 86, 4550-7.
85. Bock H., Wagner G. and Kroner J. 1972. Photoelectron spectra and molecular properties. 7. Electron lone pairs in organic sulfides and disulfides. *Chem. Ber.* 105, 3850. CA 76: 125956s.
86. Macei J.P. 1974. Photoelectron spectra of substituted naphthalene. *Helvetica Chimica Acta* 57, 994.
87. Utsunomiya C., Kobayashi T. and Nagakuri S. 1975. Configuration analysis in the LCAO Molecular Orbital theory. *Bulletin of the Chemical Society, Japan* 48, 1852.
88. Baba H., Suzuki S. and Takemura T. 1969. Molecular Orbital Analysis of Naphthalene derivatives. An application of configuration analysis to the assignment of photoelectron spectra. *Journal of Chemical Physics* 50, 2078.

89. Uzhinov B. M., Kozachenko A.I. and Kuz'min M.G. 1968. Dipole moments of singlet excited electron states of some naphthalene derivatives. Zh. Prikl. Spektrosk. 9(6) 1041-6. CA 70: 62249c.
90. Vysotskii Y.B. 1978. Effect of chemical substitution on molecular electrical properties. Zh. Strukt. Khim. 19(1) 34-41. CA 88: 189818d.
91. Karoshi A. 1964. Variations in the dipole moments of naphthols and naphthylamines. Bul. Aca. Polm. Sci. Ser. Sci. Math, Astron. Phys. 12(3) 179-82 (German). CA 61: 10137g.
92. Yoshinaga T., Hiratsuka H. and Tanizaki Y. 1977. Comparison of experimental and calculated oscillator strengths for condensed ring compounds. Bulletin of Chemical Society of Japan 50(10) 2548-53.
93. Vysotskii Y.B. 1981. Effect of chemical substitution on ionization potentials and electron affinity of systems with conjugated bonds. Teor. Eksp. Khim 17(4), 469-78. CA 95: 149757w.

94. Salem L. 1966. The Molecular Orbital Theory of Conjugated Systems. Benjamin, New York.
95. Dewar M.J.S. 1967. The Molecular Orbital Theory of Organic Chemistry. McGraw-Hill, New York.
96. Pople J.A. and Beveridge D.L. 1970. Approximate Molecular Orbital Theory. McGraw-Hill, New York.
97. Pople J.A. and Santry D.P. and Segal G.A. 1965. Approximate self-consistent molecular orbital theory I. Invariant Procedures. Journal of Chemical Physics 43, S129-S135.
98. Wheland G.N. and Mann D.E. 1949. The dipole moments of fulvene and azulene. Journal of Chemical Physics 17, 264-8.
99. Streitweisser A. (Jnr) and Nair P.M. 1959. A simple molecular orbital treatment of hyperconjugation, Tetrahedron 5, 149.
100. Streitweisser A. (Jnr) 1960. A molecular orbital study of ionization potentials of organic compounds utilizing the ω -technique. Journal of American Chemical Society 82, 4123.

101. Pople J.A. 1953. Electron interaction in unsaturated hydrocarbons. Transactions of the Faraday Society, 49, 1375.
102. Coulson C.A. 1946. Bond fixation in compounds containing the carbonyl group. Transactions of the Faraday Society, 42, 106.
103. Coulson C.A. 1939. Proceedings of Royal Society (London) A169, 413.
104. Robert J.D. Notes on Molecular Orbital Calculations, Benjamin, New York.
105. Matsen F.A. 1956. Electron affinities, methyl affinities and ionization energies of condensed ring aromatic hydrocarbons. Journal of Chemical Physics, 24, 602.
106. Davis M. Some Electrical and Optical Aspects of Molecular Behaviour, Pergamon Press, New York.
107. Daudel R., Iefebvre R. and Moser C. 1965. Quantum Chemistry Methods and Applications. Interscience Publishers, Inc. New York.

108. Atkins P.W. 1983. Physical Chemistry. 2nd Edition, Oxford.
109. Simons J.P. 1971. Photochemistry and Spectroscopy, Wiley-Interscience London and New York.
110. Straughan B.P. and Walker S. 1976. Spectroscopy, Volume 2. Chapman and Hall Limited, London P 331.
111. McRae E.G. 1956. Theory of solvent effects on molecular electronic spectra. Frequency shifts. Journal of Physical Chemistry 61, 562.
112. Suppan P. 1968. Solvent effects on the energy of electronic transitions: Experimental observations and applications to structural problems of excited molecules. Journal of Chemical Society 4, 3125.
113. Suppan P. 1980. Absolute excited-state dipole moments from solvatochromic shifts. Spectrochimica Acta 36A, 971.
114. Wheatley P.J. 1959. The Determination of Molecular Structure. Oxford University Press, London and New York.

115. O'Reilly E.J. (Jnr) and Lippincott E.R. 1955.
Vibrational spectra and assignment of naphthalene
and naphthalene d₈. Journal of Chemical
Physics, 23, 238.
116. Colthup N.B., Duly L.H. and Wiberly S.E. 1964.
Introduction to Infrared and Raman Spectroscopy.
New York and London.
117. Hodgson H.H. and Kilner E. 1924. Preparation of
2- and 4-Nitro-1-naphthols. Journal of Chemical
Society 125, 807.
118. Morgan G.T., Michlethwait F.M.G. and Winfield H.B.
1904. A study of the substitution products
of ar-Tetrahydro- α -naphthylamine. 4-
bromotetrahydro- α -naphthylamine and ar-
Tetrahydro- α -naphthylamine-4-sulphonic acid.
Journal of Chemical Society, 85, 750.
119. Price C.C. and Voong S. 1948.
Organic Synthesis 28, 80. Coll. Vol. 3,
664.
120. O'Donnell J.F., Ayres J.T. and Mann C.K. 1965.
Preparation of high purity acetonitrile. Analyt.
Chem. 37, 1161. CA 63: 8195c.

121. Vogel A.I. 1975.
A textbook of Practical Organic Chemistry,
Longmans.
122. Nilsson O. 1967. Preparation of ultraviolet
transparent, saturated hydrocarbons. Acta Chem.
Scand. 21(5) 1501-1506. CA 67: 99463w.
123. Rao C.N. R. Ultraviolet and Visible
Spectroscopy 3rd edition, Butterworths, England.
124. Ali M.A. and Coulson C.A. 1960. On the
stability of substituted diphenylenes.
Tetrahedron, 10, 41.
125. Badger G.M. 1952. The Structures and Reactions
of the Aromatic Compounds. University Press,
Cambridge.
126. Fukui K., Yonegawa T., Nagata C. and Shingu H. 1954.
Molecular Orbital Theory of Orientation in
Aromatic, Heteroaromatic and other Conjugated
Molecules. Journal of Chemical Physics 22,
1433-42.
127. Nishimoto K. and Fujishiro R. 1961. Bulletin of the
Chemical Society of Japan 35, 3.

128. UV Atlas of Organic Compounds 1966. Library of Congress Catalog Card No 66-21542, Butterworths, London.
129. Nishimoto K. 1966. Calculation of the three π - π^* Absorptions. Bulletin of Chemical Society of Japan 39, 645-650.
130. Becker R., Sen-Singh J. and Jackson E. 1963. Comprehensive spectroscopic investigation of polynuclear aromatic hydrocarbons. I. Absorption spectra and state assignments for the tetracyclic hydrocarbons and their alkyl-substituted derivatives. Journal of Chemical Physics 38, 2144.
131. Iredall T. and White J. 1960. Electronic states of monohalogen-substituted naphthalenes. Trans Faraday Soc. 56, 1719.
132. Peters D. 1957. Colour and constitution Part II. The effect of the common monatomic substituents on the ultraviolet spectrum of alternant hydrocarbons. Journal of Chemical Society 1993.

133. Hodgson H. and Hathway D. 1948. Absorption spectra of mononitro naphthylamines - their structures (II) 3-5-, 6-, 7- and 8-nitro-2-naphthylamines and 6-nitro-1-naphthylamines Trans Faraday Soc. 41, 115.
134. Baba H. and Suzuki S. 1961. Electronic spectra and hydrogen bonding. I. Phenols and Naphthols. Journal of Chemical Physics 35,1118.
135. Bayliss N.S. 1950. The effect of the electrostatic polarization of the solvent on electronic absorption spectra in solution. Journal of Chemical Physics 18(3), 292-296.
136. Bayliss N.S. and McRae E.G; 1953, Solvent effects on organic spectra. Dipole forces and the Franck-Condon principle. Journal of Physical Chemistry 58, 1002-1006.
137. Pimentel G. and McClellan A.L. 1960. The Hydrogen Bond. W.H. Freeman and Company, San Francisco.
138. Bayliss N.S. and Wills-Johnson G. 1968. Solvent effects on the intensities of the weak ultraviolet spectra of ketones and nitro-paraffins - II. Spectrochim Acta 24A, 563.

139. Pullman B., Claverie P. and Caillet J. 1965. Mechanism of molecular interactions between aromatic hydrocarbons and purine or pyrimidine bases in solution. *Science* 147, 1305. CA 63: 5487d.
140. Kamlet M.J., Abboud T.L. and Taft R.W. 1972. The solvatochromic comparison method. 6. The π^* scale of solvent polarities. *Journal of American Chemical Society* 99, 6027.
141. McClellan A.L. Tables of Experimental Dipole Moments. W.H. Freeman and Co., San Francisco and London.
142. Lippert E. 1957. Spectroscopic determination of the dipole moment of aromatic compounds in the first excited singlet state. *Z. Elektrochem* 61, 962. CA 52: 4270g.
143. Rao K.S., Nakashim H.A., Deshpande D.K. and Shashidar M.A. 1986. A new method for estimating excited state dipole moments of molecules from the solvent effect on their electronic spectra. *Spectrochim Acta* 42A5 585.

144. Bottcher C.J.F. 1952. Theory of Electric Polarisation Elsevier, Amsterdam.
145. Rice S.A. and Gelbert W.M. 1971. Relaxation phenomena in excited molecules. Pure Appl. Chem. 27(3) 361-87. CA 76: R58396u.
146. Green J.H.S., Kynastin W. and Lindsey A.S. 1961. The vibrational spectra of benzene derivatives I. Nitrobenzene, the benzoate ion, alkyl metal benzoates and salicylates. Spectrochim Acta 17, 486.
147. Evans J.C. 1960. The vibrational assignments and configurations of aniline, aniline-NHD and aniline-ND₂. Spectrochim Acta 16, 428.
148. Mecke R. and Rossmly G. 1955. Infrared spectra of aromatic hydroxyl and deuterioxyl compounds. I. Assignment of the OH in-plane deformation vibrations. Z. Elektrochem 59, 866. CA 50: 3088b.
149. Davies M. 1948. Molecular interactions and infrared absorption spectra. Journal of Chemical Physics 16, 274.

150. Cencelj L. and Hadzi D. 1955. Infrared spectra of polychloronaphthalenes. *Spectrochim Acta* 7, 274.
151. Green J.H.S. and Harrison D.J.H. 1970. Vibrational Spectra of benzene derivatives. X. Monosubstituted nitrobenzenes. *Spectrochim Acta Part A*, 26, 1925-37.
152. Dahne S. and Stanko H. 1962. The infrared spectrum of Nitrophenols - ^{15}N . *Spectrochim Acta* 18, 561.
153. Pinchas S., Samuel D. and Silver B.L. 1964. The infrared absorption spectrum of ^{18}O labelled nitrobenzene. *Spectrochim Acta* 20, 179.